NORTHWESTERN UNIVERSITY

Wireless Resource Allocation among Cooperative Relays and Non-cooperative Agents

A DISSERTATION

SUBMITTED TO THE GRADUATE SCHOOL

IN PARTIAL FULFILLMENT OF THE REQUIREMENTS

for the degree

DOCTOR OF PHILOSOPHY

Field of Electrical Engineering and Computer Science

By

Junjik Bae

EVANSTON, ILLINOIS

December 2008

ABSTRACT

Wireless Resource Allocation among Cooperative Relays and Non-cooperative Agents

Junjik Bae

This thesis focuses on resource allocation in wireless communication and networking. Resource allocation has been studied widely, for example, to maximize the system-wide throughput or to minimize the average delay per user. Moreover, the utility-based framework is becoming an important tool for addressing fairness and Quality-of-Service (QoS) for individual users. With this framework, therefore, we study wireless resource allocation for relay extensions in a cellular network and dynamic spectrum sharing among non-cooperative agents.

In the first part of the thesis, we study the centralized resource allocation problems among cooperative agents. Especially, the relay extension in a cellular network is focused on, including in-band relays in *IEEE* 802.16j and out-of-band relays with Wi-Fi access points. Here, the base station optimizes the time or power allocation such that

total throughput for data traffic or total number of active users for voice traffic is maximized. For the cases considered, a significant gain for both data traffic and voice traffic is obtained.

In the second part of the thesis, dynamic spectrum sharing with distributed resource allocation is considered with an emphasis on the development of mechanisms and their performance. First, we consider an "AP deployment" game in the commons model and show that there exists a Nash equilibrium which is efficient. In addition, we address the limitations of the commons model when interference is severe. Second, we study two auction mechanisms for resource allocation in a peer-to-peer network: The sequential second-price auction and the "Fallback" auction. For the sequential auction, the resource is divided into n units and each unit is auctioned off sequentially according to a second-price auction. The worst-case efficiency of the sequential auction is shown to be lower bounded by $1 - e^{-1}$ for a bandwidth allocation and upper bounded by $1/n$ for a power allocation. Because of the low worst-case efficiency for power allocation and the impracticality of the complete information assumption in the sequential auction, we discuss a Fallback auction, which modifies Ausubel's ascending auction. With an increasing convex utility of one agent due to interference, we show that the Fallback auction for power allocation achieves a stable outcome with minimum revenue to the seller in the core.

Acknowledgements

I would like to thank my two advisers, Professor Michael L. Honig and Professor Randall Berry. I have had a privilege to work closely with them during the past five years. They gave me support when I needed it most and they provided inspiration and dedication to my professional developments when I was wandering around.

I would like to thank Professor Rakesh Vohra and Dr. Eyal Beigman. Discussions with them always gave me insightful ideas and broadened my horizon beyond engineering mind. In addition, Professor Rakesh Vohra served as a committee member.

I also would like to thank Dr. Roger Peterson and Dr. Eugene Visotsky for valuable discussion regarding *IEEE* standard propositions. I also had a privilege working with them as a summer intern at Motorola Lab.

The Communications and Networking Lab has been a wonderful place for both research and living. I thank my present and past office mates, Manish Agarwal, Hang Zhou, Changxin Shin, Lei Zhang, Kai Hung Hui, Maximilian Riemensberger, Jianwei Huang, Naveen Arulselvan, Wiroonsak Santipach, Toni Cheng and Xiaoe Liu. I also thank other members of the lab, Ning Wen, Jieying Chen, Yalin Sagduyu, Hongxia Shen, Mingguang Xu, Jun Luo, Yan Zhu, Francisco Rubio, and Byungchul Kim.

I would like to thank my fellow grad students for my great time at Northwestern: Many from Korean student association and others from my previous group including

Hochul Lim, Shaban Ramezani-Darvish, and Katie Minder. Because of them, I have enjoyed my life here at Evanston.

Finally, many thanks to my family for their unconditional love and support. I could not have done my Ph.D. without them.

Table of Contents

List of Tables

List of Figures

CHAPTER 1

Introduction

Resource allocation is an important research topic in wireless communication and networking, due to the intrinsic scarcity of wireless resources and increasing demands for them. User devices have become increasingly sophisticated and support various multimedia applications, which require high quality-of-service (QoS). In addition, due to the prevalence of mobile devices and the popularity of Wi-Fi, more users than ever have to share the wireless spectrum. This necessitates highly efficient and robust schemes for wireless resource allocation.

There are many different wireless resources, such as frequency bands, time slots, orthogonal codes and transmit power. One or more dimensions associated with different resources can be allocated simultaneously depending on the technology and demand. Example technologies include time-division multiple access (TDMA), frequency-division multiple access (FDMA), and code-division multiple access (CDMA). In addition, orthogonal frequency division multiple access (OFDMA) is becoming increasingly important since it has been adopted for various standards such as WiMax, *IEEE* 802.11n, and next generation cellular systems such as *IEEE* 802.16m and 3GPP long term evolution (LTE) [**7, 1, 5, 9**]. Contention-based random access, as in Wi-Fi, is another spectrum sharing technology for distributed resource allocation.

Unlike wired networks, wireless networks use a common medium. This imposes challenges on designing a wireless network and allocating resources among users in the network. The common medium or spectrum is in principle open to every device, which would like to use it. Therefore, as the number of devices increases, the usability of spectrum is degraded due to interference. This is called the "tragedy of the commons" [**45**]. To avoid the tragedy of the commons, the exclusive model for allocating spectrum with a careful geographical spectrum plan has been adopted [**32, 35**]. Recently, however, a variety of studies have demonstrated that this exclusive model imposed by the Federal Communication Commission (FCC) in the U.S.A. has resulted in a great deal of spectrum lying idle [**105**]. To overcome the underutilization problem, two approaches for dynamic spectrum sharing have been studied, which will be discussed later: the commons model [**116, 97, 64**] and secondary spectrum markets [**22, 88, 112**]. Due to increasing demand on wireless resources, and efficiencies offered by dynamic spectrum sharing, the resource allocation problems become more important than ever.

Various resource allocation mechanisms in wireless networks can be applied depending on the network configuration and degree of cooperation among network entities. We can consider two classifications for resource allocation mechanisms: centralized vs. distributed and cooperative vs. non-cooperative. In centralized resource allocation, a resource manager (or "social planner") collects all related information from users and makes a decision on how to allocate resources among users. In distributed resource allocation, each user in the network allocates wireless resources based on her local information. Furthermore, users in a cooperative network work together to achieve the network's overall objective such as the sum of users' throughput or minimum blocking probability. Non-cooperative

users in a network are, on the other hand, assumed to be selfish and try to maximize their own objective[1], which might not be aligned with the system objective. An interesting problem for distributed resource allocation is to determine the efficiency loss when compared with a centralized allocation (See, for example, [**95**]).

In this thesis, we consider centralized resource allocation among cooperative base and relay stations in a cellular network (Part 1), and distributed resource allocation among non-cooperative selfish agents in the commons model, assuming a peer-to-peer network (Part 2). The resource allocation problems considered here are solved using the framework of utility functions.

1.1. Utility-Based Resource Allocation

Resource allocation and system optimization problems based on user utility functions have been widely studied in communications and networks [**57, 74, 63, 104**]. The utility function indicates the degree of satisfaction that an individual user derives from the allocated resources. The user's utility function is not necessarily aligned with system-centric "efficiency". For example, in a cellular network, to maximize total throughput, the base station (BS) might allocate all of its resources to the cellular users who have good channel gains. This, however, limits the resources available to the users with bad channel gains. By using the utility function, a balance between system efficiency and fairness can be obtained [**58**].

The utility function maps resource use (bandwidth, power, etc.) or performance criteria (data rate, delay, etc.) to private values. Different utility functions can be used in a wide range of communication models. For traditional data traffic such as file transfer

[1]This objective will be defined by a utility function.

and e-mail, increasing concave utilities as a function of data rate represent the elasticity of these services [**63, 51**]. Real-time traffic, such as Voice-over-IP (VoIP) and multi-media video streaming, has been modeled by a step function of signal-to-noise ratio (SNR) or signal-to-interference plus noise ratio (SINR), reflecting the assumption that excessive delayed data does not have any value [**67**]. In addition, a decreasing concave function of delay for delay-tolerant data traffic, and sigmoidal functions for a real-time rate adaptive application, or a frame success rate with binary phase-shift keying have been used [**66, 102, 96**].

The standard resource allocation problem using the utility framework can be described by

$$\begin{aligned} &\max_{q} \sum_{k\in\mathcal{K}} U_k(x_k(q_k, q_{-k})), \\ &\text{s.t.} \sum_{k\in\mathcal{K}} q_k \leq Q, \end{aligned} \tag{1.1}$$

where $q = (q_k, q_{-k})$ is the resource to be allocated among a set of users $\mathcal{K} = \{1, 2, \cdots, K\}$, q_k denotes the resource allocated to user k, and q_{-k} denotes the set of resources allocated to all users except for user k. In addition, Q is the total amount of resources (e.g., bandwidth or power) available in the network. Each user $k \in \mathcal{K}$ has her own utility function $U_k(x_k(q_k, q_{-k}))$, which represents her satisfaction with the allocated resources (q_k, q_{-k}). Here $x_k(q_k, q_{-k})$ can represent the QoS measurement of user k, which could be a quantity such as the queue length, queuing delay, data rate, or SINR. For example, consider allocating a total bandwidth of W among K users with elastic data traffic. If x_k represents data rate that user k has with allocated bandwidth w_k, then $U_k(x_k(w_k, w_{-k}))$ is

typically an increasing concave function, which represents the user's growing satisfaction with increasing data rate. In an FDMA network, the data rate can be represented by the Shannon capacity $x_k(w_k, w_{-k}) = r_k(w_k) = w_k \log(1 + \mathrm{SNR}(w_k))$.

Problem (1.1) can be solved either in a centralized way or in a distributed manner. The solution to the problem is called the efficient or socially optimal allocation in the economics literature [**75**]. Here we assume that the radio environment does not change for some period of time T and the optimization problem can be solved within T. (Otherwise, we could instead consider a long-term time-average optimization problem.)

1.2. Resource Allocation in Relay-Assisted Network

In the first part of this thesis, we consider centralized utility-based resource allocation in a relay-assisted network. Adding relays to a cellular network can potentially increase the network capacity, extend network coverage, and reduce congestion (e.g., see [**98, 17, 81, 20, 125, 86, 30, 41, 80, 118**]). In [**81**], the authors consider a uniform placement of in-band relays within a cell and give an upper bound on the gain for downlink throughput. In that paper, either direct transmission from the BS to each mobile station (MS), or transmission through the relay station (RS) is chosen depending on the transmission time duration, assuming each MS is required to have the same throughput. In [**17**], cell splitting using RSs in an interference-limited deployment is considered. The authors show that simple in-band RSs increase system capacity and the total cost can be reduced significantly due to the elimination of the wired backhaul. Coverage extension through multi-hop RSs is considered in [**34, 119, 30, 46**]. In addition, various cooperative schemes such as decode-and-forward, amplify-and-forward, and compress-and-forward schemes using RSs

are studied in [**62, 103, 59**]. Associated advantages have motivated the introduction of relays in emerging standards such as IEEE 802.16j [**6**] and 4G mobile systems [**91, 5, 98**].

Various relay deployment scenarios have been considered in the literature. For example, using mobile handsets as relays in a cellular system in an ad hoc manner has been considered. In that case, the incentive for each mobile to relay others' data traffic can be provided by a credit or market price [**69, 23, 73**]. Even though this kind of ad hoc extension is quite flexible and does not require additional hardware investment, it is difficult to guarantee an end-to-end QoS. In addition, it might add significant complexity to the BS for transmission scheduling.

Instead of deploying relays in an ad hoc manner, a systematic relay deployment plan might be more feasible in cellular networks [**69, 83, 114**]. One of those efforts is the fixed relay extension of WiMax. A WiMax network uses OFDM, where the base station controls the rate, power, and subchannel allocations to each mobile user. In addition, time division duplex (TDD) has been adopted for downlink and uplink transmission. The relay extension of WiMax based on the *IEEE* 802.16j standard assumes in-band relays, which use the same frequency as that of the BS within a cell [**2**]. The resource that is allocated between the BS and the RS is the time duration of the relay zone within a frame. That can be optimized centrally at the BS.

Rather than deploying new cellular relays, in some cases it may be possible for a cellular service provider to use an existing wireless LAN (WLAN) access point (AP) as a relay for cellular traffic [**114**]. In that case, although the AP potentially brings additional resources to the cellular network, those resources must be allocated across both WLAN and cellular users. If the AP service provider is different from the cellular service provider, then for

the latter to use the AP as a relay, a bargaining process between those two providers can be used to find a mutually beneficial operating point with an appropriate resource allocation.[2] On the other hand, if both the cellular and the WLAN network belong to one service provider, or are cooperative, then the optimal operating point can be computed in a centralized manner. Depending on the operating objective, which is reflected by the utility functions, total throughput or the total number of users served in the system can be maximized. Both of these problems are discussed in Chapters 2 and 3.

1.3. Dynamic Resource Allocation among Non-Cooperative Agents

In the second part of this thesis, we focus on dynamic spectrum resource allocation among non-cooperative agents. Dynamic spectrum sharing is another important issue for future wireless networks. Until now, wireless spectrum has been divided into many different bands and most bands have been allocated exclusively to a licensee by the Federal Communications Commission (FCC). Exceptions include the unlicensed bands, such as the ISM and UNII bands [**3, 8**]. It is, however, widely recognized that this "command and control" model for allocating wireless spectrum results in poor utilization of spectrum even if it might guarantee some level of QoS [**87**]. Outdoor spectrum measurements in various urban areas reveal that the use of spectrum is in general very low even during the peak time periods [**70, 115**]. Dynamic spectrum sharing approaches are alternatives to this exclusive use model, which can achieve the goal of higher utilization.

Encouraged by the success of 802.11 (Wi-Fi) and the advance of cognitive radio technology, the commons model for spectrum sharing has been studied intensively [**27, 56, 64**].

[2]For example, with the complete information assumption, the Nash bargaining solution is an efficient operating point in which the sum utility of the two service providers is maximized. Furthermore, it can be achieved distributively [**82**].

In this model, as long as certain technical requirements such as peak transmit power and a common medium access control (MAC) protocol are satisfied, users can have access to the common spectrum without a license. Sharing TV "white space" with low transmission power devices is an active area motivated by this direction [**101, 28**]. In addition, the working group on Wireless Regional Area Networks ("WRANs") is to develop an *IEEE* 802.22 standard for a cognitive radio-based PHY/MAC/air interface for use by license-exempt devices on a non-interfering basis in spectrum that is allocated to the TV broadcast service [**4**].

In the commons model, interference management is a key issue that has to be solved.[3] At a basic level this is accomplished by appropriately defining the spectrum power mask. However, this may be inadequate depending on the configuration of the network, propagation characteristics, and demand for spectrum. In [**52**], instead, the authors consider a distributed power control scheme for wireless ad hoc networks and show the convergence of the interference-price announcement algorithm using supermodular game theory. This algorithm, however, requires truthful announcement of the interference prices among nodes (users) in the ad hoc network. Moreover, cooperation or bargaining among adjacent agents in a peer-to-peer network may be a viable solution to the interference problem [**40**]. For example, adjacent BS owners may negotiate cross-rental agreements for the same spectrum, or alternatively, agree to pay "interference charges" to each other, which reflect the externality they are causing to neighboring owners. This interference payment might induce BS owners to reduce transmission power or to use neighboring BSs via routing, which lowers overall interference in the area.

[3]In fact, the main argument by opponents of the "white space" concept is the lack of interference-free technologies.

Another example of dynamic spectrum sharing is via secondary markets for spectrum, as considered by the FCC [**37, 38, 39**]. A spectrum owner, or licensee may wish to lease spectrum to secondary users depending on how their demand varies over the time of day, duration of use, number of available channels, etc. This leads to the problem of designing an efficient mechanism for allocating available wireless resources (e.g., bandwidth and/or power) among non-cooperative agents. One way to achieve this is to allow for spectrum to be allocated on a finer scale both in time and space, e.g., by a "real-time spectrum market" [**88, 24, 35, 60**] (similar to electricity markets in [**10, 53**]).

Auctions are well known techniques in economics and so are a natural approach for allocating constrained resources. An auction mechanism can be implemented through a *spectrum manager*, or *broker*. The spectrum manager can mitigate the effects of externalities (e.g., interference in wireless communication) and increase the overall efficiency by soliciting information about user utilities and channel conditions. Examples of this scenario are also presented in [**92, 54, 51**]. Other distributed spectrum sharing mechanisms, which do not rely on the presence of a spectrum manager, are considered in [**36, 52, 111**].

There are many auction mechanisms for resource allocation in the literature. The Vickrey-Clark-Groves (VCG) mechanism is especially well known because of its incentive compatibility among agents and the efficiency of the resulting resource allocation [**109, 44, 124**]. It is, however, not popular in practice because the agents are asked to submit their utility functions to the seller and, therefore, the agents reveal too much private information. The revenue of the seller through the VCG auction can be potentially very low and the seller might nullify unfavorable outcomes. In addition, it cannot block a

coalition of agents which leads to an inefficient outcome even though within the auction mechanism each agent has a dominant strategy that leads to an efficient outcome.[4]

Due to these shortcomings and impracticalities of the VCG auction, we consider two alternative auction mechanisms for wireless resource allocation. First, a sequential second price auction is considered in which each resource unit is auctioned off sequentially according to a second-price auction.[5] Sequential auctions have been used in many applications (e.g., see [**21, 126, 107, 77, 113**]), since they require relatively little computation and information exchange among the agents and the broker, compared with many other mechanisms. In addition, sequential auctions easily accommodate scenarios in which the agents enter and leave the market at arbitrary times, and allow the broker to allocate resources incrementally. However, it is well known that sequential auctions do not always achieve an efficient allocation [**77**].[6]

There is an extensive literature that investigates the properties of sequential auctions [**84, 47, 77, 113, 19, 49, 90, 61, 50**] assuming that utilities are private information. Since the assumption of private information complicates the analysis, those papers restrict attention to the case of bidders with *unit* demands and in some cases to just two bidders. On the other hand, abstracting away from private information allows us to focus on the strategic implications of bidding in sequential auctions. Indeed, in work such as [**113**], the efficiency loss is due to the information asymmetries and not the mechanism. If agents in that model have full information (each with unit demand), then it can be shown that the auction achieves an efficient outcome.

[4]See [**13**] for a more detailed discussion of these shortcoming of the VCG mechanism.
[5]Namely, each unit is allocated to the highest bidder, who pays the second highest bid.
[6]Under this mechanism, the bidders can be viewed as playing a game, in which their actions are their bids. The auction is efficient if the equilibrium of this game maximizes the total utility of the agents.

As a step toward the sequential auction with multiple-unit demands and private information, it is valuable to study the efficiency loss of the sequential auction due to the mechanism itself, ignoring possible information structures. The efficiency loss of the sequential second price auction when used to allocate bandwidth and power among selfish agents is the main topic in Chapter 5. Here we allow bidders to have multi-unit demands, but for tractability we assume full information. We also note that assuming full information is consistent with prior work, such as [**55, 95**], which also study the efficiency loss of different mechanisms.

Second, we discuss the "Fallback" auction proposed in [**14**]. In 2004, Ausubel proposed an ascending auction for multiple units of a homogeneous good and showed that the auction yields efficient outcomes with private information [**12**]. In the auction, the auctioneer announces a price and bidders respond with quantities. Each bidder "clinches" items at the current price and the price increases until the market clears. This auction, however, assumes that each bidder has a concave increasing utility function (or decreasing marginal utilities) with the number of units she receives. There are wireless resource allocation scenarios, however, for which the concavity of the utility function does not hold.[7] One example is allocating power between two peer-to-peer interfering agents with rate utility functions.

The Fallback auction, which modifies Ausubel's ascending auction, is applied to the case where one of the agents has a convex utility function due to the interference. In the auction, the market price set by the seller can be lowered by the agent with a convex utility function exactly once. The auction ends either when the market clears or when

[7]To the author's knowledge, [**42**] is the only paper in which a multi-unit auction is considered with increasing marginal utilities.

the agent falls back to a price lower than the current price. This auction assumes private information among all agents, and finds a stable outcome in the *core*. If the outcome of the auction, namely, a set of payoffs of all agents including the seller, is in the core, then there is no payoff improvement if a coalition of the agents deviates. This implies that the allocation is efficient, the bidders cannot benefit from shill bids or collusion, and the seller cannot benefit from excluding bidders [**31**]. Therefore this auction avoids the instability of the VCG and Ausubel's ascending auctions when there is an agent with an increasing convex utility function.

1.4. Overview

This thesis discusses resource allocation in wireless networks. Chapters 2 and 3 focus on cooperative relay networks. Due to the cooperative nature of the network, resources such as time or bandwidth can be allocated in a centralized way to maximize the utility of the network.

In Chapter 2, the relay extension of WiMax, or *IEEE* 802.16j is considered to increase uplink capacity (network utility). A time-division duplex (TDD) frame structure for 802.16j is discussed where the resources to be allocated are time and frequency slots in the frame. Each slot is a minimum resource allocation unit defined in the standard. To obtain an initial assessment of capacity gains, we study a one-dimensional model of a relay-enhanced cellular system. Time allocation within a frame is optimized to maximize the number of voice-over-IP (VoIP) users who require a fixed transmission rate. Furthermore, we develop a detailed system simulator based on the 802.16j standard and show that the uplink capacity for both data and VoIP traffic increases significantly when relay stations

are deployed in the system. Specifically, our system simulation results show that the number of VoIP users increases from 140 per cell to 360 per cell when two RSs per sector are deployed.

Due to the popularity of 802.11 (Wi-Fi), we consider an existing Wi-Fi AP as a relay for cellular traffic in Chapter 3. A one-dimensional model of a cellular network with two out-of-band APs is introduced. Assuming each user has a utility function, which corresponds to either the Shannon rate function for data traffic or a step function for voice traffic, the BS optimizes power allocations across both cellular and AP users to maximize the sum of utilities over active users. Furthermore, an upper bound on the gain from using APs as relays is obtained. Our analysis suggests that a modest gain in total sum throughput or total number of voice users can be obtained in the scenario considered. In addition, the coverage of the BS can be extended by using the AP.

Non-cooperative wireless networks are considered in Chapters 4, 5, and 6. The agents in the network are assumed to be selfish and maximize their own utilities. Resources such as a frequency band or transmit power are allocated in a distributed way among non-cooperative agents through best response updates (Chapter 4), or by using an auction mechanism (Chapters 5 and 6).

In Chapter 4, we consider a commons model in which a user may install an AP to serve her own, as well as other users' traffic. To avoid a "tragedy of the commons", an AP owner can provide payments to neighboring users to encourage them not to set up interfering APs. In the resulting AP deployment game, each user decides whether or not to set up an AP, depending on the interference level and the payments from other neighboring APs. We show that this game is a potential game and that best response updates converge to a Nash

equilibrium [**79**]. According to our analysis as well as simulation results, the density of APs in this game at the Nash equilibrium decreases as interference becomes severe, which leads to a large loss in efficiency. Hence, as the density of APs increases, implementing such a commons approach becomes more difficult and other forms of spectrum sharing may be more appropriate.

An alternative approach to dynamic spectrum sharing among non-cooperative agents is to apply auction mechanisms. In Chapter 5, a sequential second price auction is considered for bandwidth or power allocation in a peer-to-peer network. The resource is divided into n units of the good and each unit is auctioned off sequentially. For the bandwidth auction, the utility function of each agent is assumed to be an increasing concave function for the number of received bands. For the power auction, an increasing *convex* utility function for a single agent is assumed due to the interference. The auction is represented by an extended form game and the subgame perfect equilibrium is studied using backward induction with the complete information assumption. In addition, the worst-case efficiency, namely, the ratio of the sum utilities of agents in a subgame perfect equilibrium to the maximum sum utility, is bounded. Our analysis shows that the worst-case efficiency among two agents is lower bounded by $1 - 1/e$ for the bandwidth auction and decreases as $1/n$ for the power auction, which n is the number of (discrete) power units being allocated.

Motivated by the low worst-case efficiency of the power auction and the impracticality of the complete information assumption in the sequential second-price auction, we study the Fallback auction in Chapter 6. It is assumed that one agent has an increasing convex utility function and the others have increasing concave utility functions, similar to the

power auction in Chapter 5. In the Fallback auction, which is a modified version of Ausubel's ascending auction, the agent with a convex utility is allowed to "fall back" to a lower price than the current auction price set by the seller. We show that this Fallback auction selects a core outcome with the minimum revenue to the seller and, therefore, it achieves a full information equilibrium. In addition, for the case where the VCG outcome is in the core, this mechanism finds the VCG outcome, which is efficient and incentive compatible.

Finally, we summarize our results and propose possible directions for future work in Chapter 7.

Part 1

Resource Allocation among Cooperative Relays

CHAPTER 2

Uplink Capacity and Coverage Extension for Relay-Enhanced OFDMA Cellular System (802.16j)

Multihop Cellular Networks (MCN) have become the subject of a considerable research effort in both academia and industry. Multihop communication techniques have traditionally been applied in the field of ad-hoc networks, where radio nodes engage in peer-to-peer communication with other nodes by means of multihop routing. In such a network, any node can perform packet forwarding on behalf of another node, thereby greatly extending range and increasing robustness of the ad-hoc network. Recently, it has been recognized that by introducing multihop communication techniques into traditional single-hop cellular networks, significant performance benefits may be also obtained. For example, with the introduction of relay stations (RSs) into a cellular system, it becomes possible to break-up a long single-hop link between a base station (BS) and a distant mobile station (MS) into a series of shorter hops. As the shorter hops are more spectrally efficient, the overall system capacity of the MCN may increase relative to the legacy cellular system. RSs may also provide an opportunity for connection to a shadowed MS, thereby improving cellular coverage, or they may also serve as an attachment point for an MS out of communication range with the BS, thereby improving cellular range [**110, 81, 46, 26, 68**].

Recently, the *IEEE* 802.16j standard draft has been completed, partly encouraged by the reported benefits of relay deployments in cellular settings, as well as the successful and wide-spread application of multihop technologies in WLANs [**2**]. 802.16j is a relay-extension of the *IEEE* 802.16e standard, widely known as WiMax. To estimate the benefit associated with 802.16j, in this chapter we study the capacity and range extension of a relay-enhanced 802.16e *uplink* through a first-order analysis and detailed system simulations. Here, we define the capacity as the maximum cumulative throughput per cell (for data traffic) or the maximum number of users with a given QoS requirement (for voice traffic) supported by the system, under system-specific transmit power and scheduling constraints. Hence, the system capacity determined is necessarily less than the bound on the system capacity that may be obtained through an information-theoretic analysis. The results are encouraging, as fairly substantial capacity gain and range extension are observed from both analysis and simulations.

We first review the frame structure of 802.16j in Section 2.1 to understand how it affects the uplink capacity of the system. System analysis with a one-dimensional model is presented in Section 2.2, assuming symmetric AP deployment around the BS and uniform user density. After we estimate the capacity gain of the relays with one-dimensional model, the detailed system simulation setup and resource allocation schemes are presented in Section 2.3 and 2.4. Our simulation results on voice traffic and data traffic follow.

2.1. Frame Structure of 802.16j

The IEEE 802.16j standard has extended the IEEE 802.16e frame structure to support in-band BS-to-RS communication. A high level diagram of the 802.16j frame structure in

TDD OFDMA PHY mode is shown in Fig. 2.1 (taken from [**117**]). The frame structure supports a typical two-hop relay-enhanced communication, where some MSs are attached to an RS and communicate with a BS via the RS, and some MSs connect directly to the BS. Even though extensions of the frame structure to support more than two hops have been defined by the Task Group (TG), we only consider the two-hop scenario in this paper.

In Fig. 2.1, the horizontal dimension denotes time and the vertical dimension denotes frequency. Frame sections in gray denote receive operation, whereas sections in white denote transmit operation. The multihop-relay-BS (MR-BS) and RS frames are subdivided into Downlink (DL) and Uplink (UL) subframes to support TDD operation. Both DL and UL subframes are further subdivided into MS and RS zones. In addition, Relay-Gap (R-Gap) is placed between MS-zone and RS-zone, which allows RSs to switch from receive mode to transmit mode or from transmit mode to receive mode. The MS zones, supported at both the BS and RS, are backwards compatible with the 802.16e standard. Detailed structure of the RS zones is currently under consideration in the IEEE 802.16j TG. The RS transmits to MSs within its coverage area in the DL MS zone and receives control and data from the BS in the adjacent DL RS zone.

Here, we focus on UL capacity of the relay-enhanced system. A more detailed view of the UL subframe, as modeled in the system simulator, is shown in Fig. 2.2. In the figure, a 5 ms frame length, 50/50 TDD split and 10 MHz BW are assumed. With these parameters, there are 7 time slots and 35 frequency slots in the UL subframe, and therefore a total of 245 OFDMA slots are available for UL scheduling. A slot is the minimum resource allocation unit as defined in the 802.16 standard. The UL RS zone is one time slot wide

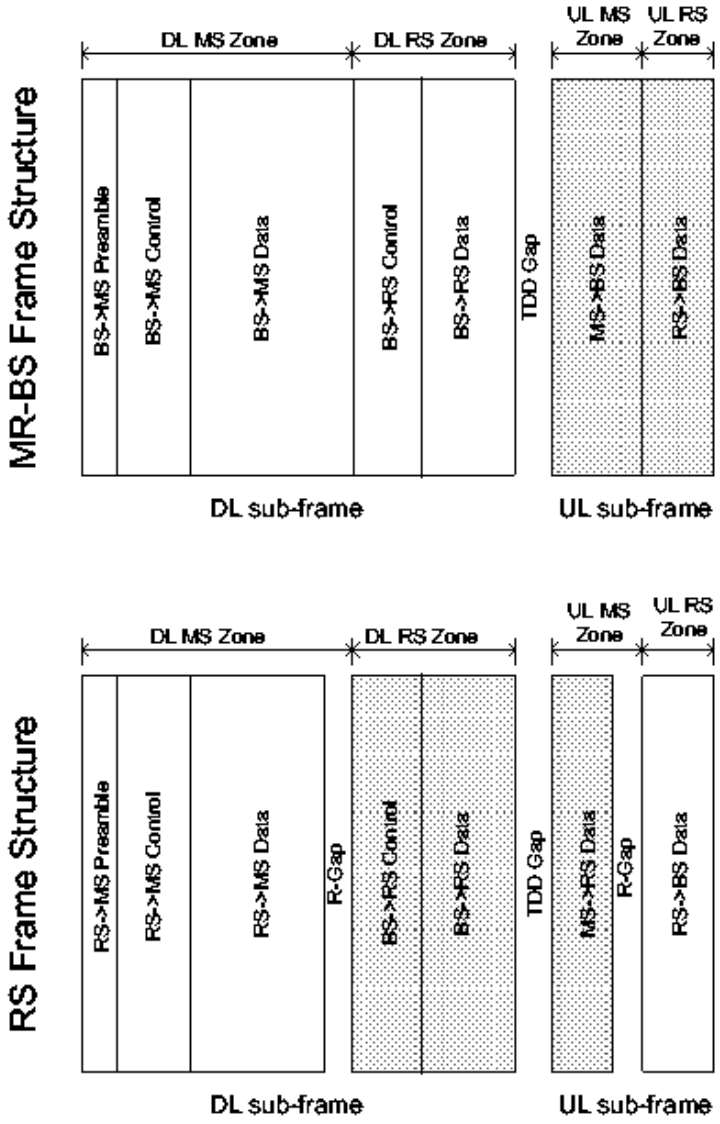

Figure 2.1. 802.16j Frame Structure in TDD OFDMA PHY mode.

in this figure. In general, the width of this zone can vary and should be optimized with respect to a given topology and user load.

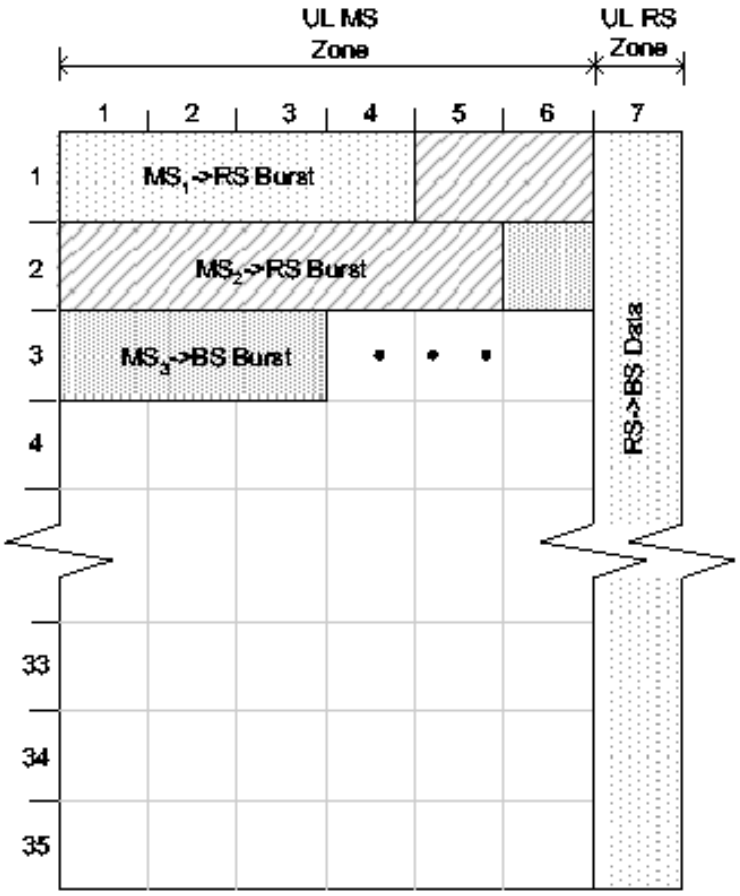

Figure 2.2. Detailed view of the UL subframe.

Within the UL MS zones at the BS and RS, bursts transmitted to the BS or RS are assigned to different time/frequency slots orthogonally by a centralized scheduler at the BS. Similar to the 802.16e UL slot allocation scheme, bursts are mapped to slots time-wise first, before wrapping to the next frequency slot if the zone boundary is reached. Furthermore, the 802.16e specification defines a randomized UL frequency-hopping scheme for interference randomization. In order to capture this effect in the simulator, all burst-to-slot assignments in the MS zone are randomly permuted prior to calculating interference.

Note in Fig. 2.2 that the overhead associated with UL control signaling is not modeled. In addition, it is assumed that the BS and the RS are synchronized, and bursts destined to the BS and RS are properly time-advanced to their respective receivers. However, since the BS and the RS are not colocated, a burst destined to the RS is not properly time-advanced to the BS, potentially resulting in interference. For simplicity, in the current simulation results the effects of mismatched time advances at the BS and the RS are assumed negligible and the resulting inter-burst interference is not modeled.

2.2. System Analysis with 1-D Model

To obtain an initial assessment of capacity gains attainable with a relay-enhanced system, we investigate the following one-dimensional model of a cellular system (See Fig. 2.3). The RS is placed at distance d from the BS. As in [**127, 15, 16**], we assume a set of static MSs, which are uniformly and continuously distributed along the line with density ρ. In addition, we consider a Voice-over-IP (VoIP) traffic model, in which all active MSs transmit a voice packet of equal size within the UL subframe. A similar model can be developed for data traffic. In the system simulation in Section 2.5, results for both data and voice traffic are presented.

First, we consider a legacy 802.16e system with no RS deployment. Due to symmetry, it is sufficient to consider the set of MSs on one side of the BS. Under a VoIP traffic model, maximizing system capacity is equivalent to maximizing the number of active MSs for a given UL subframe duration. Assuming a path-loss of $1/r^a$, where a is the path-loss exponent, the bandwidth $w(r)$ needed for a MS at distance r to transmit a voice packet

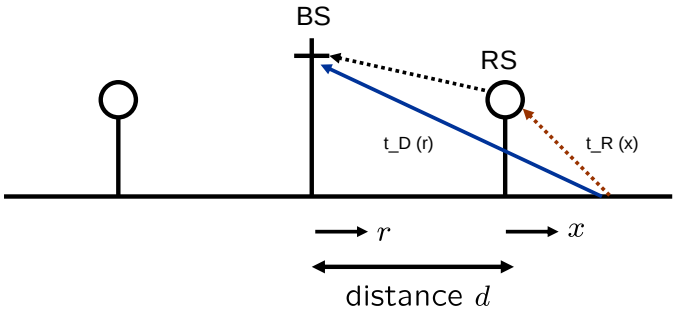

Figure 2.3. One-dimensional model of a cell with relay stations (RSs).

of size L bits during the UL subframe duration T_{UL} satisfies

$$L = w(r) \cdot \log_2 \left(1 + \alpha \frac{P_u}{N_0 w(r) r^a}\right) \cdot T_{\mathrm{UL}}, \tag{2.1}$$

where N_0 is the noise density and α is the SNR degradation factor due to various channel and receiver impairments. We assume that each MS spreads its transmission power P_u over the bandwidth $w(r)$ uniformly. Here we abstract the 802.16e resource allocation described in Section 2.1 by assuming that all bursts take up the entire subframe duration T_{UL}. Furthermore, the bursts can be allocated arbitrarily small bandwidth, instead of restricting allocations in frequency to the granularity of an OFDMA slot as in Section 2.1. Since $w(r)$ increases monotonically as r increases, the maximum number of MSs that the BS can support within the UL subframe duration is given by $\rho \cdot |\mathcal{C}_0|$, where $|\mathcal{C}_0|$ is the length of the interval containing the active MSs and satisfies $\int_0^{\mathcal{C}_0} \rho \cdot w(r)\, dr = W$, where W is the total bandwidth of the system.

Next consider a relay-enhanced system. We assume that a MS transmits a packet to *either* the BS *or* the RS. Simultaneous transmission to both are not considered. If the RS receives a packet from the MS, it relays to the BS within the UL RS zone, as shown

in Fig. 2.2. To satisfy the flow conservation constraint, the RS-to-BS link capacity should be high enough to accommodate all the voice traffic received by the RS in the UL MS zone. Given uniform MS density ρ, the maximization of the total number of active MSs is equivalent to finding the region of the active MSs, $\mathcal{C}$, namely,

$$\max_{\mathcal{C}} \rho \cdot |\mathcal{C}|, \tag{2.2}$$

subject to the total bandwidth and flow conservation constraints. Here, $|\cdot|$ denotes the length of the corresponding region, where the region may consist of a set of disjoint intervals. With the RS, the coverage set $\mathcal{C}$ can consist of two or more disjoint intervals $\mathcal{C}_d$ and $\mathcal{C}_r$, where $\mathcal{C}_d = \cup_i \mathcal{C}_{d,i}$ is the union of non-overlapping intervals corresponding to the MSs served directly by the BS and similarly, $\mathcal{C}_r$ corresponds to the MSs relayed by the RS [**16**].

To solve the optimization problem (2.2), we first assume that the BS allocates time γT_{UL} for the RS zone, and subsequently optimize over $\gamma \in [0, 1]$. With this assumption the constraints of the preceding optimization problem become

$$\int_{\mathcal{C}_d} \rho \cdot w_D(r)\, dr + \int_{\mathcal{C}_r} \rho \cdot w_R(x)\, dx \leq W, \tag{2.3}$$

$$\rho \cdot |\mathcal{C}_r| \leq \gamma T_{\mathrm{UL}} R_{\mathrm{RB}}/L, \tag{2.4}$$

where $w_D(r)$ ($w_R(x)$) is the bandwidth needed for a MS at distance r (x) from the BS (RS) to transmit during the UL MS zone duration $(1-\gamma)\cdot T_{\mathrm{UL}}$ and $R_{\mathrm{RB}} = W \cdot \log_2\left(1 + \alpha \frac{P_{\mathrm{RS}}}{N_0 W d^b}\right)$ is the capacity of the link between the RS and the BS. It is assumed that the path-loss

exponent $b \leq a$, as it is likely that the propagation conditions on the RS-to-BS link are less severe than that on the MS-to-RS link.

Instead of giving detailed proof of the optimization problem (2.2) with constraints (2.3) and (2.4), we present a graphical explanation, especially when γ is relatively small. It can be shown that $w_D(r)$ and $w_R(x)$ are increasing functions in r and x (See in Fig. 2.4). For given horizontal bar λ in Fig. 2.4, we assume that MSs who require the bandwidth for a voice packet of size L less than λ are served either by the BS or the RS. The idea for the solution of (2.2) is to serve MSs who need less bandwidth with higher priority. As λ increases from 0 to λ', MSs of the interval $[0, \bar{r}(\lambda')]$ are included in $\mathcal{C}_d$ and MSs in the interval $[-\bar{x}(\lambda'), \bar{x}(\lambda')]$ in $\mathcal{C}_r$. Here, λ' is obtained from the constraint (2.4) or

$$2\rho \cdot w_R(\lambda') = \gamma T_{UL} R_{RB}/L, \tag{2.5}$$

since we assume γ is small. As λ increases further from λ', the RS cannot support additional MSs and only the BS adds more MSs in $\mathcal{C}_d$ until the constraint (2.3) becomes tight. For example, suppose that the constraint (2.3) is tight with λ'' as shown in Fig. 2.4. Then, the interval for MSs served by the BS is given by $\mathcal{C}_d = [0, d-\bar{x}(\lambda')] \cup [d+\bar{x}(\lambda'), \bar{r}(\lambda'')]$. λ'' can be calculated from the constraint (2.3). Similarly, we can obtain the intervals of active users for all $\gamma \in [0, 1]$.

We give some numerical results to illustrate the capacity gains attainable with a relay-enhanced system. Fig. 2.5 shows the ratio of the total number of users with relaying to that without relaying as a function of γ. The UL subframe duration is $T_{\mathrm{UL}} = 2.2 \times 10^{-3}$ s, and the path-loss exponents are $a = 5.0$ and $b = 4.2$ (corresponding to Type A and Type C models in Section 2.3). In addition, the RS is located at $0.7 \times |\mathcal{C}_0|$. The remaining

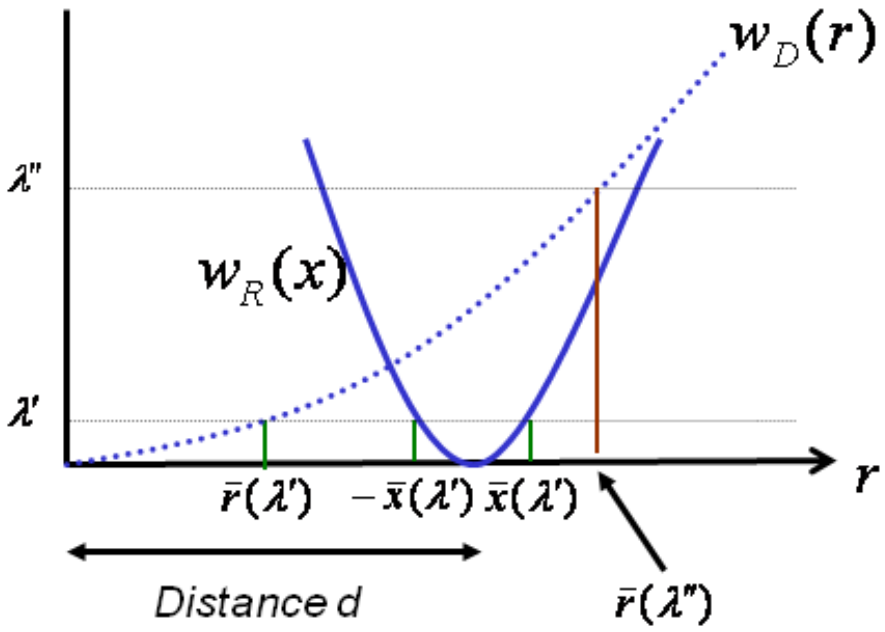

Figure 2.4. Graphical explanation of the optimization problem (2.2) assuming γ is small. In this example, the intervals of active MSs are given by $\mathcal{C}_r = [-\bar{x}(\lambda'), \bar{x}(\lambda')]$ and $\mathcal{C}_d = [0, d - \bar{x}(\lambda')] \cup [d + \bar{x}(\lambda'), \bar{r}(\lambda'')]$.

parameters are indicated in the caption. The maximum gain with the RS is approximately 60% to 65% at $\gamma \approx 0.17$ to 0.3 depending on MS density. These gains are relatively insensitive to variations of ρ over a wide range (from 40 users per km to 70 users per km).

2.3. System Simulation Setup

The preceding analysis provides a first indication of the potential capacity gains to be achieved with a relay deployment. The analysis only considers a single-cell linear model of a cellular system. In practice, cellular systems are deployed in two-dimensional uneven terrain exhibiting various propagation impediments and giving rise to shadow loss and fast fading phenomena. A system analysis, taking into account these propagation effects

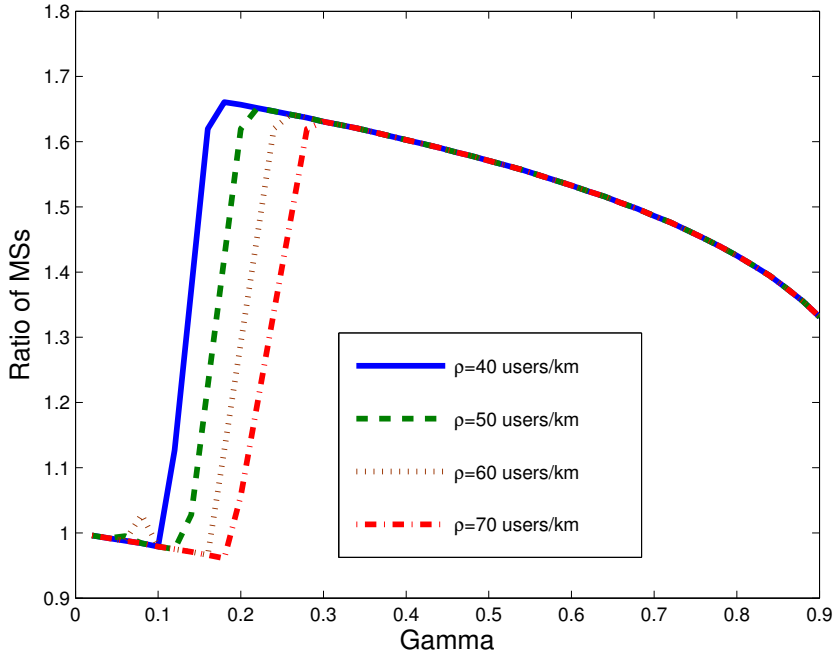

Figure 2.5. Ratio of the total number of users served with and without the RS as a function of γ. The voice packet length is $L = 544$ bits including overhead, $N_0 = -174\,\text{dBm/Hz}$ and $\alpha = 0.3981$, $P_u = 23\,\text{dBm}$, and $P_{RS} = 33\,\text{dBm}$. The antenna gain for the MS-BS and MS-RS links is assumed to be $+10\,\text{dB}$, and that for RS-BS link is $+25\,\text{dB}$.

is largely intractable, and we resort to system simulations to characterize performance of the RS deployment in such a setting.

A custom multihop cellular system simulator capable of modeling various aspects of the relay deployment has been developed. More specifically, the simulator includes the following features:

(1) Correlated shadow loss model,

(2) Resource allocation procedure with the granularity of an OFDMA slot,

(3) Multi-sector per-slot interference calculations,

(4) Power control and scheduling procedures as detailed below,

(5) Models for both VoIP and data traffic.

The simulator models a service area covered by a grid of hexagonal cells. A BS is placed at the center of every cell with sectorized antennas, and a certain number of the RSs per sector are placed uniformly at the same distance from the BS. The RS is assumed to be less complex than the BS, but capable of performing decode-and-forward operations.

Fig. 2.6 shows a typical cell layout that we consider with our system simulator. In this example, a 3-sector deployment with two RSs per sector is depicted. Each RS is deployed at fraction a of the cell radius away from the BS. Note that identical positioning of RSs in all cells creates a regular topology with colinear RSs and BSs. If a narrow-beam, high-gain directional antenna is installed at a RS pointing toward its serving BS, transmissions from this RS may create significant interference at other RSs and BSs that are colinear with it. To mitigate this situation and to better reflect a realistic deployment scenario, RSs in each cell, after being uniformly placed on a circle around the serving BS, are rotated by a random angle drawn from a uniform distribution with finite support $[-\frac{\pi}{k}, \frac{\pi}{k}]$, where k is the number of relays per cell.

2.3.1. Path-loss and Shadow loss

The simulator separately models path-loss on the MS-to-BS, MS-to-RS, and RS-to-BS links. The particular path-loss models used in this paper are defined by the IEEE 802.16j TG in document [**99**]. The document defines three terrain types for suburban macro-cell: Hilly with moderate to heavy tree densities (Type A), intermediate path-loss condition (Type B), and flat terrain with light tree densities (Type C). For the results reported

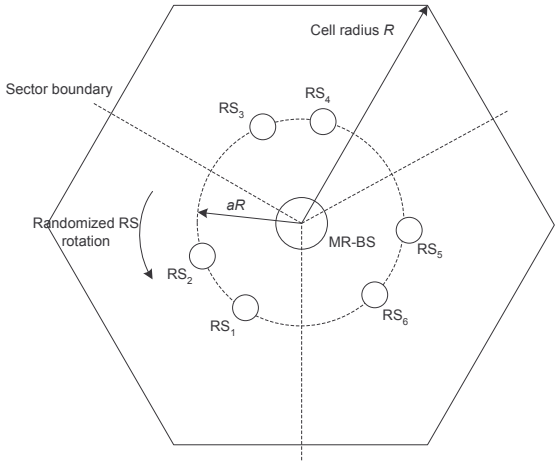

Figure 2.6. Example of a cell layout in the simulator.

here, Type A terrain profile is used for the MS-to-BS and MS-to-RS links and Type C terrain profile for the RS-to-BS links. For details of the path-loss calculations, refer to [**99**].

In addition, the system simulator creates a system-wide grid, which is used to evaluate shadow loss for a particular path. A decorrelation distance and log-normal standard deviation are specified as input parameters. When shadow loss calculations are performed during a simulation run, the resulting values are spatially correlated and repeatable. The technique used for shadow loss calculations is described in [**89**].

2.3.2. Spectrum Reuse

A number of different spectrum reuse strategies can be supported in IEEE 802.16e/j deployments. A single spectrum reuse plan is selected for this study. It is assumed that all cells are deployed on a single carrier (10 MHz BW) and every sector of every cell of the system utilizes the available BW. For a three-sector system this is usually denoted

as a 1/3/1 reuse plan. Therefore, each sector has 245 OFDMA slots available for UL as explained in section 2.1.

2.3.3. Antenna Configuration

A 3-sector antenna configuration is considered at the BS. Sector antennas are assumed to be ideal in the sense that antenna gain as a function of azimuth angle has a "brick wall" characteristic with a front lobe width of the antenna pattern of 120°. An MS is presumed to have an omni-directional antenna. An RS is equipped with both an omni-directional antenna used for the MS-to-RS communication and a directional antenna used for the RS-to-BS communication with 20° front lobe width. A front-to-back ratio of +25 dB is used for all antenna patterns.

2.4. Resource Allocation for Relay-Enhanced Uplink

2.4.1. MS Link Models

The MS-to-BS and MS-to-RS link models for the data traffic are obtained in the form of link spectral efficiency (information bits per subcarrier) as a function of the receiver SINR. A link simulator is constructed to obtain an estimate of the attainable spectral efficiency on the MS-to-BS and MS-to-RS links in fading channel conditions. The simulator assumes an infinitely backlogged data source and an N-channel stop-and-wait HARQ protocol at the link-layer, thus closely modeling the 802.16e UL specifications.

For VoIP, a certain maximum packet error rate requirement is assumed (1% for the results in this paper). Given this requirement, SINR thresholds are determined, based on link-level simulations, for a discrete set of modulation and coding schemes (MCSs)

supported by link adaptation procedures on the 802.16e UL MS link. Specifically, a set of MCSs with the following spectral efficiencies is considered: 1/4, 1/2, 1, 2, and 3 information bits per subcarrier. These SINR thresholds are used in the VoIP scheduler.

2.4.2. RS Link Model

The RS-BS link is not modeled in detail in the simulator. As in Section 2.2, the spectral efficiency achievable on that link, as a function of average SINR per subcarrier, is computed by

$$R_{\mathrm{RB}} = \log_2(1 + \alpha \times \mathrm{SINR}), \tag{2.6}$$

where R_{RB} denotes the number of information bits per subcarrier and α is a factor less than one accounting for the rate degradation. For the results in this paper, $\alpha = 0.3981\,(-4\mathrm{dB})$ is used.

2.4.3. VoIP Scheduler

The VoIP scheduler attempts to maximize the number of VoIP users served in the system. In particular, the scheduler iteratively searches for a resource allocation solution, where each user is assigned the most spectrally efficient MCS so that the required number of slots for the user's voice packet is minimized.

The scheduling procedure is initialized by assigning all users the MCS with maximum spectral efficiency (3 bits per subcarrier), and assigning the maximum transmit power. In each iteration of the scheduler, a user's link SINR is updated based on the desired and interferers' power settings from the previous iteration subject to the MS power constraint. Based on the updated SINR, the user is assigned the highest possible MCS such that

the user's link SINR is greater than or equal to the SINR threshold of the assigned MSC. A user is considered blocked if no MCS can be found satisfying the updated SINR condition or if the number of slots required for the assigned MCS is less than the number of unoccupied slots in the sector.

The VoIP scheduler enforces a flow conservation constraint at each RS, as discussed in Section 2.2. Namely, at a given RS, the number of VoIP users attached to that RS times the VoIP packet size must be less than the per-frame throughput of that RS's link to the BS. If this condition is violated, a number of users assigned to the RS are blocked until it is satisfied.

2.4.4. Data Scheduler

In the UL MS zone, the data scheduler allocates a *fixed number of OFDMA slots* to every user. The slots are allocated time-wise first, as in the example of Fig. 2.2, and then their positions are randomized throughout the UL MS zone. Following user slot assignment and randomization, interference calculations and iterative power control procedures are performed on the MS-to-RS and MS-to-BS links to attain target link SINRs, subject to the transmit power constraint at the MS. Note that due to randomization, each slot of a user allocation sees a different interference level and therefore different SINR. The link SINR is defined as the average of the per-slot SINRs.

Upon convergence of the iterative power control procedure, the attained link SINRs are mapped to the link spectral efficiencies obtained for the data traffic model. The per-user link throughput (per frame) is then simply computed as the size of slots allocated to the user times the link spectral efficiency. Similar calculations are performed to obtain

throughput on the RS-to-BS links. Again, the flow conservation constraint at all RSs should be satisfied. The scheduler checks at each RS whether this constraint is violated and if so reduces the throughput on all MS-to-RS links by a faction, so that the constraint is met with equality.

2.5. Simulation Results in Uplink Capacity

2.5.1. VoIP Capacity Results

An 8 kbps voice coder, a 20 ms voice frame duration, and a 40 Byte IP/RTP/UDP header are assumed, resulting in a VoIP packet size of 544 bits including MAC header. Voice activity detection is not considered. The VoIP capacity results are shown in Fig. 2.7. In this case, the UL sub-frame is split into 4 time slots devoted to the MS zone and 3 time slots to the RS zone. This UL subframe split is consistent with the split value analytically predicted in Section 2.2. The curves in Fig. 2.7 display VoIP call blocking probability as a function of user load per cell. For example, 802.16e system supports about 140 VoIP users at 5% blocking probability. On the other hand, about 190 (360) users are supported with one RS (two RSs) per sector. Therefore, a significantly higher user load can be accommodated by the relay-enhanced system. The system capacity is expected to grow with increasing number of RSs deployed per sector.

It is interesting to compare these results with capacity gains analytically predicted in section 2.2 for a one-dimensional system. The capacity gain 65% from 1-D analysis is in the range shown in Fig. 2.7 (between 35% gain with one RS and 100% gain with two RS). The higher capacity gain in the simulation could be partially due to the fact that with uniformly distributed users over the cell area, more users are concentrated around

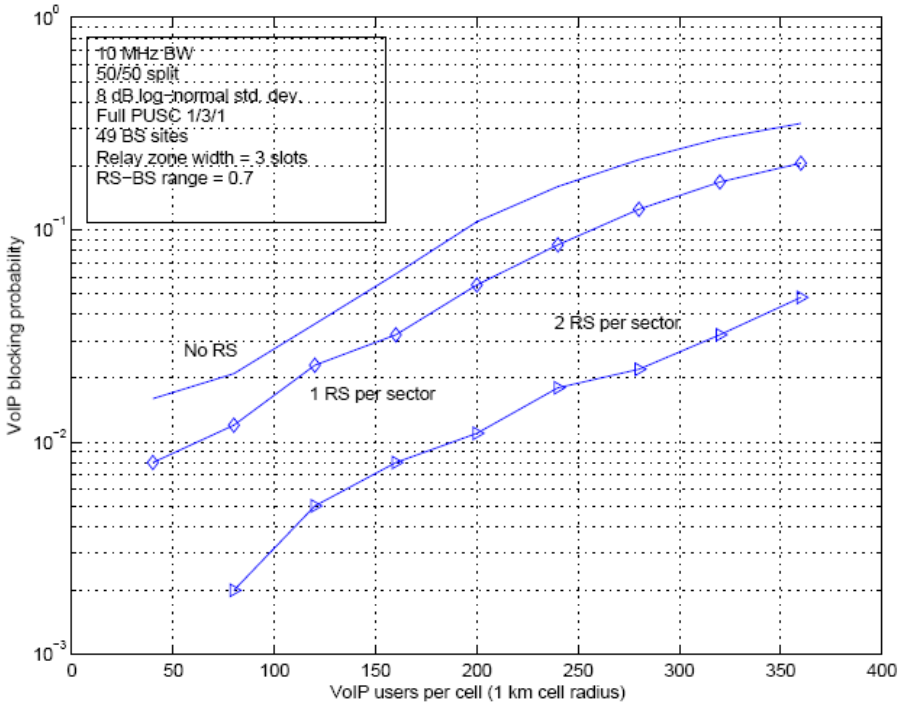

Figure 2.7. Blocking probability vs. the number of users per cell for voice traffic.

each RS in two dimensions than in one dimension. In addition, relay deployment is more beneficial in a system exhibiting shadow loss effects. Recall that the analysis in Section 2.2 does not take shadow losses into account.

2.5.2. Data Capacity Results

The data capacity results are displayed in Fig. 2.8. The plot displays sum throughput per base site as a function of the number of MSs randomly dropped in a cell. The cell radius of 1 km is used. Throughput is displayed with no RS, 1 RS, 2 RSs deployed per sector. The 'No RS' curve corresponds to the performance of the 802.16e UL, with all 245 OFDMA slots available for scheduling MS-to-BS bursts. The remaining two curves

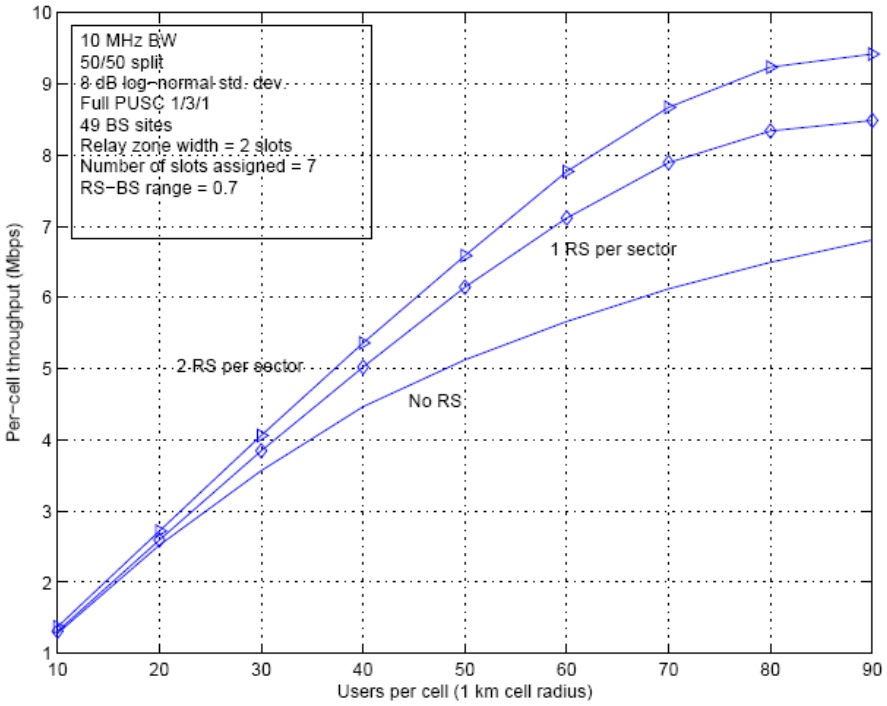

Figure 2.8. Per-cell throughput vs. the number of users per cell for data traffic.

characterize the performance of the 802.16j uplink, with 5 slots in the time dimension devoted to the UL MS zone and 2 slots to the UL RS zone. This particular split of the UL subframe is determined via simulations to result in the highest cell throughput. The data scheduler assigns 7 OFDMA slots per user in the UL MS zone. Power control thresholds of 19 dB for the MS-to-BS and MS-to-RS link and 24 dB for the RS-to-BS link are empirically determined for the highest cell throughput and used in the simulations. As seen in Fig. 2.8, RS deployment with 2 RSs per sector provides a significant capacity gain at higher user loads. For example, when there are 70 users per cell, the per-cell throughput increases about 40 % from 6.1 Mbps with no RS to more than 8.5 Mbps with two RSs.

2.6. Parametric Cost Analysis of Relay Deployment

For conciseness, cost-benefit analysis of the relay deployment is performed for VoIP capacity results only. To capture the trade-off of increased network capacity with the RS deployment versus costs of RS installation and maintenance, the following metric of the network cost per user is proposed:

$$C_k = \frac{c_b + kc_r}{N_k}, \tag{2.7}$$

where c_b denotes a BS cost, including *backhaul*, installation, maintenance and hardware; c_r denotes an RS cost, including installation, maintenance and hardware, but *no backhaul cost*; k denotes the number of RS deployed per cell; finally, N_k denotes the number of VoIP users at capacity accommodated with k RS per cell. Note that C_0 denotes the normalized cost per user of the 802.16e system.

To gauge cost-effectiveness of the RS solution, the following ratio is of interest:

$$R \equiv \frac{C_0}{C_k} = \frac{N_k}{N_0} \frac{1}{1 + k\frac{c_r}{c_b}}. \tag{2.8}$$

Clearly, the RS deployment is cost-effective if the ratio R is greater than unity. Specific to the simulation results in this paper, with $N_0 \approx 144$ and $N_6 \approx 360$ (corresponding to 5% blocking probability in Fig. 2.7), it readily follows that $R \geq 1$ implies the normalized cost of the RS relative to that of the BS needs to satisfy $\frac{c_r}{c_b} \leq 0.25$.

2.7. Chapter Summary

We have investigated through both analysis and simulations the capacity gains attainable with a relay-enhanced wideband cellular system. Our results show that UL capacity

for both data and VoIP traffic increases significantly when RSs are deployed in the system (more than 40% gain for data and 100% gain for voice with two RSs). However, these gains are realized at the cost of relay deployment in the system. Our cost analysis attempts to capture this trade-off and indicates that the relay-enhanced cellular system is economically viable only when the cost of the RS is relatively small (less than 25%) compared to that of the BS. As the hardware and installation costs of the RS and BS are expected to be similar, the cost of backhaul emerges as the primary factor driving the cost effectiveness of 802.16j deployments, and relay-enhanced cellular systems in general.

CHAPTER 3

Power Allocation for Relay-Assisted Downlink Transmission

Relay extensions for cellular networks were studied in the previous chapter along with a simple cost analysis. Due to the success and the popularity of Wi-Fi WLANs, we turn our attention to the relay extension of cellular networks using Wi-Fi access points (APs) as the relays. There are many possible network scenarios depending on the relationship between the base stations (BSTs) and APs. For example, if the BST and AP are non-cooperative, bargaining can be used to share the AP resources for relaying traffic to and from the BST. In this chapter, however, we assume that APs cooperative with the BST, and willingly share their resources to maximize the social welfare (sum utilities of both BST and AP users).

Specifically, we focus on power allocation across the BST and AP for downlink transmissions in a relay-assisted cellular network. We consider a single cell with two relays (AP nodes), and a static user population, and optimize the allocation of power across cellular and AP users, in addition to the BST-AP link. We then study the corresponding increase in rate and coverage provided by sharing AP resources. In contrast to previous work (e.g., [**80, 125, 118**]) in which all AP resources are available to the BST, here we assume that the APs are serving a separate group of (non-cellular) users. Hence serving as a relay for cellular users requires the AP to reduce the amount of power allocated to serving its own users.

To obtain insight into the effect of the relay on power and rate allocations, we consider a one-dimensional model in which cellular users are uniformly distributed along a line. Two relay nodes are placed symmetrically on either side of BST, and serve a separate set of users, which are uniformly distributed around the relay. This corresponds to the large system model presented in the last chapter and in [**127**]. All users (both cellular and AP) are assumed to be orthogonal in time, frequency, and/or signature space, and do not interfere. Furthermore, the AP is assumed to use a different band from the cellular band, so that cellular users do not interfere with non-cellular users. Also, here we consider only the power allocation problem subject to a total power constraint. We assume that each user receives a single unit of bandwidth (i.e., channel, time slot, or signature), and that the total number of users does not exceed a bandwidth constraint. Finally, in the model considered path loss is determined only by distance. Random propagation effects, such as shadowing, are not explicitly modeled, but can be incorporated in the model by changing the distance metric.[1]

For the one-cell model, we wish to allocate available BST and AP power across *both* cellular and AP users, and from the BST to the AP, to maximize the total sum rate over all users for *data traffic*, or to maximize the total number of active users for *voice traffic*. We solve this problem for the following two scenarios: (i) the information flows to the cellular users served by the relay are jointly encoded and transmitted from the BST to the AP; and (ii) the preceding information flows are transmitted in parallel (separately encoded) from the BST to the AP. Joint encoding requires less power to transmit the data destined for relayed users from the BST to the AP, but requires that the received data at

[1]This change in distance metric effectively amounts to changing the distribution of users along the line.

the AP be demultiplexed. We also give an upper bound on the increase in total sum rate (data traffic) or in total number of users (voice traffic) provided by the AP, based on the scenario in which the AP and BST have a wireline connection, so that the BST does not expend any power to communicate with the AP.

3.1. System Model

The one-dimensional cellular model is illustrated in Fig. 3.1. We assume a symmetric cell in which two APs are placed at the same distance d from the BST. As in [**127**], we assume a static set of users, which are uniformly and continuously distributed along the line. The density of the cellular users, served by the BST, is ρ_B, and the density of the AP users is ρ_A. This corresponds to a large system limit in which the number of users in the system tends to infinity in proportion with the available bandwidth (i.e., fixed users per Hz). Given a finite total power constraint, the BST and AP each serve a finite number of users. In what follows, we assume that each active user receives a fixed unit of bandwidth, and that the corresponding number of available channels (and/or time slots and/or signatures) exceeds the total number of active users.

We consider two different types of traffic for downlink transmission: data and voice. For data traffic, the BST and the AP allocate the transmission power to maximize the total sum rate over all users (both cellular and AP users) ignoring fairness considerations. For voice traffic, on the other hand, each user requires a certain fixed data rate, and the BST and AP allocate the transmission power to maximize the total number of active users.

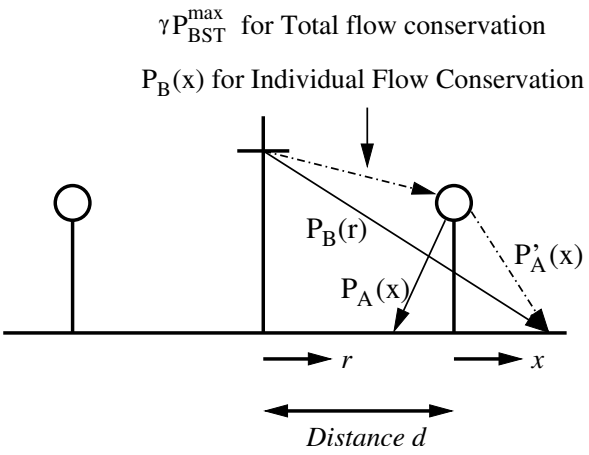

Figure 3.1. One-dimensional model of a cell with relay nodes (APs) placed at the same distance from the BST. Depending on the flow conservation between the BST and the AP, the power allocations at the BST are different.

3.1.1. Data Traffic

We first consider the situation in which the BST does not use the AP as a relay. From symmetry, we only need to consider the power allocation and set of active users on one side of the BST. Suppose that the BST transmits to a cellular user at distance r with power $P_B(r)$. Assuming a path loss of $1/r^a$, where a is the path-loss exponent, the received Signal-to-Noise Ratio (SNR) is $\frac{P_B(r)}{N_0 W_B r^a}$, where N_0 is the noise density, and W_B is the cellular bandwidth/user. We further assume optimal coding, so that the corresponding rate is $W_B \log\left(1 + \frac{P_B(r)}{N_0 W_B r^a}\right)$. Similarly, the AP transmits to an AP user at distance x with power $P_A(x)$, and the corresponding received rate is $W_A \log\left(1 + \frac{P_A(x)}{N_0 W_A x^a}\right)$, where W_A is the AP bandwidth/user.

We wish to select $P_B(r)$ and $P_A(x)$ to maximize the total transmission rate summed over all users, i.e.,

$$\begin{aligned}\max_{\{P_B(r),P_A(x)\}} &\int \rho_B W_B \log\left(1+\tfrac{P_B(r)}{N_0 W_B r^a}\right) dr \\ &+ \int \rho_A W_A \log\left(1+\tfrac{P_A(x)}{N_0 W_A x^a}\right) dx,\end{aligned} \tag{3.1}$$

subject to total power constraints

$$\int \rho_B P_B(r)\, dr \le P_{BST}^{max}, \tag{3.2}$$

$$\int \rho_A P_A(x)\, dx \le P_{AP}^{max}. \tag{3.3}$$

Note that the total number of active users served by the BST and AP, and hence the total bandwidth, depends on the total powers P_{BST}^{max} and P_{AP}^{max}.[2]

The optimal power allocations for the preceding problem are determined by water-filling, i.e.,

$$P_B(r) = N_0 W_B (r_{B0}^a - r^a)^+, \qquad r \in [0, r_{B0}], \tag{3.4}$$

$$P_A(x) = N_0 W_A (x_{A0}^a - x^a)^+, \quad x \in [-x_{A0}, x_{A0}], \tag{3.5}$$

where $r_{B0} = (\frac{a+1}{a}\frac{P_{BST}^{max}}{N_0 W_B \rho_B})^{\frac{1}{a+1}}$ is the BST coverage radius, $x_{A0} = (\frac{a+1}{2a}\frac{P_{AP}^{max}}{N_0 W_A \rho_A})^{\frac{1}{a+1}}$ is the AP coverage radius, and $(x)^+ = \max(x, 0)$. Here, we assume $x_{A0} \le d$. The coverages of the BST and AP obtained by water-filling are shown in Fig. 3.2. The total rates supported by the BST and the AP summed over their own users (first and second terms in (3.1))

[2]The total BST power for users on both sides of the BST is then $2 \cdot P_{BS}^{max}$.

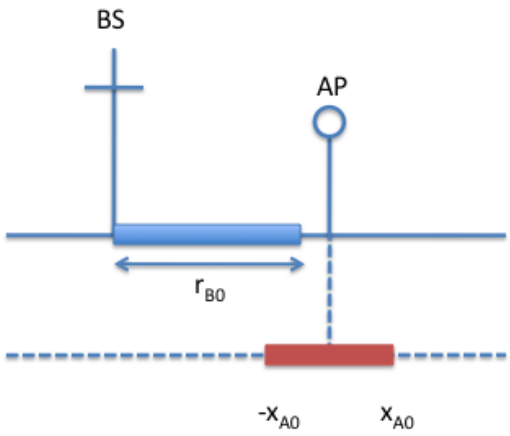

Figure 3.2. Coverage of the BST and AP by water-filling. One-sided coverage of the BST is $[0, r_{B0}]$ and coverage of the AP is $[-x_{A0}, x_{A0}]$.

are

$$R_{B0} = a\,\rho_B W_B\, r_{B0}, \tag{3.6}$$

$$R_{A0} = 2a\,\rho_A W_A\, x_{A0}, \tag{3.7}$$

and the sum rate over all users on one side of BST is, therefore, $R_0 = R_{B0} + R_{A0}$.

Now we consider the case where the BST uses the AP to relay data. We assume that a cellular user can receive data *simultaneously* from the BST and the AP.[3] The relay poses an additional *flow* constraint, namely, the total rate that the AP provides to the cellular (relayed) users must be the same as the total rate it receives from the BST. The channel between the BST and the AP is also assumed to be orthogonal to those used by the BST

[3]Although splitting data streams in this manner is more complicated than receiving data from either the BST or the AP, this assumption simplifies the power allocation problem, and gives an upper bound on the performance when data streams are not split.

and the AP. The power allocation problem then becomes

$$\begin{aligned}\max_{\{P_B(r),P'_A(x),P_A(x)\}} &\int \rho_B W_B \log\left(1+\tfrac{P_B(r)}{N_0 W_B r^a}\right) dr \\ &+ \int \rho_B W_A \log\left(1+\tfrac{P'_A(x)}{N_0 W_A x^a}\right) dx \\ &+ \int \rho_A W_A \log\left(1+\tfrac{P_A(x)}{N_0 W_A x^a}\right) dx\end{aligned} \tag{3.8}$$

subject to the power and flow conservation constraints, where $P'_A(x)$ is the power allocated by the AP to a cellular user at distance x from the AP. That is, a cellular user at distance r from the BST ($x = r - d$ from the AP) may receive positive power allocations $P_B(r) > 0$ and $P'_A(x) > 0$, corresponding to splitting the data stream between the direct path from the BST and the relay path.

3.1.2. Voice Traffic

Because each active user receives a certain target rate for voice service, our objective is to maximize the number of active users for a given power constraint. As in section 3.1.1, we first study the case where the BST does not use the AP as a relay. The power needed to transmit at rate R_B to a cellular user at distance r is $P_B(r) = N_0 W_B\big(e^{\frac{R_B}{W_B}} - 1\big) r^a \equiv B r^a$. The maximum number of cellular users that the BST can support with power P_{BS}^{max} is then $\rho_B|\mathcal{C}_0|$, where $\mathcal{C}_0$ is the one-sided interval containing the active users and satisfies $\int_0^{\mathcal{C}_0} \rho_B P_B(r) dr = P_{BS}^{max}$, i.e.,

$$\mathcal{C}_0 = \left(\frac{a+1}{\rho_B B} P_{BS}^{max}\right)^{\frac{1}{a+1}}. \tag{3.9}$$

Here, $|\cdot|$ denotes the size (i.e. Lebesgue measure) of the corresponding region.

Similarly, assuming non-cellular and cellular users have the same path-loss exponents, the minimum power needed by the AP to transmit at rate R_A to a user at distance x is $P_A(x) = N_0 W_A\big(e^{\frac{R_A}{W_A}} - 1\big)x^a \equiv Ax^a$. The maximum number of non-cellular users that the AP can support with power P_{AP}^{max} is therefore $2\rho_A|\mathcal{D}_0|$, where $\mathcal{D}_0 = (\frac{a+1}{\rho_A A}\frac{P_{AP}^{max}}{2})^{\frac{1}{a+1}}$ is the one-sided AP coverage (i.e., for users at distance $d + x$, with $x \geq 0$).[4] Therefore, without relaying, the total number of active cellular and non-cellular users (on one side of the BST) is $\rho_B|\mathcal{C}_0| + 2\rho_A|\mathcal{D}_0|$.

Now we consider the case where the BST uses the AP to relay voice traffic to cellular users. We assume that a cellular user receives data either from the BST directly or through AP, but *not simultaneously*.[5] With target rates R_B and R_A for BST and AP users, respectively, the power allocation problem is then to maximize the total number of BST and AP users served, namely,

$$\max_{\{\mathcal{C},\mathcal{D}\}} \rho_B|\mathcal{C}| + 2\rho_A|\mathcal{D}|, \tag{3.10}$$

subject to the power and flow conservation constraints. Here, $\mathcal{C}$ and $\mathcal{D}$ are the regions of active cellular and non-cellular users, respectively. It can be easily shown that $\mathcal{D}$ is always a single connected interval. However, since each cellular user can receive data from either the BST or the AP, the cellular coverage set $\mathcal{C}$ can consist of two or more disjoint intervals $\mathcal{C}_d$ and $\mathcal{C}_r$, where $\mathcal{C}_d = \cup_i \mathcal{C}_{d,i}$ is the union of non-overlapping intervals corresponding to the direct (non-relayed) cellular users and similarly, $\mathcal{C}_r$ corresponds to the relayed users.

[4]Note we are assuming that the AP coverage region is symmetric about the AP location. This will only be the case if $|\mathcal{D}_0| \leq d$, which implies $P_{AP}^{max} \leq 2\frac{\rho_A A}{a+1}d^{a+1}$. Otherwise the coverage would be bounded on the left at zero (since the other users would be covered by the AP to the left of the BST).

[5]This is in contrast to the model for data service considered in section 3.1.1 where the BST and AP can simultaneously transmit to a cellular user.

We assume that $\mathcal{C}_r$ is one (connected) segment for simplicity even though it might not be optimal.

3.1.3. Joint Coding vs. Individual Coding

We investigate two different techniques for coding the streams transmitted from the BST to the AP for the relayed users. *Joint coding* assumes that the BST jointly encodes all of the data destined for relayed users, and transmits the resulting stream to the AP. The AP then decodes and demultiplexes the individual data flows. In that case, the total rate from the BST to the AP is equal to the sum rate of the flows from the AP to relayed users. In the second technique, *individual coding*, data flows, which are to be relayed by the AP, are transmitted in parallel from the BST to the AP. The AP then decodes the packets for each data flow separately. Hence the code rate used by the BST to transfer the data to the AP is the same as that used by the AP to transmit to the relayed user. Joint coding generally requires less power for the BST-AP link than individual coding, but is more complex, since the relayed users must be multiplexed at the BST and demultiplexed at the AP.

3.2. Data Traffic

3.2.1. Joint Coding

The BST aggregates and jointly encodes the data destined for relayed users, and transmits this to the AP. The rate optimization problem is then to maximize (3.8) subject to

$$\int \rho_B P_B(r)\, dr + \gamma P_{BST}^{max} \leq P_{BST}^{max}, \tag{3.11}$$

$$\int \rho_A P_A(x)\, dx + \int \rho_B P'_A(x)\, dx \leq P_{AP}^{max}, \tag{3.12}$$

$$\begin{aligned} &W_{BA} \log\left(1 + \tfrac{\gamma P_{BST}^{max}}{N_0 W_{BA} d^b}\right) \\ &\quad = \int \rho_B W_A \log\left(1 + \tfrac{P'_A(x)}{N_0 W_A x^a}\right) dx, \end{aligned} \tag{3.13}$$

where W_{BA} is the bandwidth between the BST and the AP, and γP_{BST}^{max}, where $\gamma \in [0, 1]$, is the BST power allocated to the relay channel. Also, the path-loss exponent between the BST and the AP is b, which can differ from the direct path-loss exponent a. That is, through proper placement of the AP, it may be the case that $b < a$. The first and second constraints are the total power constraints for the BST and the AP, respectively. The last constraint is for the aggregate flow rate conservation.

To solve this optimization problem, we decompose it into two separate optimization problems. Namely, we first assume that the AP allocates power αP_{AP}^{max}, to relayed users, where $\alpha \in [0, 1]$, and subsequently optimize over α. With this assumption the problem decomposes into two independent power allocation problems for the BST and AP. Namely, the AP problem is

$$\textbf{AP:} \max_{\{P_A(x)\}} \int \rho_A W_A \log\left(1 + \tfrac{P_A(x)}{N_0 W_A x^a}\right) dx \tag{3.14}$$

subject to

$$\int \rho_A P_A(x)\, dx \leq (1-\alpha) P_{AP}^{max} \tag{3.15}$$

and the BST problem is

$$\begin{aligned} \textbf{BST:} \max_{\{P_B(r), P'_A(x)\}} & \int \rho_B W_B \log\left(1 + \tfrac{P_B(r)}{N_0 W_B r^a}\right) dr \\ & + \int \rho_B W_A \log\left(1 + \tfrac{P'_A(x)}{N_0 W_A x^a}\right) dx \end{aligned} \tag{3.16}$$

subject to (3.11), (3.13), and

$$\int \rho_B P'_A(x)\, dx \leq \alpha P_{AP}^{max}. \tag{3.17}$$

The optimum power allocation for the AP problem is water-filling and the total rate is $R_A(\alpha) = 2a\,\rho_A W_A x_A(\alpha)$, where $x_A(\alpha) = \left(\frac{a+1}{2a}\frac{(1-\alpha)P_{AP}^{max}}{N_0 W_A \rho_A}\right)^{\frac{1}{a+1}}$ is the AP coverage radius for its own users. If the portion of the BST power allocated to the relay, γ, is fixed, then for the BST problem the optimal $P_B(r)$ and $P'_A(x)$ at the BST and the AP, respectively, are also water-filling distributions. Therefore, the BST problem reduces to finding the $\gamma^*(\alpha)$, which maximizes the total rate from the BST, i.e.,

$$\begin{aligned} \max_{\gamma} R_B(\alpha, \gamma) = & \, a\,\rho_B W_B\, r_B(\gamma) \\ & + \min\left\{ W_{BA} \log\left(1 + \tfrac{\gamma P_{BST}^{max}}{N_0 W_{BA}\, d^b}\right), 2a\,\rho_B W_A\, x_R(\alpha) \right\}, \end{aligned} \tag{3.18}$$

where $r_B(\gamma) = \left(\frac{a+1}{a}\frac{(1-\gamma)P_{BST}^{max}}{N_0 W_B \rho_B}\right)^{\frac{1}{a+1}}$ is the coverage radius of the BST for direct transmissions, and $x_R(\alpha) = \left(\frac{a+1}{2a}\frac{\alpha P_{AP}^{max}}{N_0 W_A \rho_B}\right)^{\frac{1}{a+1}}$ is the coverage radius for relayed users measured from the AP. Since the total rate for relayed users from the BST to the AP, $W_{BA} \log\left(1 + \frac{\gamma P_{BST}^{max}}{N_0 W_{BA} d^b}\right)$, increases monotonically with γ, and is zero for $\gamma = 0$, the BST

rate simplifies to

$$\max_{\gamma\in[0,\gamma^\bullet]} R_B = a\,\rho_B W_B\, r_B(\gamma) + W_{BA}\log\Big(1+\tfrac{\gamma P_{BST}^{max}}{N_0 W_{BA} d^b}\Big), \tag{3.19}$$

where $\gamma^\bullet$ satisfies

$$W_{BA}\log\Big(1+\tfrac{\gamma^\bullet P_{BST}^{max}}{N_0 W_{BA} d^b}\Big) = 2a\,\rho_B W_A x_R(\alpha) \tag{3.20}$$

if the solution is in $[0,1]$. Otherwise, $\gamma^\bullet = 1$. Since R_B is a concave function of γ, it is straightforward to solve for the optimal value, $\gamma^*(\alpha)$, given α. Finally, joint optimization of the AP and BST power allocations is achieved by searching for the optimal $\alpha \in [0,1]$, i.e.,

$$\max_{\alpha}\ R = R_A(\alpha) + R_B(\gamma^*(\alpha)). \tag{3.21}$$

A relatively simple upper bound on the total transmission rate with the relay can be obtained by assuming that the BST does not require any power to transmit data flows to the AP, which are destined for relayed users. This might correspond to the situation in which the BST and AP are co-located, or are connected by a wired line. In that case, the BST serves cellular users with density ρ_B, and the AP serves both its users and cellular users together with density $\rho_B + \rho_A$. The total transmission rate is therefore

$$\begin{aligned} R^{WL} = {} & a\,\rho_B W_B\Big(\frac{a+1}{a}\frac{P_{BST}^{max}}{N_0 W_B \rho_B}\Big)^{\frac{1}{a+1}} \\ & + 2a\,(\rho_B+\rho_A) W_A\Big(\frac{a+1}{2a}\frac{P_{AP}^{max}}{N_0 W_A(\rho_B+\rho_A)}\Big)^{\frac{1}{a+1}}, \end{aligned} \tag{3.22}$$

and the relative rate increase is

$$\frac{R^{WL}}{R_0} = \frac{1+2(1+\frac{\rho_A}{\rho_B})^{\frac{a}{a+1}}(\frac{W_A}{W_B})^{\frac{a}{a+1}}(\frac{P_{AP}^{max}}{P_{BST}^{max}})^{\frac{1}{a+1}}}{1+2(\frac{\rho_A}{\rho_B})^{\frac{a}{a+1}}(\frac{W_A}{W_B})^{\frac{a}{a+1}}(\frac{P_{AP}^{max}}{P_{BST}^{max}})^{\frac{1}{a+1}}}. \tag{3.23}$$

If $\rho_A = \rho_B$, $W_A = W_B$, and $P_{AP}^{max} = P_{BST}^{max}$, then this becomes $R^{WL}/R_0 = (1 + 2^{\frac{2a+1}{a+1}})/3$, and for $a = 5$ this evaluates to a 52.1% gain from using the relay. If the AP does not have its own users to serve ($\rho_A = 0$), then this ratio becomes

$$\frac{R^{WL}}{R_0} = 1 + 2\Big(\frac{W_A}{W_B}\Big)^{\frac{a}{a+1}}\Big(\frac{P_{AP}^{max}}{P_{BST}^{max}}\Big)^{\frac{1}{a+1}}. \tag{3.24}$$

Hence if $W_A = W_B$, $P_{AP}^{max} = P_{BST}^{max}$, then the relay can at most triple the total rate, independent of the path loss exponents and the density of cellular users.

3.2.2. Individual Coding

The BST individually encodes all data destined to the relayed users and transmits these individual streams in parallel to the AP. Assuming the AP allocates power αP_{AP}^{max} to the relayed users, we can again decompose the optimization problem (3.8) into two separate problems. The AP problem is still given by (3.14) and (3.15). The BST problem now becomes

$$\begin{aligned}\textbf{BST:} \max_{\{P_B(r),P_B(x),P'_A(x)\}} &\int \rho_B W_B \log\Big(1 + \tfrac{P_B(r)}{N_0 W_B r^a}\Big)\, dr \\ &+ \int \rho_B W_B \log\Big(1 + \tfrac{P_B(x)}{N_0 W_B d^b}\Big)\, dx\end{aligned} \tag{3.25}$$

subject to (3.17),

$$\int \rho_B P_B(r)\, dr + \int \rho_B P_B(x)\, dx \le P_{BST}^{max}, \tag{3.26}$$

and

$$W_B \log\Big(1 + \tfrac{P_B(x)}{N_0 W_B d^b}\Big) = W_A \log\Big(1 + \tfrac{P'_A(x)}{N_0 W_A x^a}\Big), \tag{3.27}$$

where $P_B(x)$ is the BST power allocated for relayed data to a cellular user at distance x from the AP. Hence, when a cellular user at distance r from the BST ($x = r - d$ from the AP) receives data from both the direct and relay path, we have $P_B(r) > 0$, $P_B(x) > 0$, and $P'_A(x) > 0$.

To simplify our discussion of this case, we will assume in the rest of this section that $W_A = W_B = W$, i.e. the AP and the BST have the same bandwidth/user. With this assumption, the individual flow conservation constraint (3.27) is reduced to $\frac{P_B(x)}{d^b} = \frac{P'_A(x)}{x^a}$. We first consider the solution when $b = a$, i.e. the path loss exponent between the BST and the AP is the same as the direct path loss exponent. We then consider the general case where $b < a$.

3.2.2.1. Equal path-loss exponents. For any fixed rate R, the power required for the BST to transmit at that rate over the direct path to a user at distance r is proportional to r^a. With equal path loss exponents, the power required for the BST to transmit at that rate over the relay path to the same user is proportional to d^a, with the same constant of proportionality. Hence, it is clear that under the optimal power allocation, the BST will not send any relayed data to a cellular user at distance $r < d$ (but it may send direct data). On the other hand, for the users at distance $r > d$, using the relay channel is beneficial to the BST because it can save the power. Recall that r_{B0} was defined to be the BST coverage radius without relaying. For a given α, the solution to BST problem can be classified into two cases depending on if $r_{B0} \leq d$ or $r_{B0} > d$.

Case 1: $r_{B0} \leq d$. In this case, the coverage radius of BST without relaying does not extend beyond the AP location, and so even when the AP can be used for relaying, it will not benefit the BST. It follows that the solution to the BST problem will be to only

use direct channels, i.e. to set $P_B(x) = 0$ for all x and $P_B(r)$ is again given by the water-filling allocation in (3.4). For any α, the maximum total rate achieved by the BST is $R_B(\alpha) = R_{B0}$, where R_{B0} is given in (3.6). Since this does not depend on α, clearly it is optimal to set $\alpha = 0$, when optimizing the total rate. Therefore, the AP solution is also the same as in the no-relay case.

Note that the condition $r_{B0} \leq d$ is equivalent to $P_{BST}^{max} \leq \frac{a}{a+1} N_0 \rho_B W d^{a+1}$, and this case will arise when the BST power is small enough, or equivalently when the user density ρ_B is large enough.

Case 2: $r_{B0} > d$. When the coverage radius of the BST extends beyond the AP, the BST can increase its throughput by using the relay path. Note that for a given data rate, the BST requires the same power to transmit at that rate to any user via the relay path. Hence, the power allocation to the relayed users is determined by the AP power constraint (3.17) and the individual flow constraint (3.27). To characterize the resulting power allocation, we consider the following Lagrangian for the BST problem:

$$\begin{aligned} L(P_B(r), P_B(x)) &= \int \rho_B W \log\Big(1 + \frac{P_B(r)}{N_0 W r^a}\Big)\, dr \\ &+ \int \rho_B W \log\Big(1 + \frac{P_B(x)}{N_0 W d^a}\Big)\, dx \\ &- \lambda_1 \Big(\int \rho_B P_B(r)\, dr + \int \rho_B P_B(x)\, dx - P_{BST}^{max} \Big) \\ &- \lambda_2 \Big(\int \rho_B P_B(x) \frac{x^a}{d^a}\, dx - \alpha P_{AP}^{max} \Big), \end{aligned} \tag{3.28}$$

where λ_1 and λ_2 are Lagrange multipliers corresponding to the constraints in (3.26) and (3.17), respectively. Note that we have used the individual flow constraint (3.27) to

express $P'_A(x)$ in terms of $P_B(x)$. The corresponding first order optimality conditions are

$$\frac{\partial L}{\partial P_B(r)} = \frac{W}{N_0 W r^a + P_B(r)} - \lambda_1 = 0, \tag{3.29}$$

$$\frac{\partial L}{\partial P_B(x)} = \frac{W}{N_0 W d^a + P_B(x)} - \lambda_1 - \lambda_2 \frac{x^a}{d^a} = 0. \tag{3.30}$$

Clearly, under the optimal solution, the BST power constraint will be tight. Suppose that the AP power constraint (3.17) is not tight. Then $\lambda_2 = 0$ and the resulting power allocations are

$$P_B(r) = N_0 W \left(r_B^a - r^a\right)^+, \tag{3.31}$$

$$P_B(x) = \begin{cases} N_0 W \left(r_B^a - d^a\right)^+, & x \geq 0, \\ 0, & x < 0, \end{cases} \tag{3.32}$$

where $r_B = \left(\frac{1}{N_0 \lambda_1}\right)^{1/a}$ is the coverage radius of the direct channel. To satisfy the BST power constraint (3.26), it must be that $r_B \leq d$, but in this case, since by assumption $r_{B0} > d$, this will result in the BST not using all of its power. Hence, $\lambda_2 > 0$ and the AP power constraint must be tight. Therefore, the optimal power allocations at the BST are

$$P_B(r) = N_0 W \left(r_B^a - r^a\right)^+, \tag{3.33}$$

$$P_B(x) = \begin{cases} N_0 W d^a \left(\frac{\frac{r_B^a}{d^a}}{1 + \lambda_2 N_0 \frac{r_B^a}{d^a} x^a} - 1\right)^+, & x \geq 0, \\ 0, & x < 0, \end{cases} \tag{3.34}$$

where r_B (λ_1) and λ_2 are chosen so that the power constraints are tight. The resulting coverage of relayed users measured from the AP is $x_R = \left(\frac{1}{\lambda_2 N_0}\left(1 - \frac{d^a}{r_B^a}\right)\right)^{1/a}$, and the

solution to the BST problem is

$$R_B(\alpha) = a\,\rho_B W_B\, r_B + \int_0^{x_R} \rho_B W_B \log\Big(\frac{\frac{r_B^a}{d^a}}{1+\lambda_2 N_0 \frac{r_B^a}{d^a} x^a}\Big)\, dx. \tag{3.35}$$

As in Section 3.2.1, the rates of the BST and AP can then be jointly optimized by searching for the optimal $\alpha^* \in [0,1]$.

3.2.2.2. Unequal path-loss exponents. Now we consider the case where $b < a$, i.e. the channel between the BST and AP has a lower path-loss exponent than the direct channel. This case can be solved using the same approach as in the previous section. Therefore, we omit the arguments except for pointing out the main differences.

First note that the power required by the BST to send at any fixed rate R to a user at distance r over the direct channel is still proportional to r^a. However, if the BST sends at rate R to this user over the relay path, the power is now proportional to d^b. Hence, the BST would like to use the relay channel to send data to users at distance greater than $d_1 = d^{b/a} < d$. In other words, when $r_{B0} > d_1$, the solution to the BST problem uses the relay. Second, note that to efficiently utilize the AP power, the users nearest the AP will receive relay traffic. A result of this is that when the AP power for relaying is small enough, the cellular users which are served may be divided into two disjoint intervals. Specifically, the BST may transmit directly to all users in $[0, d_1]$, then there may be a gap in service, and the AP may then continue serving users in a small radius around it.

3.3. Voice Traffic

3.3.1. Joint Coding

The optimization problem in this case is to maximize (3.10) subject to

$$\int_{\mathcal{C}_d} \rho_B P_B(r)\, dr + \gamma P_{BS}^{max} \leq P_{BS}^{max}, \tag{3.36}$$

$$2\int_{\mathcal{D}} \rho_A P_A(x)\, dx + \int_{\mathcal{C}_r} \rho_B P'_A(x)\, dx \leq P_{AP}^{max}, \tag{3.37}$$

$$W_{BA} \log\left(1 + \frac{\gamma P_{BS}^{max}}{N_0 W_{BA} d^b}\right) = R_B \rho_B |\mathcal{C}_r|, \tag{3.38}$$

$$\mathcal{C} = \mathcal{C}_d \cup \mathcal{C}_r,\ \mathcal{C}_d \cap \mathcal{C}_r = \emptyset,\ \gamma \in [0,1] \tag{3.39}$$

where γ is a variable to be optimized, which indicates the fraction of BST power allocated to the relay channel. The AP power allocation for a relayed cellular user at distance x from the AP is $P'_A(x) = N_0 W_A\big(e^{\frac{R_B}{W_A}} - 1\big)|x|^a = A'|x|^a$. Constraints (3.36) and (3.37) are the total power constraints for the BST and AP, respectively, and (3.38) is the total flow rate conservation.

Similar to Section 3.2, we first assume that the AP allocates power αP_{AP}^{max} for relayed cellular users, where $\alpha \in [0,1]$, and subsequently optimizes over α. Then the problem decomposes into two independent optimization problems for the BST users and the AP users. Given α, the AP optimization problem is to maximize the number of active non-cellular users. The solution is $2\rho_A|\mathcal{D}(\alpha)|$, where $|\mathcal{D}(\alpha)| = (\frac{a+1}{\rho_A A}\frac{(1-\alpha)P_{AP}^{max}}{2})^{\frac{1}{a+1}}$. The BST optimization problem is to maximize the coverage of the cellular users $|\mathcal{C}(\alpha)|$ for given density ρ_B.

To solve the BST optimization problem, we first write constraints on the interval containing relayed users, which follow from the AP power allocation αP_{AP}^{max} and the BST power allocation γP_{BS}^{max}. Denote the interval of relayed users by $[d+\underline{x}, d+\bar{x}]$, where $\underline{x} \geq -d$. Given $\underline{x}$, from (3.37) $\bar{x} \leq \bar{x}_A(\underline{x})$, where $\bar{x}_A(\underline{x})$ is the value of $\bar{x}$ that satisfies

$$\int_{\underline{x}}^{\bar{x}} \rho_B P_A'(x)\, dx = \alpha P_{AP}^{max}. \tag{3.40}$$

Likewise, from (3.38), we have $\bar{x} \leq \bar{x}_B(\underline{x})$, where

$$\bar{x}_B(\underline{x}) = \underline{x} + \frac{W_{BA}}{R_B \rho_B} \log\left(1 + \frac{\gamma P_{BS}^{max}}{N_0 W_{BA} d^b}\right). \tag{3.41}$$

Combining these, we must have that

$$\bar{x} \leq \bar{x}(\underline{x}) \equiv \min\{\bar{x}_A(\underline{x}), \bar{x}_B(\underline{x})\}. \tag{3.42}$$

Given α and γ, to maximize the total coverage this bound will be met with equality.

The BST allocates $(1-\gamma)P_{BS}^{max}$ for the direct-path cellular users. Consider the two possible inequalities

$$\int_0^{d+\underline{x}} \rho_B P_B(r)\, dr \gtrless (1-\gamma) P_{BS}^{max}. \tag{3.43}$$

The left side of the inequality is the BST power required to activate users in the interval $[0, d+\underline{x}]$. This can be rewritten as

$$\underline{x} \gtrless \tilde{x} = \left(\frac{a+1}{\rho_B B}(1-\gamma) P_{BS}^{max}\right)^{\frac{1}{a+1}} - d, \tag{3.44}$$

where $[0, d+\tilde{x}]$ is the largest interval of users which can be served directly by the BST given the available power. For a given interval of relayed users $[d+\underline{x}, d+\bar{x}]$, if $\underline{x} > \tilde{x}$,

then there is a gap between the cellular users served directly by the BST and the cellular users served by the AP. The total cellular user coverage is then

$$\mathcal{C}(\gamma, \alpha, \underline{x}) = d + \tilde{x} + \bar{x} - \underline{x}. \tag{3.45}$$

If $\underline{x} \leq \tilde{x}$, then there is no gap in the coverage of cellular users. That is, the BST power needed to activate users in $[0, d+\underline{x}]$ is less than $(1-\gamma)P_{BS}^{max}$. Hence, there will be a second interval of cellular users served directly by the BST given by $[d + \bar{x}, \mathcal{C}(\gamma, \alpha, \underline{x})]$, where

$$\mathcal{C}(\gamma, \alpha, \underline{x}) = \left[(d + \tilde{x})^{a+1} + (d + \bar{x})^{a+1} - (d + \underline{x})^{a+1}\right]^{\frac{1}{a+1}} \tag{3.46}$$

is the total cellular coverage.

Given α, the BST optimization problem reduces to optimizing $\underline{x}$, which determines the interval of relayed users, and γ, i.e.,

$$\mathcal{C}(\alpha) = \max_{0 \leq \gamma \leq 1} \max_{\underline{x} \geq -d} \mathcal{C}(\alpha, \gamma, \underline{x}). \tag{3.47}$$

Finally, the maximum total number of users served by both the BST and AP is given by

$$\max_{0 \leq \alpha \leq 1} \rho_B |\mathcal{C}(\alpha)| + 2\rho_A |\mathcal{D}(\alpha)|. \tag{3.48}$$

Although we are unable to obtain a closed-form solution to the preceding optimization problem, we can follow the approach in Section 3.2 to derive a closed-form upper bound on the total number of users served by the BST and the AP. Namely, we assume that the connection between the BST and the AP is "free", i.e., does not require any expenditure

of power. In that case, the intervals of users served by the BST and the AP have lengths

$$|\mathcal{C}^{WL,\infty}| = \left(\frac{a+1}{\rho_B B} P_{BS}^{max}\right)^{\frac{1}{a+1}} + 2\left(\frac{a+1}{2} P_{AP}^{max}\right)^{\frac{1}{a+1}} \times \left(\frac{\rho_B}{A'^{1/a}} + \frac{\rho_A}{A^{1/a}}\right)^{-\frac{1}{a+1}} \frac{\rho_B}{A'^{1/a}}, \tag{3.49}$$

$$|\mathcal{D}^{WL,\infty}| = \left(\frac{a+1}{2} P_{AP}^{max}\right)^{\frac{1}{a+1}} \left(\frac{\rho_B}{A'^{1/a}} + \frac{\rho_A}{A^{1/a}}\right)^{-\frac{1}{a+1}} \frac{1}{A^{1/a}} \tag{3.50}$$

provided that the distance d between the BST and the AP is large enough so that there is no coverage overlap between the users directly served by the BST and the relayed users. The relative increase in the total number of users due to the addition of the relay is then

$$\begin{aligned} &\frac{\rho_B|\mathcal{C}^{WL,\infty}| + 2\rho_A|\mathcal{D}^{WL,\infty}|}{\rho_B\mathcal{C}_0 + 2\rho_A\mathcal{D}_0} \\ &= \frac{1 + 2\left(\frac{P_{AP}^{max}}{2}\frac{1}{P_{BS}^{max}}\right)^{\frac{1}{a+1}}\left(\frac{B^{1/a}}{A'^{1/a}} + \frac{\rho_A}{\rho_B}\frac{B^{1/a}}{A^{1/a}}\right)^{\frac{a}{a+1}}}{1 + 2\left(\frac{\rho_A}{\rho_B}\right)^{\frac{a}{a+1}}\left(\frac{B}{A}\frac{P_{AP}^{max}}{2}\frac{1}{P_{BS}^{max}}\right)^{\frac{1}{a+1}}}. \end{aligned} \tag{3.51}$$

If the AP does not have a separate set of non-cellular users to serve ($\rho_A = 0$), then this ratio becomes

$$\frac{\rho_B|\mathcal{C}^{WL,\infty}| + 2\rho_A|\mathcal{D}^{WL,\infty}|}{\rho_B\mathcal{C}_0 + 2\rho_A\mathcal{D}_0} = 1 + 2\left(\frac{B}{A'}\frac{P_{AP}^{max}}{2}\frac{1}{P_{BS}^{max}}\right)^{\frac{1}{a+1}}. \tag{3.52}$$

Even with a wired connection between the BST and the AP, the preceding bound is not tight unless the distance d between the BST and AP is large enough so that the intervals covered by BST and AP do not overlap. With small d this bound can be improved by optimizing the total number of users served over $\underline{x}$ and α as before, assuming that the

BST-AP link requires no power consumption (since the BST-AP link requires no power, we no longer have to optimize over γ).

3.3.2. Individual Coding

Assuming the AP allocates power αP_{AP}^{max} to the relayed users, we can again decompose the optimization problem (3.10) into two separate problems. The AP problem is still the same as the one for total flow rate conservation. The BST problem for given user density ρ_B now becomes maximizing the cellular user coverage $|\mathcal{C}| = |\mathcal{C}_d| + |\mathcal{C}_r|$ subject to

$$\int_{\mathcal{C}_d} \rho_B P_B(r)\, dr + \int_{\mathcal{C}_r} \rho_B P_B(d)\, dx \leq P_{BS}^{max}, \tag{3.53}$$

$$\int_{\mathcal{C}_r} \rho_B P_A'(x)\, dx \leq \alpha P_{AP}^{max}. \tag{3.54}$$

Note in this case, (3.53) combines the BST power constraint and the individual flow constraint; namely, $P_B(d) = Bd^a$ is the power required from the BST to deliver each relayed flow to the AP. As before, $\mathcal{C}_d$ and $\mathcal{C}_r$ are also constrained to be disjoint sets.

3.3.2.1. Equal path-loss exponents. We consider the case where $b = a$. Then for a cellular user at distance $r < d$, the BST will not receive any power savings by using the relay. Therefore, if the BST power P_{BS}^{max} is less than $\frac{\rho_B B}{a+1} d^{a+1}$, the BST will not use the relay even when $\alpha > 0$. In this case, the total coverage is $\mathcal{C}(\alpha) = \mathcal{C}_0 = (\frac{a+1}{\rho_B B} P_{BS}^{max})^{\frac{1}{a+1}} < d$. However, if $P_{BS}^{max} > \frac{\rho_B B}{a+1} d^{a+1}$, using the relay reduces the power needed by the BST. Again, denote the interval of relayed users by $[d+\underline{x}, d+\bar{x}]$. Given $\underline{x}$ and α, $\bar{x}$ is again constrained by $\bar{x} \leq \bar{x}_A(\underline{x})$, where $\overline{x}_A(\underline{x})$ is the value of $\bar{x}$ that satisfies (3.40). The following proposition shows that when the relay is used, the optimal relay user interval starts at $\underline{x} = 0$.

Proposition 1. *Given AP power* αP_{AP}^{max} *and* $b = a$*, if* $P_{BS}^{max} > \frac{\rho_B B}{a+1} d^{a+1}$*, then the optimal relay user interval is given by* $[d, d + \overline{x}]$*, where* $\overline{x} \leq \overline{x}_A(0)$*.*

Proof. See Section 3.6. □

3.3.2.2. Unequal path-loss exponents. Now we consider the case where $b < a$. Then the power required by the BST to transmit directly to a user at distance r at rate R_B is $P_B(r) = Br^a$ and the power required by the BST to transmit a relayed packet to the AP for this user is $P_B(d) = Bd^b$. Hence, the BST can save power by using the relay if $r > d_1 = d^{b/a}$. When the BST power is small enough so that it can only serve users at distance less than d_1, it will not use the relay. As its power increases, it will begin to serve the relayed users. Initially, the set of relayed users will lie in a symmetric interval around the AP. Given AP power αP_{AP}^{max}, let $[d - \Delta, d + \Delta]$ be the largest symmetric interval of relayed users that can be supported around the AP, where $\Delta = (\frac{a+1}{\rho_B A'} \frac{\alpha P_{AP}^{max}}{2})^{\frac{1}{a+1}}$. As the BST power further increases, the resulting coverage will follow two possible evolutions, depending on whether or not $d - \Delta \geq d_1$, and they are shown in Figure 3.3. On the left is the case where $d - \Delta \geq d_1$. In this case the relay always serves a symmetric set of cellular users, and as the BST power increases, it will eventually serve some users to the right of the relayed set. On the right is the case where $d - \Delta < d_1$. In this case, when there is sufficient relayed traffic, the relayed set is not symmetric, but extends further in the positive direction. This is because the users to the left are served directly by the BST. For the former case ($d - \Delta \geq d_1$), the coverage as a function of the BST power is given in Table 3.1 and for the latter case ($d - \Delta < d_1$) in Table 3.2.

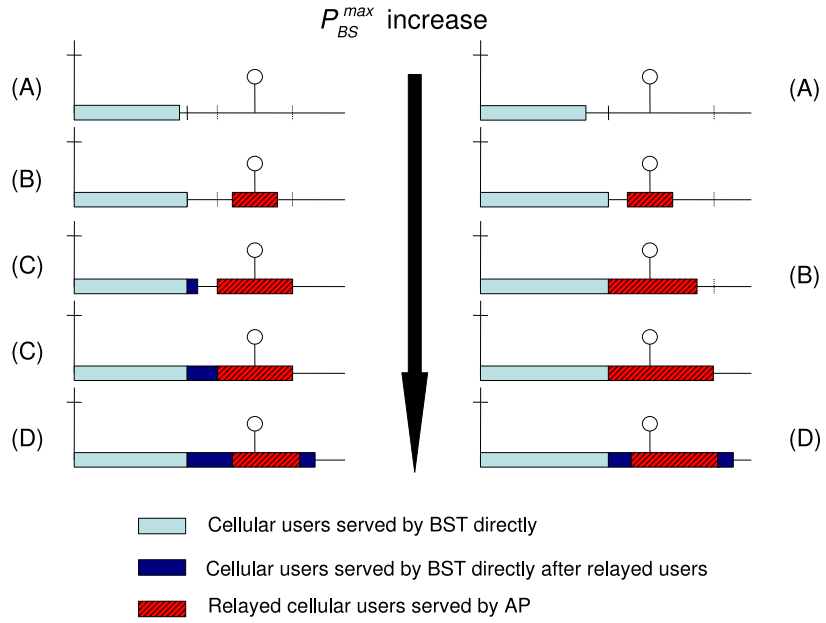

Figure 3.3. Cellular user coverage as a function of P_{BS}^{max}. On the left is the case where $d - \Delta \geq d_1$ and on the right is the case where $d - \Delta < d_1$.

Table 3.1. Cellular coverage as a function of P_{BS}^{max} when $b < a$ and $d - \Delta \geq d_1$.

	BST Power P_{BS}^{max}	BST coverage $\lvert\mathcal{C}(\alpha)\rvert$
A	$0 < P_{BS}^{max} \leq \frac{\rho_B B}{a+1} d_1^{a+1}$	$\lvert\mathcal{C}(\alpha)\rvert = \lvert\mathcal{C}_0\rvert = \left(\frac{a+1}{\rho_B B} P_{BS}^{max}\right)^{\frac{1}{a+1}}$
B	$P_{BS}^{max} \leq \frac{\rho_B B}{a+1} d_1^{a+1} + \rho_B B d^b \cdot 2\Delta$	$\lvert\mathcal{C}(\alpha)\rvert = d_1 + \frac{P_{BS}^{max} - \frac{\rho_B B}{a+1} d_1^{a+1}}{\rho_B B d^b}$
C	$P_{BS}^{max} \leq P_{BS}^{max}(\text{critical})$ $= \frac{\rho_B B}{a+1}(d-\Delta)^{a+1} + \rho_B B d^b \cdot 2\Delta$	$\lvert\mathcal{C}(\alpha)\rvert = \left\{\frac{a+1}{\rho_B B}\left(P_{BS}^{max} - \rho_B B d^b \cdot 2\Delta\right)\right\}^{\frac{1}{a+1}} + 2\Delta$
D	$P_{BS}^{max} > P_{BS}^{max}(\text{critical})$	$\lvert\mathcal{C}(\alpha)\rvert$ – See (3.55) and (3.56)

In Table 3.1, $P_{BS}^{max}(\text{critical})$ represents the minimum power such that when $P_{BS}^{max} > P_{BS}^{max}(\text{critical})$, the BST serves users to the right of the relayed interval. In this case, the

Table 3.2. Cellular coverage as a function of P_{BS}^{max} when $b < a$ and $-\Delta < d_1 - d$

	BST Power P_{BS}^{max}	BST coverage $\lvert\mathcal{C}(\alpha)\rvert$
A	$0 < P_{BS}^{max} \leq \frac{\rho_B B}{a+1} d_1^{a+1}$	$\lvert\mathcal{C}(\alpha)\rvert = \lvert\mathcal{C}_0\rvert = \left(\frac{a+1}{\rho_B B} P_{BS}^{max}\right)^{\frac{1}{a+1}}$
B	$P_{BS}^{max} \leq P_{BS}^{max}(\text{critical})$ $= \frac{\rho_B B}{a+1} d_1^{a+1} + \rho_B B d^b \{\bar{x}_A(d_1 - d) - (d_1 - d)\}$	$\lvert\mathcal{C}(\alpha)\rvert = d_1 + \frac{P_{BS}^{max} - \frac{\rho_B B}{a+1} d_1^{a+1}}{\rho_B B d^b}$
D	$P_{BS}^{max} > P_{BS}^{max}(\text{critical})$	$\lvert\mathcal{C}(\alpha)\rvert$ – See (3.55) and (3.56)

cellular coverage as a function of $\underline{x}$ becomes

$$|\mathcal{C}(\alpha, \underline{x})| = \left[\frac{a+1}{\rho_B B} P_{BS}^{max} + (d + \overline{x}_A(\underline{x}))^{a+1} - (a+1) d^b (\overline{x}_A(\underline{x}) - \underline{x}) - (d + \underline{x})^{a+1}\right]^{\frac{1}{a+1}}, \tag{3.55}$$

where $\underline{x}$ is constrained to be no smaller than $\max\{-\Delta, d_1 - d\}$. Therefore, the optimal cellular coverage for a given α is

$$|\mathcal{C}(\alpha)| = |\mathcal{C}(\alpha, \min\{x^*, \dot{x}\})|, \tag{3.56}$$

where x^* and $\dot{x}$ are obtained by solving $\frac{\partial |\mathcal{C}(\alpha, \underline{x})|}{\partial \underline{x}}|_{\underline{x}=x^*} = 0$ and $|\mathcal{C}(\alpha, \dot{x})| = d + \overline{x}_A(\dot{x})$, respectively. The optimal number of cellular and AP users can then be found by searching for the optimal $\alpha^* \in [0, 1]$.

3.4. Numerical Results

3.4.1. Data Traffic

We give some numerical results to illustrate the gains from relaying under the two flow conservation constraints. First, we consider the total flow constraint. Fig. 3.4 shows the ratio of the total rate with relaying to that without relaying as a function

of the distance between the BST and the AP. The simulation parameters are $P_{BS}^{max} = 36\,\text{dBm}, P_{AP}^{max} = 20\,\text{dBm}, W_B = W_A = 30\,\text{Khz}, W_{BA} = 1\,\text{MHz}, \rho_B = \rho_A = 50\,\text{users/Km}$ and $N_0 = 10^{-20}\,\text{Watt/Hz}$. Without using the AP as a relay, the (one-sided) radius and (one-sided) throughput for the BST are respectively given by $r_{B0} = 758.9\,\text{m}$ and $R_{B0} = 9.49 \times 10^6\,\text{nats/sec}$ when the pathloss exponent between BST and users is $a = 5$. Similarly, the radius and throughput for the AP are $x_{A0} = 365.9\,\text{m}$ and $R_{A0} = 9.15 \times 10^6\,\text{nats/sec}$. By using the AP as a relay, the total throughput of the system increases by $\sim 11\%$ when the pathloss exponents $a = b = 5$ and by $\sim 40\%$ when $a = 5$ and $b = 4$, as shown in Fig. 3.4. As expected, the better channel between the BST and the AP improves the total throughput significantly. In this case, the wire-line upperbound from (3.23) is 1.406, which is approached when the AP is moved towards to the BST.

Overall, however, the total transmission rate is not much improved with relaying, especially when the AP is relatively far from the BST. This is due to our objective of maximizing the total rate. Users closest to the BST, who do not use the relay, contribute the most to the total rate, and, due to the water-filling power allocation, receive most of the power. However, using a relay in this setting can improve the coverage and the rate allocation of cellular users farther away from the BST. This is illustrated in Fig. 3.5, which shows the rate distribution of cellular users with and without relaying under the total flow constraint when the distance between the BST and AP is $0.7 \times r_{B0}$. It can be seen that the relay improves the rate of the users near the AP while the rates of users near the BST are only slightly reduced.

Figures 3.6 and 3.7 show the corresponding plots under individual flow constraints. The same trends can be observed. Comparing these with the total flow constraint, it can

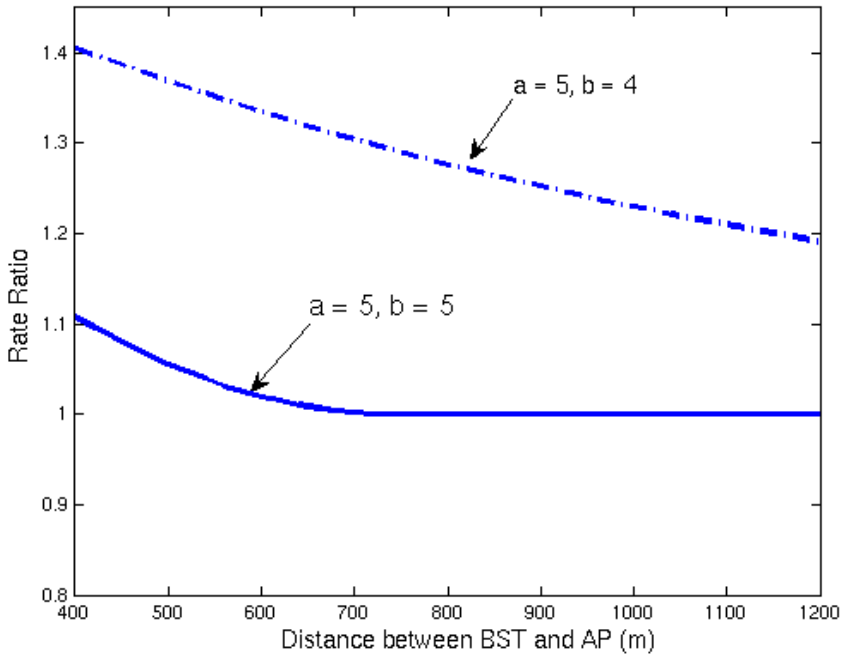

Figure 3.4. Ratio of total data rate with and without relaying as a function of distance between the BST and AP under total flow conservation.

be seen that the gain in total rate is less under this constraint. However, from Fig. 3.7, the increase in coverage is greater in this case ($\sim 30\%$).

3.4.2. Voice Traffic

The required rates for the voice application are assumed to be $R_B = R_A = 30\,\text{Kbps}$. The other parameters are the same as those used for data traffic. Without relaying, the coverage of the BS and the AP are $|\mathcal{C}_0| = 365.2\,\text{m}$ and $|\mathcal{D}_0| = 176.1\,\text{m}$ with $a = 5$.

First, we consider total flow rate conservation. Fig. 3.8 shows the ratio of the total number of users (BST+AP) with relaying to that without relaying as a function of distance d between the BST and the AP. Two different path-loss scenarios are considered: $a =$

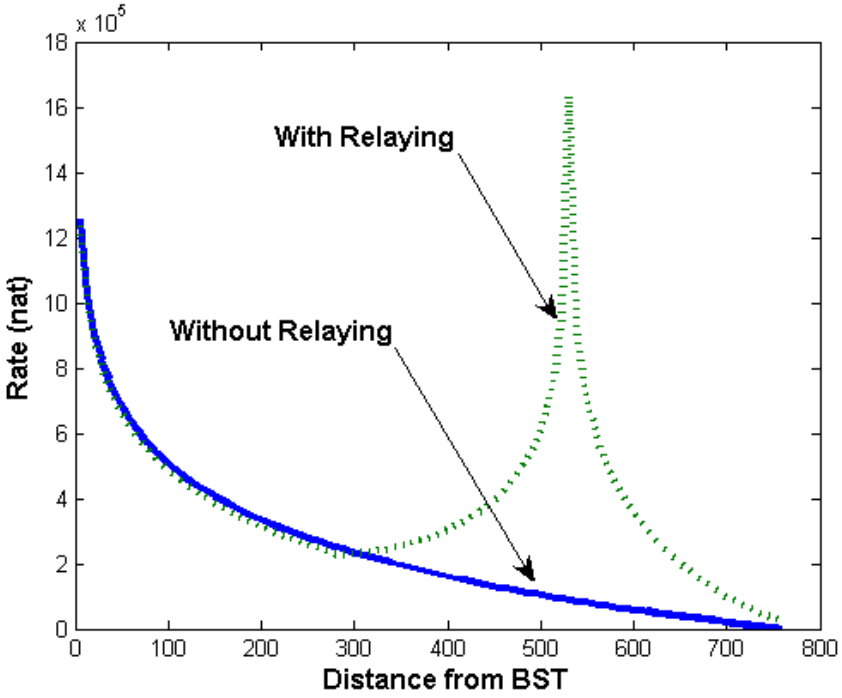

Figure 3.5. Rate distribution of cellular data users with and without relaying as a function of distance from the BST under total flow conservation ($a = 5$ and $b = 4$).

$5, b = 4$ and $a = b = 5$. For each case the ratio of the total number of cellular users is also shown (BST only). Note there is clearly an optimal location of the relay for maximizing each of these ratios. When the path-loss exponent b between the BST and the AP is the same as the path-loss exponent a between the BST and each user, the increase in the total number of active users with the relay is relatively moderate (less than $\sim 21.5\%$ when $a = b = 5$). As the path-loss between the BST and the AP improves, however, the ratio of the total number of users with/without relaying increases more significantly. The relay achieves more than a 37.9% increase in total number of users served when $a = 5$ and $b = 4$. In this case the cellular users served increase by more than 95.6%. (This is offset

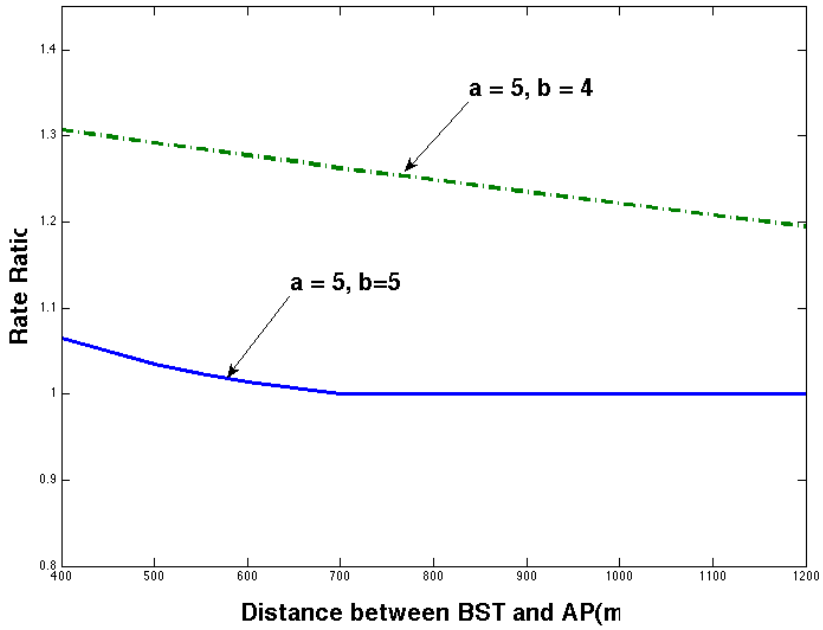

Figure 3.6. Ratio of total data rate with and without relaying as a function of distance between the BST and AP under individual flow conservation.

by a decrease in the number of AP users.) It follows that the increase in the total number of cellular users is larger than 95.6% when the AP only serves as a relay (i.e., $\rho_A = 0$). The upper bound we obtained by assuming the wired connection between the BST and the AP (equation (3.51)) is 1.384, which is very close to the gain shown with $a = 5$ and $b = 4$. The loss due to the power consumption on the link between the BST and the AP is small in this example (38.4 % vs. 38.9%). This is partially because we only consider one AP. In a two dimensional model that has more APs, the loss due to the BST-AP link should be larger.

Results for the individual flow conservation constraint are shown in Fig. 3.9. This figure is very similar to that with total flow conservation. In this case, the gains are lower due to the increasing power needed for the BST-AP link. For example, in the case of

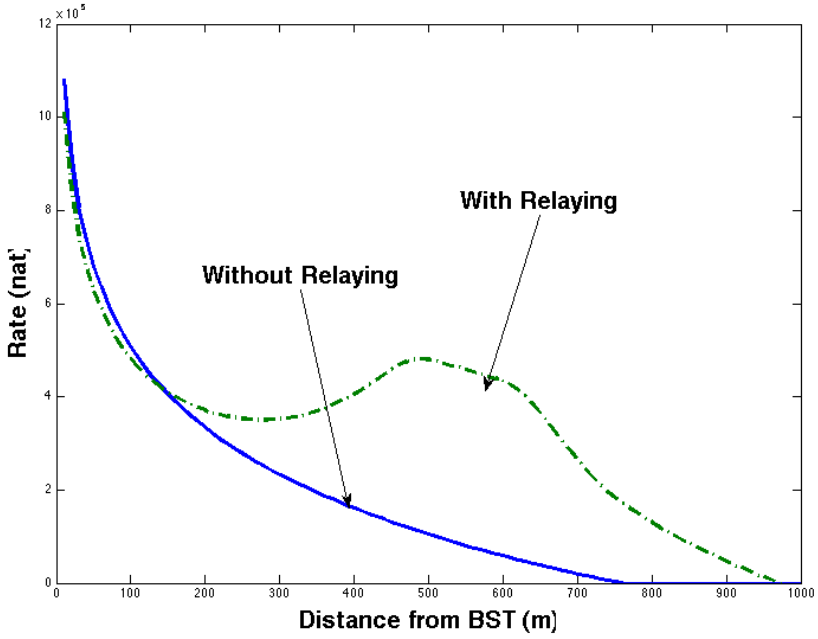

Figure 3.7. Rate distribution of cellular data users with and without relaying as a function of distance from the BST under individual flow conservation ($a = 5$ and $b = 4$).

$a = 5$, $b = 5$, the maximum percentage increase in the total number of users served is about 7.4% (vs.$\sim$ 21.5% in the total flow case). On the other hand, with $a = 5$, $b = 4$, the maximum percentage increase is about the same (37.8% with the individual flow constraint vs. 37.9% with the total flow constraint). In these examples the gain from joint encoding is, in general, very small and may not warrant the additional implementation complexity required.

3.5. Chapter Summary

We have considered a one-dimensional cellular model with two APs placed symmetrically at a fixed distance from the BST and have studied the gain from using the APs as

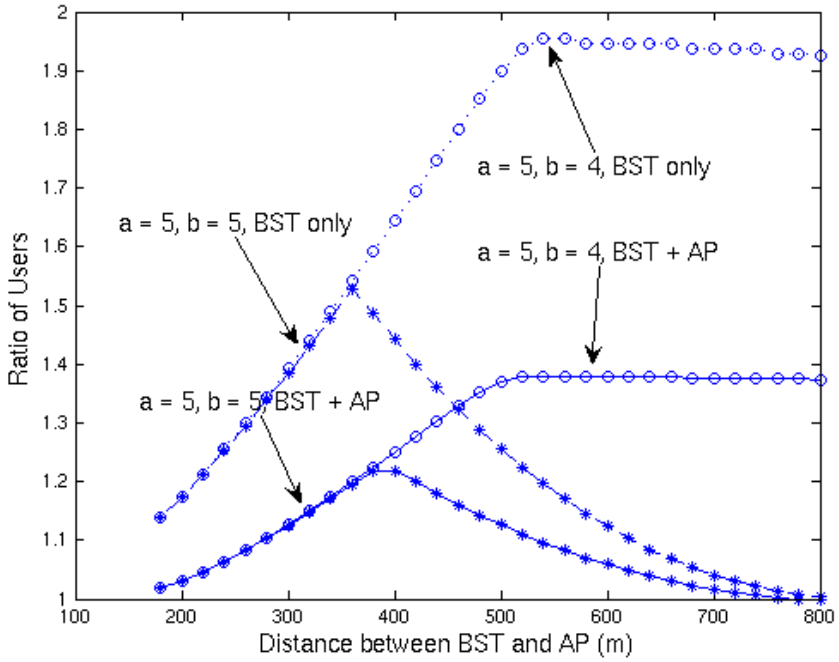

Figure 3.8. Ratio of the total number of voice users served under total flow conservation as a function of distance between the BST and AP.

relays. In addition to relayed traffic, we have assumed that each AP has its own customers to serve. We considered two different flow conservation models depending on whether or not the relay traffic is multiplexed when sent to the AP.

For data traffic, we have studied the maximum total rate for the downlink without considering fairness. Our results show that under both flow constraints, the total transmission rate increases by at most 40%, where the most significant gains are with the total flow conservation model and small traffic density for the relay. Moreover, each relay scheme alters the cellular user rate distribution by slightly reducing the rate of users near the BST and increasing the rate of users near the relay. In addition, the BST coverage can be extended by using the relay.

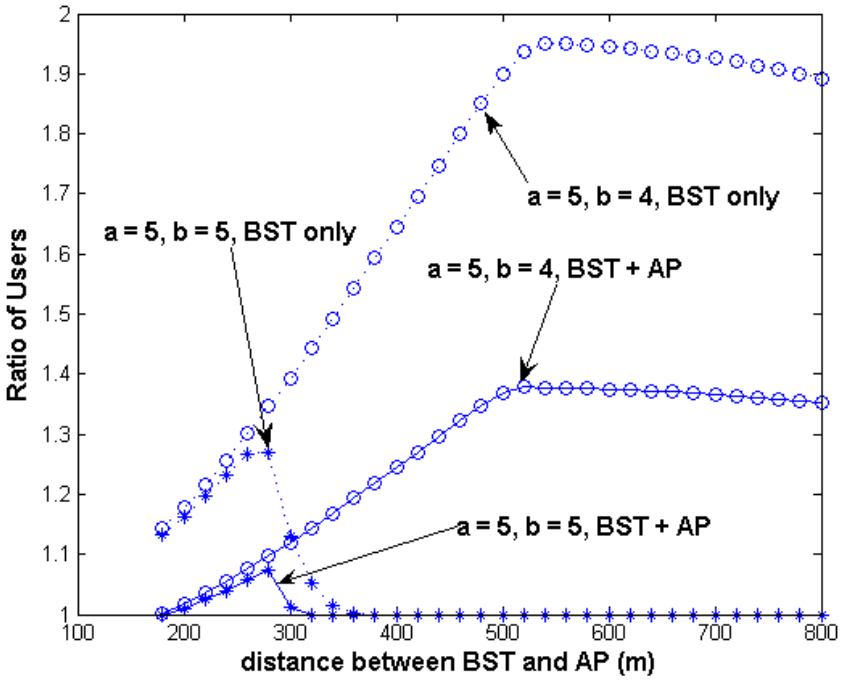

Figure 3.9. Ratio of the total number of voice users served under individual flow conservation as a function of distance between the BST and AP.

For voice traffic, the gain in total number of active users has been studied. When the sets of active users are optimized, the total number of cellular users increases significantly under both flow rate conservation schemes, but at the cost of reducing the AP users. This corresponds to a coverage extension of the cellular network. Our numerical results show that the total number of active users increases by $\sim 38\%$ when the distance between the BST and the AP is optimized.

3.6. Supplement: Proof of Proposition 1

First consider the case when

$$\frac{\rho_B B}{a+1} d^{a+1} < P_{BS}^{max} \leq \frac{\rho_B B}{a+1} d^{a+1} + \int_0^{\overline{x}_A(0)} \rho_B P_B(x)\, dx = \frac{\rho_B B}{a+1} d^{a+1} + \rho_B B d^a \overline{x}_A(0). \quad (3.57)$$

Then the direct channel user coverage is $|\mathcal{C}_d(\alpha)| = d$ (or interval $[0, d]$), and the relayed user coverage is $|\mathcal{C}_r(\alpha)| = \frac{\left(P_{BS}^{max} - \frac{\rho_B B}{a+1} d^{a+1}\right)}{\rho_B B d^a}$. The interval for the relayed cellular users is, therefore, $[d + \underline{x}, d + \underline{x} + C_r(\alpha)]$, where $\underline{x} \in [0, \hat{x}]$. The upper bound $\hat{x}$ can be calculated from $\overline{x}_A(\hat{x}) - \hat{x} = \mathcal{C}_r(\alpha)$. As P_{BS}^{max} increases from $\frac{\rho_B B}{a+1} d^{a+1}$, $\hat{x}$ decreases. When $P_{BS}^{max} = \frac{\rho_B B}{a+1} d^{a+1} + \rho_B B d^a \overline{x}_A(0)$, $\hat{x} = 0$ and the relayed interval becomes $[d, d + \overline{x}_A(0)]$. Therefore, the optimal relay user interval is $[d, d + \overline{x}]$, where $\overline{x} \leq \overline{x}_A(0)$, and the cellular user coverage is

$$|\mathcal{C}(\alpha)| = |\mathcal{C}_d(\alpha)| + |\mathcal{C}_r(\alpha)| = d + \frac{\left(P_{BS}^{max} - \frac{\rho_B B}{a+1} d^{a+1}\right)}{\rho_B B d^a}. \quad (3.58)$$

Next consider the case where $P_{BS}^{max} > \frac{\rho_B B}{a+1} d^{a+1} + \rho_B B d^a \overline{x}_A(0)$. The relayed user interval becomes $[d + \underline{x}, d + \overline{x}] = [d + \underline{x}, d + \overline{x}_A(\underline{x})]$, where $\underline{x} \in [0, \dot{x}]$. Here, we obtain $\dot{x}$ from

$$\int_0^{d+\dot{x}} \rho_B P_B(r)\, dr + \int_{\dot{x}}^{\overline{x}_A(\dot{x})} \rho_B P_B(x)\, dx = P_{BS}^{max}. \quad (3.59)$$

The total cellular user coverage including the relayed users is, then, calculated by

$$\int_0^{d+\underline{x}} \rho_B P_B(r)\, dr + \int_{\underline{x}}^{\overline{x}_A(\underline{x})} \rho_B P_B(x)\, dx + \int_{d+\overline{x}_A(\underline{x})}^{|\mathcal{C}|} \rho_B P_B(r)\, dr = P_{BS}^{max}, \quad (3.60)$$

or

$$|\mathcal{C}(\alpha,\underline{x})|^{a+1} = \frac{a+1}{\rho_B B} P_{BS}^{max} + (d+\overline{x}_A(\underline{x}))^{a+1} - (a+1)\, d^a\, (\overline{x}_A(\underline{x}) - \underline{x}) - (d+\underline{x})^{a+1}. \tag{3.61}$$

It can be shown easily that $\frac{\partial |\mathcal{C}(\alpha,\underline{x})|^{a+1}}{\partial \underline{x}} \leq 0$ for all $\underline{x} \in [0, \dot{x}]$ as long as $a \geq 1$. Therefore, the optimal relayed user interval for given α is $[d, d+\overline{x}_A(0)]$ and the cellular user coverage is given by

$$|\mathcal{C}(\alpha)| = \left[\frac{a+1}{\rho_B B} P_{BS}^{max} + (d+\overline{x}_A(0))^{a+1} - (a+1)\, d^a\, \overline{x}_A(0) - d^{a+1}\right]^{\frac{1}{a+1}}. \tag{3.62}$$

Part 2

Resource Allocation among Non-cooperative Agents

CHAPTER 4

Incentives and Resource Sharing in Spectrum Commons

So far we have considered wireless resource allocation in cellular networks with cooperative relays and studied the maximization of the social welfare. Now we shift our focus and consider resource allocation among non-cooperative agents. In that case, there arise important issues such as developing efficient distributed mechanisms for resource allocation and estimating the efficiency loss if the allocation mechanism is not efficient.

Here we consider a commons model for spectrum sharing in which users may install access points (APs) to serve their own as well as other users' traffic.[1] In the latter case, the AP owner may receive a payment for this [**72**]. One concern with such a model is that as the density of APs increases, the users may eventually suffer a "tragedy of the commons," because of increasing interference [**45**]. It has been suggested that it is enough to lightly regulate the commons to mitigate the tragedy. Schemes such as etiquette protocols, restricted design of devices and bargaining amongst users have been proposed [**97, 64**]. In this paper we model the effect of regulation in reduced form through a shared rate. Namely, an AP owner can provide payments to neighboring users to encourage them not to set up interfering APs. This payment may take the form of providing discounted service and/or providing a share of revenue to potential interferers.

[1]Although this work is motivated by 802.11 systems, here "Access Point" could refer to other types of systems sharing a common band.

Given such a scheme, we study a game theoretic model, which reflects user behavior. In this game, each user decides whether or not to set up an AP, which operates on a particular (single) band. If a user sets up an AP, she provides payments to each neighbor who does not and suffers a disutility depending on the number of interfering APs. On the other hand, if a user does not set up an AP, she receives payments from each neighbor that does. Clearly, if the payments are large enough, the user may decide not to set up an AP and thereby reduce interference. For a given model of the agents' payoffs, we show that the resulting game is a *potential game* and that best response updates converge to a Nash equilibrium of the game.

A game is called a potential game if all players in the game change their strategy as if they jointly optimize a common objective function, i.e., a potential function [**79**]. Potential games have been used to model various network resource allocation problems, including distributed power control [**122, 48, 120**], non-cooperative routing in wired networks [**11**], and multihoming of users to APs in WLANs [**100**].[2]

Using the potential function of the AP deployment game, we analyze the Nash equilibrium under various assumptions. First, we assume that users are located on a two-dimensional lattice and that interference only comes from the nearest APs. This models a situation where either the density of APs or transmission power of each AP is relatively low. In this case, we show that Nash equilibria exist in both pure and mixed strategies and that at least one Nash equilibrium achieves the socially optimal density of APs with the appropriate payment. We then account for interference from outside of the nearest neighbors. Our results suggest that as the transmission power increases relative to the

[2]Other related work, in which a game theoretic approach is used to analyze the performance of ad hoc networks (including IEEE 802.11), is presented in [**106, 121, 25, 108, 36**].

node density, implementing such a commons approach becomes more difficult and other forms of spectrum sharing (e.g. a secondary market) may be more appropriate.

4.1. The Model

Consider a two-dimensional $L_1 \times L_2$ lattice. Every lattice point has a selfish agent who decides whether she sets up an AP or not. Namely, agent l_{ij} at lattice point (i, j) chooses a strategy $y_{ij} \in Y_{ij}$, based on interference and the shared data rate from the nearest APs. This shared data rate among nearest neighbors is the regulatory measure we introduce and is discussed later in detail. The strategy space Y_{ij} of agent l_{ij} is $Y_{ij} = \{0, 1\}$, where $y_{ij} = 1$ if agent l_{ij} decides to set up an AP and $y_{ij} = 0$ if she decides not to set up an AP. If both agents l_{kl} and l_{ij} set up their own APs, the inference from l_{kl} to l_{ij} is given by $I_{kl\to ij}$. On the other hand, if agent l_{ij} decides not to set up the AP, then she shares rate $\gamma_{kl\to ij}$ from agent l_{kl}'s AP, assuming agent l_{kl} sets up the AP.[3] This rate sharing can be justified by the fact that agent l_{ij} is more likely to set up an AP if there is no rate sharing resulting in increased interference to agent l_{kl}. If the rate degradation from this interference is severe enough, then agent l_{kl} has an incentive to share her rate with agent l_{ij}. For tractability we assume that the nodes are placed at lattice points in the plane, and that rate sharing occurs only between nearest neighbors in the lattice.[4] Therefore, $\gamma_{kl\to ij} = 0$ if l_{kl} is not in the set of agent l_{ij}'s nearest neighbors, H_{ij}.[5]

[3]We assume payoff functions that are linear in rate and so this rate sharing can be equally viewed as a transfer payment.

[4]We can relax this assumption and allow rate sharing between non-neighboring agents. This relaxation, however, increases the total amount of information that an agent should know before she makes a decision, and may not be practical.

[5]Depending on the boundary condition, the set of nearest neighbors, H_{ij} can be different. For a periodic boundary condition in a two-dimensional (torus) lattice, considered in Section 4.3, the set of nearest neighbors of agent l_{11} is given by $H_{11} = \{(1, 2), (1, L_1), (2, 1), (L_2, 1)\}$. Without the periodic boundary condition $H_{11} = \{(1, 2), (2, 1)\}$.

The payoff function of agent l_{ij} depends on her own strategy as well as those of other agents. Here, we restrict attention to the following payoff function. If agent l_{ij} decides to set up her own AP given the other agents' decisions, her payoff becomes

$$\begin{aligned}\pi_{ij}^{A}(y_{ij}=1,y_{-ij}) = R - C - \sum_{kl\in\{L_1\times L_2\}} y_{kl}\cdot I_{kl\to ij} \\ - \sum_{kl\in H_{ij}} (1-y_{kl})\cdot\gamma_{ij\to kl},\end{aligned} \tag{4.1}$$

where R is the total rate generated from her own AP and C is the fixed cost for setting up the AP. y_{-ij} denotes the set of decisions of all agents except agent l_{ij}. This payoff function can be motivated by viewing R as the total rate an agent can achieve over a coverage area if there are no interferers, and $I_{kl\to ij}$ as the reduction in coverage caused by each interfering AP. Of course, assuming this linear relation is a simplification, but it provides a tractable model that captures the key interaction among agents. On the other hand, if agent l_{ij} decides not to set up her own AP, then she shares the rate from the APs in her nearest neighborhood H_{ij} and her payoff becomes

$$\pi_{ij}^{N}(y_{ij}=0,y_{-ij}) = \sum_{kl\in H_{ij}} y_{kl}\cdot\gamma_{kl\to ij}. \tag{4.2}$$

Note that we can write the payoff function of agent l_{ij} as the following:

$$\pi_{ij}(y_{ij},y_{-ij}) = y_{ij}\cdot\pi_{ij}^{A} + (1-y_{ij})\cdot\pi_{ij}^{N}. \tag{4.3}$$

For the preceding payoff functions, we consider a non-cooperative game $\Gamma(\pi_{11},\cdots,\pi_{L_1L_2})$ among agents in the lattice. In this game, given fixed actions for all other agents, a rational agent decides whether or not to set up an AP as follows. If $\pi_{ij}^{A}\geq\pi_{ij}^{N}$, then agent

l_{ij} sets up the AP at her lattice point. Otherwise, she chooses to share the rate from the APs in the nearest neighborhood instead of setting up her own AP. We show later that this game Γ is a potential game under certain conditions. This allows us to assert the existence of a Nash equilibrium and characterize the efficiency of Nash equilibria as a function of the amount of rate sharing.

No coordination or no regulatory measure among agents can be represented by $\gamma_{kl \to ij} = 0$. Without rate sharing, agent l_{ij}'s payoff if she decides not to set up the AP becomes $\pi_{ij}(0, y_{-ij}) = 0$ from (4.2). Therefore, an agent is encouraged to set up her own AP unless interference from other APs is so large that her payoff with the AP is negative. This can lead to a situation where a large number of agents in the lattice set up the APs and experience severe interference. As we see later in Section 4.5, the payoffs of all agents can become very low, especially when the density of agents is high. This is an example of the "tragedy of the commons" [**45**].

4.1.1. Model Limitations

Here we briefly discuss the limitations associated with the preceding model, which is analyzed in subsequent sections. First, we assume that the wireless nodes are placed in a lattice, whereas in practice the agents are likely to be randomly distributed over the geographic area of interest. The regular spacing of nodes in a lattice implies that the interference externality imposed by each active node on its nearest neighbor is the same. This enables us to characterize properties of the AP deployment game, such as the existence of equilibria along with the associated efficiency, with a *single* shared rate.[6]

[6]Also, in Section 4.4 we show that the AP deployment game on a lattice is a potential game with different shared rates across the network.

Of course, the shared rate (or equivalently, a transfer payment) scheme can be applied to more general configurations of AP nodes, but then it is likely that different payments would be needed to prove similar results. Such an analysis would be significantly more complicated than that presented here.

The second simplifying assumption is that each AP in the lattice uses the same set of frequencies. Namely, if an agent decides to set up an AP, then she transmits over the entire band. Our model therefore does not directly account for the possibility of using dynamic channel assignment schemes to avoid interference, such as those proposed for *IEEE* 802.11 in [**65, 78, 71, 94**]. (An alternative interpretation of our model is that the particular band considered has already been assigned to each AP by such a channel assignment algorithm, and that the transfer payment scheme is subsequently being used to mitigate interference within that band.)

Finally, as discussed earlier, the payoff depends linearly on the interference. A more accurate model might account for the degradation due to interference by computing the received SINR at each node. The linear payoff assumed here facilitates tractability while providing insight into the benefits of using transfer payments for more realistic scenarios. We also point out that although we initially consider rate sharing between nearest neighbors in the lattice, we relax this assumption in Section 4.2 and show that the AP deployment game is a potential game if rates are shared between non-neighboring agents. However, that increases the total amount of information that an agent needs to make a decision.

4.2. Potential Games

We begin by giving some background on potential games. These are a class of games with several desirable properties, which we will exploit. First, pure Nash equilibrium strategies exist (assuming finite strategy sets) and are relatively easy to compute using a potential function. Second, in these games, a Nash equilibrium can be justified as being the outcome of a boundedly rational learning process such as best response updates.

Let $\Gamma(\pi_1, \pi_2, \ldots, \pi_n)$ be a game with a finite number of players. The set of players is $N = \{1, 2, \ldots, n\}$, the set of strategies of player i is Y_i, and the payoff function of player i is $\pi_i : Y \to R$, where $Y = Y_1 \times Y_2 \times \cdots \times Y_n$ is the set of strategy profiles. A function $P : Y \to R$ is a potential function for Γ if for every $i \in N$ and for every $y_{-i} \in Y_{-i}$

$$\pi_i(x, y_{-i}) - \pi_i(z, y_{-i}) = P(x, y_{-i}) - P(z, y_{-i}) \tag{4.4}$$

for every $x, z \in Y_i$, where Y_{-i} is the Cartesian product of the strategy space of all players except player i.

Definition A game Γ is called a *potential game* if it admits a potential function.

Namely, a game is considered a potential game if the improvement of the player's payoff by changing her strategy can be expressed in terms of the potential function, which is the same for all players. This definition leads to the following Lemma.

Lemma 2 ([**79**])**.** *Let P be a potential function for $\Gamma(\pi_1, \pi_2, \ldots, \pi_n)$. Then the equilibrium set of $\Gamma(\pi_1, \pi_2, \ldots, \pi_n)$ coincides with the equilibrium set of $\Gamma(P, P, \ldots, P)$. That*

is, $y \in Y$ is an equilibrium point for Γ if and only if for every $i \in N$

$$P(y) \geq P(x, y_{-i}) \quad \textit{for every } x \in Y_i. \tag{4.5}$$

Corollary 3 ([**79**])**.** *Every finite potential game possesses a pure-strategy equilibrium.*

Lemma 2 and Corollary 3 show the existence of a Nash equilibrium and how to compute it using the potential function.

In the potential game with a finite set of strategies, the Nash equilibrium can be reached by best response updates [**79**]. Best response updates of the game $\Gamma(\pi_{11}, \cdots, \pi_{L_1 L_2})$ are described by the following. At time $t+1$, an agent l_{ij} is randomly selected among all agents in the lattice $L_1 \times L_2$ and she chooses her strategy, which maximizes her payoff for given strategies of the other agents at time t. Namely, agent l_{ij} chooses the best response $y_{ij}(t+1)$ according to

$$y_{ij}(t+1) = \arg \max_{y_{ij} \in Y_{ij}} \pi_{ij}(y_{ij}, y_{-ij}(t)). \tag{4.6}$$

Initial strategies $y_{ij}(0)$ for all agents are randomly chosen. This best response at time $t+1$ is repeated for $t = 0, 1, 2, \ldots$ with a randomly selected agent. Note that agent l_{ij}'s best response $y_{ij}(t)$ at time t might be different from her best response $y_{ij}(t')$ at time $t' \neq t$. For the AP deployment game, changing actions in this way is reasonable when the fixed cost C is small enough.

Lemma 4. *In every finite potential game, a Nash equilibrium can be reached by best response updates.*

The following Lemma will be useful when we discuss the mixed Nash equilibrium in the potential game considered later.

Lemma 5 ([**79**]). *Let* Γ *be a finite game. Then* Γ *is a potential game if and only if the mixed extension of* Γ *is a potential game.*

4.3. Periodic Boundary Condition with Nearest Neighbor Interference

Initially we study the game discussed in Section 4.1, assuming a periodic boundary condition for the lattice $L_1 \times L_2$[7], namely, $L_1 + 1 = 1$ and $L_2 + 1 = 1$. Then the set of the nearest neighbors of $(1, 1)$, for example, is $H_{11} = \{(1, 2), (1, L_2), (2, 1), (L_1, 1)\}$. This assumption simplifies our analysis by removing boundary effects. (In Section 4.4 we consider a game *without* this periodic boundary condition.) Furthermore, we assume that interference comes only from the nearest neighbor APs. This nearest neighbor interference models a situation where either the density of APs or transmission power of each AP is relatively low. Therefore,

$$I_{kl \to ij} = \begin{cases} I, & (k, l) \in H_{ij}, \\ 0, & (k, l) \notin H_{ij}, \end{cases} \tag{4.7}$$

[7]The resulting lattice is also called a torus-lattice.

where I is a constant, which represents the interference level between two neighboring APs. The payoff function (4.3) for agent l_{ij}, then, is given by

$$\begin{aligned}
&\pi_{ij}(y_{ij}, y_{-ij}) \\
&= y_{ij} \cdot \left(R - C - \sum_{kl \in H_{ij}} y_{kl} \cdot I - \sum_{kl \in H_{ij}} (1 - y_{kl}) \cdot \gamma \right) \\
&\quad + (1 - y_{ij}) \cdot \left(\sum_{kl \in H_{ij}} y_{kl} \cdot \gamma \right) \\
&= y_{ij} \cdot \left(R - C - \sum_{kl \in H_{ij}} y_{kl} \cdot I - \sum_{kl \in H_{ij}} \gamma \right) \\
&\quad + \sum_{kl \in H_{ij}} y_{kl} \cdot \gamma.
\end{aligned} \tag{4.8}$$

For the time being, we assume that the shared rate from the AP of each agent $l_{kl} \in H_{ij}$ to each agent l_{ij} is $\gamma_{kl \to ij} = \gamma$. Namely, it is the same for all agents in the lattice.

Let Γ_{PBNN} denote the resulting game under these assumptions.

Lemma 6.

$$\begin{aligned}
&P(y_{11}, y_{12}, \ldots, y_{L_1 L_2}) \\
&= (R - C) \left(\sum_{i=1}^{L_1} \sum_{j=1}^{L_2} y_{ij} \right) - \sum_{i=1}^{L_1} \sum_{j=1}^{L_2} y_{ij} \left(\sum_{kl \in H_{ij}} \gamma \right) \\
&\quad - \frac{1}{2} \sum_{i=1}^{L_1} \sum_{j=1}^{L_2} y_{ij} \left(\sum_{kl \in H_{ij}} y_{kl} \cdot I \right).
\end{aligned} \tag{4.9}$$

is a potential function for Γ_{PBNN}.

The proof of this follows by noting that for given y_{-ij},

$$\begin{aligned} &\pi_{ij}(y'_{ij}, y_{-ij}) - \pi_{ij}(y_{ij}, y_{-ij}) \\ &\qquad = P(y'_{ij}, y_{-ij}) - P(y_{ij}, y_{-ij}), \end{aligned} \tag{4.10}$$

for all $y_{ij}, y'_{ij} \in Y_{ij}$ and all agents in the Lattice $L_1 \times L_2$. Therefore, according to Definition 4.2, Γ_{PBNN} is a potential game with the potential function P given by (4.9).

On the other hand, the social welfare is the sum of the payoffs of all agents and is not affected by the shared rate γ since it is an exchange between two agents. The social welfare of all agents in the $L_1 \times L_2$ lattice is, therefore, given by

$$\begin{aligned} &SW(y_{11}, y_{12}, \ldots, y_{L_1 L_2}) \\ &= (R - C) \left(\sum_{i=1}^{L_1} \sum_{j=1}^{L_2} y_{ij} \right) - \sum_{i=1}^{L_1} \sum_{j=1}^{L_2} y_{ij} \left(\sum_{kl \in H_{ij}} y_{kl} \cdot I \right). \end{aligned} \tag{4.11}$$

We next compare a Nash equilibrium strategy with a strategy, which maximizes the social welfare and discuss the efficiency loss at the Nash equilibrium.

4.3.1. Pure Nash Equilibrium

The first-order derivative of the potential function (4.9) is given by

$$\frac{\partial P}{\partial y_{ij}} = (R - C) - \sum_{kl \in H_{ij}} \gamma - \sum_{kl \in H_{ij}} y_{kl} \cdot I. \tag{4.12}$$

Note that $\frac{\partial P}{\partial y_{ij}}$ does not depend on y_{ij}. If the strategy space is restricted to $\{0, 1\}$ for all agents, the best response of agent l_{ij} for $\frac{\partial P}{\partial y_{ij}} > 0$ ($\frac{\partial P}{\partial y_{ij}} < 0$) is $y_{ij} = 1$ ($y_{ij} = 0$). By Lemma 4, best response updates of randomly selected agents converge to a Nash

equilibrium. In a similar way, if $\frac{\partial SW}{\partial y_{ij}} > 0$ ($\frac{\partial SW}{\partial y_{ij}} < 0$), then $y_{ij} = 1$ ($y_{ij} = 0$) to maximize the social welfare given by (4.11).

Let H_{ij}^A be the set of nearest neighbors of agent l_{ij} which set up an AP. Then from (4.12) it can be seen that agent l_{ij}'s action in a Nash equilibrium is to set up an AP if

$$\frac{R - C - \sum_{kl \in H_{ij}} \gamma}{I} > |H_{ij}^A| \tag{4.13}$$

and not to set up an AP when

$$\frac{R - C - \sum_{kl \in H_{ij}} \gamma}{I} < |H_{ij}^A|. \tag{4.14}$$

The agent is indifferent when equality holds. For Γ_{PBNN}, $\sum_{kl \in H_{ij}} \gamma = 4\gamma$ for all l_{ij}, and so the preceding threshold on the number of neighbors is

$$\mathbf{H}_{th} = \frac{R - C - 4\gamma}{I}. \tag{4.15}$$

There are 5 cases of interest for this quantity.

4.3.1.1. $0 < \mathbf{H}_{th} < 1$**.** In this case, an agent will set up an AP in a Nash equilibrium only if none of her neighbors does. For fixed $R - C$, this is true if γ and I satisfy

$$\begin{cases} R - C - 4\gamma - I \cdot 0 & > & 0, \\ R - C - 4\gamma - I \cdot 1 & < & 0. \end{cases} \tag{4.16}$$

In addition, we assume $\gamma \leq I$. Otherwise, an agent would always prefer having a neighboring AP over sharing the rate. Similarly, the following conditions must hold if an agent sets up an AP to maximize social welfare, assuming there is no AP in the nearest

neighborhood:

$$\begin{cases} R - C - 2I \cdot 0 & > & 0, \\ R - C - 2I \cdot 1 & < & 0. \end{cases} \tag{4.17}$$

4.3.1.2. $1 < \mathbf{H}_{th} < 2$**.** In this case, an agent will set up an AP in a Nash equilibrium only if no more than one of her neighbors sets up an AP. γ and I must satisfy

$$\begin{cases} R - C - 4\gamma - I \cdot 1 & > & 0, \\ R - C - 4\gamma - I \cdot 2 & < & 0. \end{cases} \tag{4.18}$$

The analogous conditions for maximizing social welfare must hold:

$$\begin{cases} R - C - 2I \cdot 1 & > & 0, \\ R - C - 2I \cdot 2 & < & 0. \end{cases} \tag{4.19}$$

4.3.1.3. $2 < \mathbf{H}_{th} < 3$**.** An agent will set up an AP in a Nash equilibrium only if no more than two neighbors set up APs. For this case, γ and I must satisfy

$$\begin{cases} R - C - 4\gamma - I \cdot 2 & > & 0, \\ R - C - 4\gamma - I \cdot 3 & < & 0, \end{cases} \tag{4.20}$$

and to maximize social welfare,

$$\begin{cases} R - C - 2I \cdot 2 & > & 0, \\ R - C - 2I \cdot 3 & < & 0. \end{cases} \tag{4.21}$$

For the remaining two cases ($3 < \mathbf{H}_{th} < 4$ and $\mathbf{H}_{th} > 4$), similar conditions for the potential function P and the social welfare SW can be obtained easily and we omit them here.

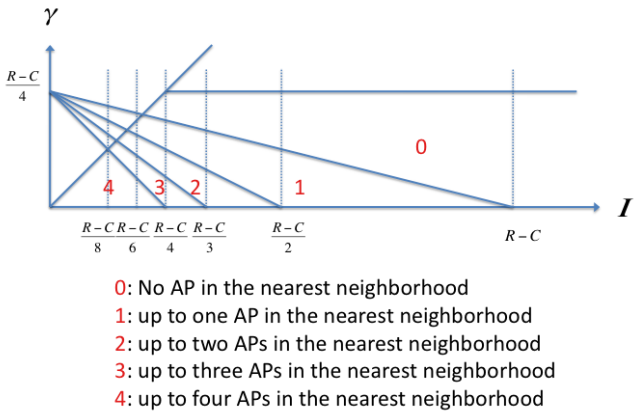

Figure 4.1. Maximum number of APs allowed in the nearest neighbors for pure Nash equilibrium and the feasible region for Interference I and shared rate γ.

Figures 4.1 and 4.2 summarize these cases. Figure 4.1 shows the values of I and γ for pure strategy Nash equilibria to exist in each case. These values lie in one of five regions; each region is labeled with the maximum number of neighboring APs for which an agent's best response will be to set up an AP (e.g., region 0 corresponds to case $0 < \mathbf{H}_{th} < 1$). Figure 4.2 shows the values of I and γ for the socially optimum solution to have the same structure.

Proposition 7. *Consider the game Γ_{PBNN} with the set of strategies $Y_{ij} = \{0, 1\}$. For given interference level I, there exist a set of γ such that a Nash equilibrium achieves the optimal social welfare.*

For example, if $I \geq \frac{R-C}{2}$, a set of γ, which satisfies the conditions of the potential function for the case $0 < \mathbf{H}_{th} < 1$ induces a Nash equilibrium which might correspond to the optimal strategy. On the other hand, if $I \in [\frac{R-C}{4}, \frac{R-C}{2}]$, a set of γ, which satisfies the conditions of the potential function in case $2 < \mathbf{H}_{th} < 3$, might generate a Nash

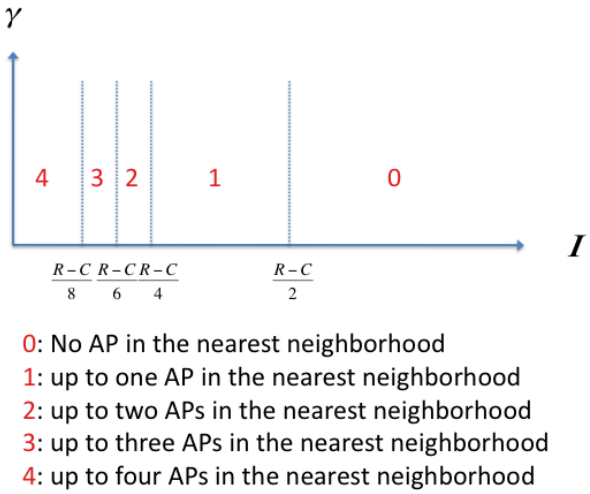

Figure 4.2. Maximum number of APs allowed in the nearest neighbors for the optimal social welfare and the feasible region for interference I and shared rate γ.

equilibrium in which there exists an AP with two APs in the nearest neighborhood. This Nash equilibrium cannot be socially optimal.

The AP deployment game may not have a unique Nash equilibrium. Consider a 3×3 lattice with the periodic boundary condition as an example. If γ and I are such that no AP in the nearest neighborhood H_{ij} is allowed when agent l_{ij} sets up an AP ($0 < \mathbf{H}_{th} < 1$), then there exists only one Nash equilibrium with three APs in the lattice. Namely, three among nine agents decide to set up APs at the Nash equilibrium. On the other hand, if up to two APs are allowed in the nearest neighborhood ($2 < \mathbf{H}_{th} < 3$), then there exist two Nash equilibria with either 5 or 6 APs in the lattice.

4.3.2. Mixed Nash Equilibrium

We next consider the mixed extension of the potential game Γ_{PBNN}. In this game, each agent l_{ij} can be viewed as having strategy space $Y_{ij} = [0, 1]$, where an action $y_{ij} \in Y_{ij}$ can be viewed as the probability that l_{ij} sets up an AP. An agent's payoff is then the expected value of (4.3) with respect to the actions chosen by every other agent. Since the payoff is linear in the action, it can be seen that the first-order derivative of the potential function is given by (4.12) and the second-order derivative is given by

$$\frac{\partial^2 P}{\partial y_{ij} \partial y_{kl}} = \begin{cases} -I, & (k,l) \in H_{ij}, \\ 0, & (k,l) \notin H_{ij}. \end{cases} \tag{4.22}$$

Since the Hessian of the potential function P is negative semi-definite, P is a concave function with a unique global maximum. In addition, $\frac{\partial P}{\partial y_{ij}} = \frac{\partial \pi_{ij}}{\partial y_{ij}}$ for all agents $l_{ij} \in L_1 \times L_2$. Therefore, the best response updates of agents in the potential game reach this global maximum of the potential function, which corresponds to the unique mixed Nash equilibrium. This gives the following proposition.

Proposition 8. *Γ_{PBNN} has a unique mixed strategy Nash equilibrium, which is symmetric.*

The mixed extension of Γ_{PBNN} can be interpreted as a game in which all agents install an AP, but only use it a fraction of the time, indicated by y_{ij}. Individual agents do not coordinate their usage.

Assume each agent chooses the same strategy, namely, $y_{11} = y_{12} = \cdots = y_{L_1 L_2} = y$. We can then rewrite the potential function as

$$P(y) = (L_1 \cdot L_2)\{(R - C - 4\gamma)y - 2Iy^2\}, \tag{4.23}$$

and so

$$\frac{\partial P(y)}{\partial y} = (L_1 \cdot L_2)\{(R - C - 4\gamma) - 4Iy\}. \tag{4.24}$$

It follows that the mixed Nash equilibrium strategies are given by $y_{ij}^{\mathrm{NE}} = y^{\mathrm{NE}}$ for all agents, where

$$y^{\mathrm{NE}} = \begin{cases} 0, & \frac{R-C-4\gamma}{4I} < 0, \\ 1, & \frac{R-C-4\gamma}{4I} > 1, \\ \frac{R-C-4\gamma}{4I}, & \text{otherwise.} \end{cases} \tag{4.25}$$

Similarly, assuming symmetric strategies, the social welfare[8] and its first-order derivative are given by

$$SW(y) = (L_1 \cdot L_2)\{(R - C)y - 4Iy^2\}, \tag{4.26}$$

and

$$\frac{\partial SW(y)}{\partial y} = (L_1 \cdot L_2)\{(R - C) - 8Iy\}. \tag{4.27}$$

[8]The social welfare function is also concave since its Hessian is given by

$$\frac{\partial^2 SW}{\partial y_{ij} \partial y_{kl}} = \begin{cases} -2I, & (k,l) \in H_{ij} \\ 0, & (k,l) \notin H_{ij} \end{cases}$$

and is negative semi-definite.

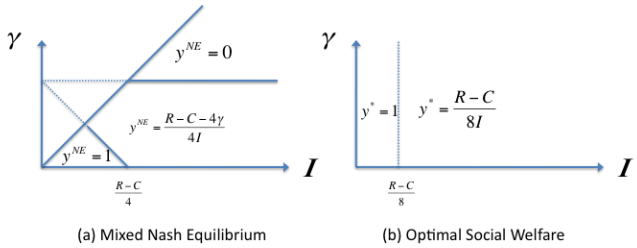

Figure 4.3. Interference I and shared rate γ for mixed Nash equilibrium and social optimum.

It follows that the social welfare is maximized if $y_{ij} = y^*$ for all l_{ij}, where

$$y^* = \begin{cases} 0, & \frac{R-C}{8I} < 0, \\ 1, & \frac{R-C}{8I} > 1, \\ \frac{R-C}{8I}, & \text{otherwise.} \end{cases} \tag{4.28}$$

Figure 4.3 shows the values of I and γ corresponding to different mixed Nash equilibria and the optimal social welfare. In the overlapped region where $y^{\text{NE}} = 1$ and $y^* = 1$, the mixed Nash equilibrium achieves the optimal social welfare. In general, however, the social welfare at the Nash equilibrium does not correspond to the optimal social welfare. We consider the efficiency of the Nash equilibrium for three possible ranges of I next.

4.3.2.1. $I \in [0, \frac{R-C}{8}]$**.** As we can see from Figure 4.3, for given interference $I \in [0, \frac{R-C}{8}]$, the mixed strategy Nash equilibrium is $y^{\text{NE}} = 1$ and the probability for setting up an AP to achieve the optimal social welfare is $y^* = 1$. Therefore, the efficiency at the Nash equilibrium, defined by the ratio of the social welfare at y^{NE} vs. at y^* is given by

$$\varepsilon = \frac{SW(y^{\text{NE}} = 1)}{SW(y^* = 1)} = 1, \tag{4.29}$$

regardless of $\gamma \in [0, I]$.

4.3.2.2. $I \in [\frac{R-C}{8}, \frac{R-C}{4}]$**.** In this case, there are two possible regions depending on the shared rate γ. If $0 \leq \gamma \leq \frac{R-C-4I}{4}$, then the Nash equilibrium strategy is $y^{\mathrm{NE}} = 1$, whereas the optimal probability is $y^* = \frac{R-C}{8I}$. The efficiency is then given by

$$\varepsilon = \frac{SW(y^{\mathrm{NE}} = 1)}{SW(y^* = \frac{R-C}{8I})} = \frac{16I}{(R-C)} - \frac{64I^2}{(R-C)^2}, \tag{4.30}$$

and, therefore, the efficiency does not depend on the shared rate γ. If $\frac{R-C-4I}{4} \leq \gamma \leq I$, then the Nash equilibrium strategy and the optimal probability are $y^{\mathrm{NE}} = \frac{R-C-4\gamma}{4I}$ and $y^* = \frac{R-C}{8I}$, respectively, and the efficiency is

$$\begin{aligned} \varepsilon &= \frac{SW(y^{\mathrm{NE}} = \frac{R-C-4\gamma}{4I})}{SW(y^* = \frac{R-C}{8I})} \\ &= 4\left\{ \frac{R-C-4\gamma}{R-C} - \left(\frac{R-C-4\gamma}{R-C} \right)^2 \right\}. \end{aligned} \tag{4.31}$$

Since $\frac{R-C-4I}{4} \leq \gamma \leq I$, the range of the efficiency for given I is $\varepsilon_{\min} \leq \varepsilon \leq 1$, where $\varepsilon_{\min}$ is given by (4.30).

4.3.2.3. $I \in [\frac{R-C}{4}, \infty]$**.** Similarly, there are two possible regions depending on the shared rate γ. If $0 \leq \gamma \leq \frac{R-C}{4}$, the efficiency is given by (4.31) and the range is $0 \leq \varepsilon \leq 1$. On the other hand, if $\frac{R-C}{4} \leq \gamma \leq I$, the efficiency is $\varepsilon = 0$ because $y^{\mathrm{NE}} = 0$.

Proposition 9. *For any R, C, and I, there exists a γ so that the unique mixed strategy Nash equilibrium of Γ_{PBNN} is efficient.*

If the interference level is $I \in [0, \frac{R-C}{8}]$, then the mixed strategy Nash equilibrium is efficient for any $\gamma \leq I$. If $I > \frac{R-C}{8}$, then the rate sharing should be $\gamma = \frac{R-C}{8}$ to have an efficient Nash equilibrium.

4.4. Generalization

In this section, we generalize the previous results. First, we relax the constraint on the same shared rate γ among all agents in the lattice and allow this rate to be different. The shared rate from the AP of agent l_{kl} to agent l_{ij} is denoted by $\gamma_{kl \to ij}$. Assuming $\gamma_{kl \to ij} = \gamma_{ij \to kl}$,[9] we can show that the potential function is now given by

$$\begin{aligned} & P(y_{11}, y_{12}, \ldots, y_{L_1 L_2}) \\ & = (R-C) \left(\sum_{i=1}^{L_1} \sum_{j=1}^{L_2} y_{ij} \right) - \sum_{i=1}^{L_1} \sum_{j=1}^{L_2} y_{ij} \left(\sum_{kl \in H_{ij}} \gamma_{kl \to ij} \right) \\ & \quad - \frac{1}{2} \sum_{i=1}^{L_1} \sum_{j=1}^{L_2} y_{ij} \left(\sum_{kl \in H_{ij}} y_{kl} \cdot I \right). \end{aligned} \tag{4.32}$$

Second, we can remove the periodic boundary condition and consider edge effects in the lattice. We can still show that the game is a potential game with the potential function in (4.32). Note that H_{ij} does not always contain 4 nearest neighbors as with the periodic boundary condition. In addition, if mixed strategy Nash equilibria are considered (as in

[9] If this condition does not hold, (4.32) is no longer a potential function.

Section 4.3.2), the potential function (4.32) can be simplified to

$$\begin{aligned} & P(x,y,z) \\ & = (R-C)L^2 - 4(L-2)^2\gamma x - 12(L-2)\gamma y - 8\gamma z \\ & \quad - 2(L^2-5L+6)Ix^2 - 4(L-2)Ixy \\ & \quad - 4(L-3)Iy^2 - 8Iyz, \end{aligned} \tag{4.33}$$

where $x \in [0,1]$ is the strategy of an agent who has 4 nearest neighbors, $y \in [0,1]$ is that of an agent who has 3 nearest neighbors, and $z \in [0,1]$ is that of an agent who has 2 nearest neighbors. Here, we assume $L_1 = L_2 = L$ for simplicity. Since the potential function (4.33) is a concave function, the mixed Nash equilibrium can again be found easily.

Finally, we can include interference from APs beyond the nearest neighbors. This might be relevant when the density of APs increases or the transmission power of each AP increases relative to the node density. Assuming interference only depends on the distance between two APs, interference from the AP of agent l_{kl} to the AP of agent l_{ij} is given by

$$I_{kl \to ij} = \frac{I}{|(k,l)-(i,j)|^a}, \tag{4.34}$$

where a is the path-loss exponent. Note that $I_{kl\to ij} = I_{ij\to kl}$. The potential function of the game is then given by

$$\begin{aligned} & P(y_{11}, y_{12}, \ldots, y_{L_1 L_2}) \\ & = (R - C)\left(\sum_{i=1}^{L_1}\sum_{j=1}^{L_2} y_{ij}\right) - \sum_{i=1}^{L_1}\sum_{j=1}^{L_2} y_{ij}\left(\sum_{kl\in H_{ij}} \gamma_{kl\to ij}\right) \\ & \quad - \frac{1}{2}\sum_{i=1}^{L_1}\sum_{j=1}^{L_2} y_{ij}\left(\sum_{kl\in\{L_1\times L_2\}} y_{kl}\cdot I_{kl\to ij}\right). \end{aligned} \tag{4.35}$$

Here, we are still assuming that rate sharing is only between nearest neighbors. As discussed in Section 4.1, we can relax this constraint. The social welfare function is the same as in (4.11) except that the interference from the APs beyond the nearest neighbors is included. As we will see in Section 4.5, if interference is severe, then an agent is less likely to set up her own AP at a Nash equilibrium even when $\gamma > 0$ and this reduces the sum of the agents' payoffs in the lattice. This suggests that as interference becomes severe due to an increase in AP density, implementing such a commons approach becomes more difficult and other forms of spectrum sharing (e.g., a secondary market) may be more appropriate.

4.5. Simulation Results

We now present Matlab-simulation results to illustrate properties of the AP deployment game. We begin with a game with periodic boundary conditions and nearest neighbor interference, as in Figure 4.4. The strategy space of an agent in the game is $Y_{ij} = \{0, 1\}$ for all agents l_{ij}. Figure 4.5 shows one realization of the convergence of best response updates to a pure Nash equilibrium with parameters $L_1 = L_2 = 100$, $R = 10$, $C = 3$, $I = 1.6$

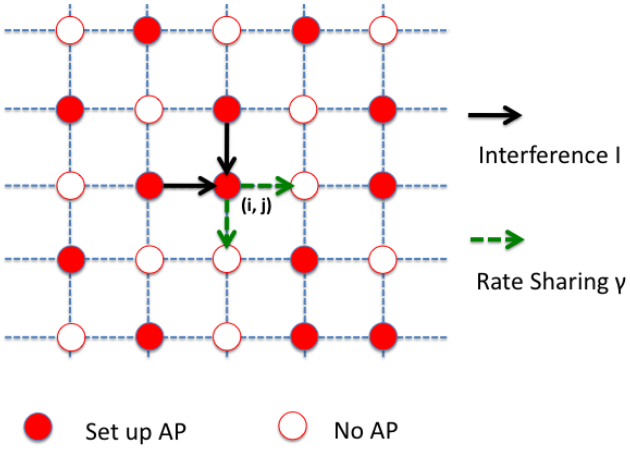

Figure 4.4. Agents in the lattice decide whether or not to set up their own APs. Here we only consider interference from the nearest neighbor APs.

and $\gamma = 0.7$. Initial decisions of agents in the lattice are randomly chosen. At each iteration, all agents in the lattice are randomly ordered and sequentially choose their best response. Therefore, during one iteration in Figure 4.5, $100 \times 100 = 10^4$ agents make their decisions.

The above parameters allow up to two nearest APs at a pure Nash equilibrium, which corresponds to the case $2 < \mathbf{H}_{th} < 3$ in Section 4.3.1.3. As we can see easily, the optimal configuration with these parameters is to have a chess board-like deployment of APs in the lattice, so that there is no AP in the nearest neighborhood when a user sets up her own AP. Therefore, the average number of APs per agent (per lattice point) at the optimal configuration is 0.5 with the average payoff per agent $\frac{10-3}{2} = 3.5$. On the other hand, in the commons model without shared rate ($\gamma = 0$), every selfish agent in the lattice sets up her own AP. This reduces the average payoff per agent to $10 - 3 - 4 \times 1.6 = 0.6$,

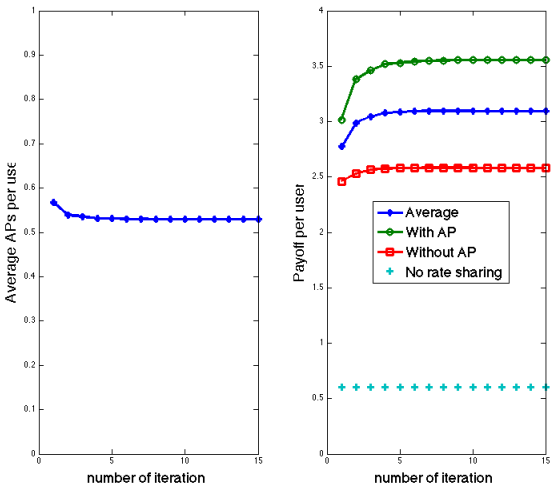

Figure 4.5. Game in the lattice with a periodic boundary condition. $L_1 = L_2 = 100, R = 10, C = 3, I = 1.6$ and $\gamma = 0.7$. (a) Average number of APs per agent (b) Average payoff per agent for different decisions.

which is substantially lower than the payoff at the optimal configuration. As discussed in Section 4.1, this outcome can be viewed as an example of the "tragedy of the commons".

Now we consider the shared rate $\gamma = 0.7$. From Section 4.3, this allows up to two APs in the nearest neighborhood at a Nash equilibrium. The Best response updates of agents in the game converge to a Nash equilibrium with a more desirable average payoff per agent. After a transition period, Figure 4.5 shows that the average number of APs per agent converges to ~ 0.527 and the average payoff per agent to ~ 3.1, which are closer to the socially optimal configuration of APs. In addition, it shows the average payoff per agent with and without an AP. We achieve this near optimality simply by introducing rate sharing among agents.

Note that the Nash equilibrium is not unique as we discussed before and the final results (average number of APs and average payoff per agent) may be different at each

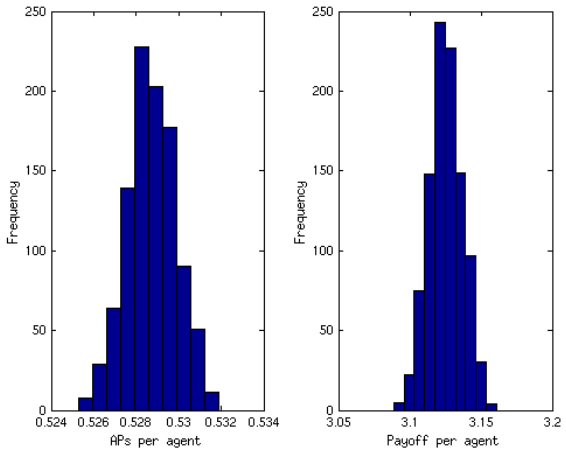

Figure 4.6. Histogram of average number of APs and average payoff per agent at Nash equilibrium. Total number of simulation runs is 1000. $L_1 = L_2 = 100, R = 10, C = 3, I = 1.6$ and $\gamma = 0.7$.

simulation run. With a large lattice size, however, these differences are relatively small. We simulated 1000 times with the same parameters and our results (See Figure 4.6) show that average of the average number of APs and the average payoff per agent over 1000 realizations are 0.5287 (standard deviation 0.0011) and 3.1254 (standard deviation 0.0116) respectively. However, this does not mean we sampled all possible Nash equilibria in the simulation. In fact, we did not realize the optimal density of 0.5 even though it is possible with the chosen parameters.

Figure 4.7 shows one realization of the average number of APs and the average payoff per agent as a function of the shared rate γ. If we consider many realizations of the simulation, each point in the figure should be replaced by a distribution such as Figure 4.6. The overall trend of the figure with mean values, however, will be the same. From the figure, we can see that over a wide range of γ, the average payoff per agent is close to the optimal value.

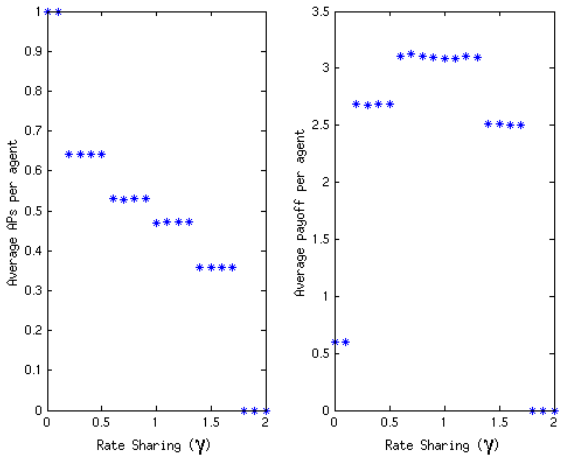

Figure 4.7. Average number of APs and average payoff per agent at a Nash equilibrium as a function of the shared rate γ. Every point in the Figure is one particular realization. Other parameters are the same ($L_1 = L_2 = 100, R = 10, C = 3, I = 1.6$).

Now we remove the periodic boundary condition from the game. Agents at the edge of the lattice have fewer nearest neighbors and this encourages them to set up the APs. One realization shows that the average APs per agent increases to ~ 0.546. The average payoff per agent does not change much. We further generalize this game and include interference from the APs beyond the nearest neighbors. As we expect, fewer agents decide to set up their own APs due to excessive interference. If the path-loss exponent in (4.34) is assumed to be $a = 4$, then the average number of APs per agent is ~ 0.475 (average payoff per agent ~ 2.15). With the path-loss exponent $a = 3$, the average number of APs per agent becomes ~ 0.357 (average payoff per agent ~ 1.30).

As interference increases, more agents decide not to set up an AP even though there are no APs available with which she can share the rate. This configuration with relatively low density of APs in the lattice is close to the optimal configuration with severe interference.

Our calculations in Section 4.7 show that the optimal density of APs per agent is ~ 0.424 when $a = 4$ and ~ 0.330 when $a = 3$. However, even if the shared rate scheme achieves the near optimal configuration, the overall average payoff per agent becomes small because of the commons model itself. When interference becomes severe, a frequency-division scheme with some frequency reuse factor might increase the average payoff substantially compared to the commons model.

4.6. Chapter Summary

We have considered a game theoretic model of a spectrum commons where non-cooperative users in a lattice decide whether or not to set up their own APs. A simple regulatory measure, rate sharing, is proposed to mitigate the tragedy of the commons. We have shown that the AP deployment game on a lattice is a potential game and that there exist pure and mixed Nash equilibrium. Moreover, by choosing the shared rate appropriately, we achieve a Nash equilibrium in the game, which is efficient. However, with pure strategies other inefficient equilibria may also exist. The potential game was also extended to the case where interference comes from the APs beyond the nearest neighbors. The density of APs in the lattice decreases at the Nash equilibrium as interference becomes severe. This result suggests that as interference becomes severe due to the increase in AP density, implementing such a commons approach becomes more difficult and other forms of spectrum sharing (e.g., a secondary market) may be more appropriate.

4.7. Supplement: Optimal Density of APs in 2-D lattice

We would like to compute the optimal density of APs in two-dimensional lattice even when there exists interference from APs beyond the nearest neighbors. This is, however,

difficult because of the integer optimization nature of the problem. Here we solve the problem approximately by applying mean-field theory, which was originally introduced in the context of statistical physics [**93**].[10]

We consider infinite two-dimensional lattice, namely L_1 and $L_2 \to \infty$ to apply mean-field theory. This implies that the approximation can be used only when the lattice size is relatively large. Assuming interference only depends on the distance between two APs, interference from the AP of a lattice site (k, l) to the AP of a lattice site (i, j) is given by $1/r^a$ as in (4.34), where $r = |(k, l) - (i, j)|$ is the distance between two APs. Since interference decreases as $1/r^a$, we ignore interference from the APs at distance $r > D_m$, where D_m is called an effective interference radius and defined later.

A contribution of a particular lattice site (i, j) to the social welfare is given by

$$SW_{ij} = (R - C)\, y_{ij} - y_{ij} \left(\sum_{|kl-ij|=D_1} y_{kl} \cdot I_{D_1} + \sum_{|kl-ij|=D_2} y_{kl} \cdot I_{D_2} + \cdots + \sum_{|kl-ij|=D_m} y_{kl} \cdot I_{D_m} \right), \tag{4.36}$$

where D_n is the distance of n-th nearest neighbors from the site (i, j) and $I_{D_n} = \frac{I}{|D_n|^a}$ is interference from the n-th nearest neighbor AP. Here interference from the nearest neighbor AP is given by I. The social welfare of the entire lattice is obtained by $SW = \sum_i \sum_j SW_{ij}$. As an approximation we replace sum of interference from all the APs at

[10]We can obtain the exact solution for the optimal density of APs for a one-dimensional lattice.

distance $r \leq D_m$ in the second term of (4.36) by its mean value, or

$$\begin{aligned} H_m &\equiv \left\langle \sum_{|kl-ij|=D_1} y_{kl} \cdot I_{D_1} + \cdots + \sum_{|kl-ij|=D_m} y_{kl} \cdot I_{D_m} \right\rangle \\ &=< y > \cdot \left(\sum_{n=1}^{m} N_{D_n} \cdot I_{D_n} \right), \end{aligned} \tag{4.37}$$

where $< \cdot >$ represents an ensemble average and N_{D_n} is the number of nearest neighbor APs at distance D_n. H_m should be determined in such a way that it leads to a self-consistent solution of the statistical problem. Then, (4.36) is represented by

$$SW_{ij} = (H - H_m) \cdot y_{ij}, \tag{4.38}$$

where $H = R - C$. Since $y_{ij} \in \{0, 1\}$, the ensemble average of the strategy is given by

$$\begin{aligned} < y > &= 1 \times \text{Prob}(SW_{ij} = H - H_m) \\ &\quad + 0 \times \text{Prob}(SW_{ij} = 0) \\ &= \frac{e^{\beta(H-H_m)}}{1 + e^{\beta(H-H_m)}} \end{aligned} \tag{4.39}$$

from statistical physics, where β is a temperature parameter and it is inversely proportional to temperature [**93**]. From (4.37) and (4.39), we can compute H_m and $< y >$. The parameter $\beta \to \infty$ to obtain an average number of APs per user $< y >_{\text{opt}}$ when the optimal social welfare is achieved. The parameter $\beta \to \infty$ means that temperature of the physical system goes to absolute zero. Then the system reaches the ground state, which

is the optimal social welfare in the case considered here. The solution is given by

$$< y >_{\text{opt}} = \begin{cases} 1, & \sum_{n=1}^{m} N_{D_n} \cdot I_{D_n} \leq H, \\ \frac{H}{\sum_{n=1}^{m} N_{D_n} \cdot I_{D_n}}, & \sum_{n=1}^{m} N_{D_n} \cdot I_{D_n} > H. \end{cases} \tag{4.40}$$

We consider the same example as in Section 4.5. If we assume $a = 4$ and $m = 10$, then the total interference within the effective interference radius D_{10} is $\sum_{n=1}^{10} N_{D_n} \cdot I_{D_n} = 16.530$. The average density of APs per user with the optimal social welfare is, then, given by $< y >_{\text{opt}} = 7/16.5307 = 0.424$. This is close to ~ 0.475, which is obtained by simulation in Section 4.5. With $a = 3$, the average density of APs per user is $< y >_{\text{opt}} = 0.330$ (~ 0.357 from simulation). The total interferences with $m = 10$ and $m = 30$ are not much different (16.530 vs. 16.565), and therefore this justifies the assumption of the effective interference radius D_m.

CHAPTER 5

Sequential Second Price Auction as a resource allocation mechanism

One dynamic spectrum sharing method among non-cooperative agents based on a commons model was studied in the previous chapter. In this chapter, we consider an auction mechanism, the sequential second price auction, for dynamic spectrum sharing and examine its efficiency when each user has full information about the other users' utilities.[1] In the sequential second price auction, the resource is divided into n identical units, and each unit is auctioned off sequentially. Assuming full information, the auction can be viewed as an extended form game, and we investigate the subgame perfect equilibrium through backward induction and lower bound its efficiency. Although having full information may not be true in practice, it makes the corresponding game relatively tractable. In addition, it provides substantial insight into advantages and shortcomings of the mechanism.

For two users and an arbitrary number of resource units, our results show that the sequential second price auction has a unique allocation among two users in a subgame perfect equilibrium.[2] We characterize the worst-case efficiency loss of this equilibrium for the case where each agent has a concave utility for the spectrum resource, and the case

[1]This is in contrast to previous work in which the utilities are assumed to be private, and bidders have unit demand [**77, 113**].
[2]See Section 5.2 for a precise definition of the equilibrium concept we use.

where one agent has a concave utility and the other agent has a convex utility. The former case models the bandwidth auction, while the latter can arise in the power auction, when a user bids to reduce interference.

We also present simulation results for the efficiency loss when the two users' channel gains are randomly generated. The utility function for each user is the maximum achievable (Shannon) rate, where interference is treated as background noise. The results show that except for a small fraction of realizations, the equilibrium allocation is efficient. Furthermore, we show that lower bound of the worst-case efficiency for the bandwidth auction increases due to constraints on the marginal utilities imposed by logarithmic properties of the Shannon rate function.

For more than two users, each with a concave utility function, we show that the auction has at least one pure strategy equilibrium. Furthermore, the equilibrium allocation may not be unique. Hence, some coordination of the users may be required to decide on a particular outcome. This makes characterizing the efficiency loss more difficult. Numerical results show that the empirical distribution of the efficiency for the bandwidth auction with three users is stochastically better than that with two users. This suggests that the worst-case efficiency loss is attained with two users.

5.1. Spectrum Sharing Model

We consider a model for spectrum sharing among k users, where each user consists of a distinct transmitter-receiver pair. As in [**36, 52**], we model this as a k-user Gaussian interference channel with frequency flat fading. The channel gain between user i's transmitter and user j's receiver is denoted by h_{ij}. Each transmitter has an average power

constraint P, and the total available bandwidth is W Hz. We further assume that each transmitter uses an optimal (capacity achieving) code, where the received interference is treated as background noise (i.e., no interference cancellation is used).

We focus on two spectrum sharing techniques: frequency division multiplexing (FDM) and spread-spectrum signaling with frequency-flat power allocations across the entire band.[3] With FDM, each user i receives bandwidth W_i, where $\sum_j W_j = W$, and achieves rate

$$r_i(W_i) = W_i \log(1 + \tfrac{h_{ii}P}{N_0 W_i}), \tag{5.1}$$

where N_0 is the power spectral density of the additive noise. With full spreading, user i receives power $P_i \in [0, P]$ and achieves rate

$$r_i(P_i, P_{-i}) = W \log(1 + \tfrac{h_{ii}P_i}{N_0 W + \sum_{j \neq i} h_{ji} P_j}), \tag{5.2}$$

where P_{-i} is the vector of powers of all users except i. Each agent is endowed with a utility function, $U_i(r_i)$, which is increasing and concave.

Assume that agent 1 is initially using the spectrum with a given bandwidth or power allocation, and agents $2, \ldots, k$ want to share this spectrum. The spectrum manager divides the appropriate resource into n units and re-allocates these units among the k agents. In the FDM case, each resource unit represents a frequency band of W/n Hz. The manager either re-allocates a unit to some agent i or lets agent 1 continue to use that unit. Let u_s^i be agent i's marginal utility for receiving her s-th unit, i.e., $u_s^i =$

[3]More generally, the users could each pick a power allocation over frequency; our choices represent two specific classes of power allocations. Restricting ourselves to these classes simplifies resource allocation. Furthermore, for many choices of channel gains, the optimal power allocation is in this set [**36**].

$U_i(r_i(sW/n)) - U_i(r_i((s-1)W/n))$. From (5.1), it follows that the marginal utilities of each agent are decreasing, i.e. $u_1^i \geq \ldots \geq u_n^i$.

In the full-spread case, the manager allows each agent $i \neq 1$ to continue transmitting at its current power, P_i, and only allocates the power of agent 1 ($P_1 = P$) among all agents. Each allotted unit represents a power increment of P/n. A unit allocated to agent 1 allows her to increase her transmission power, whereas a unit allocated to agent $i \neq 1$ decreases the power assigned to agent 1, thereby reducing agent i's interference. Agent 1's marginal utility for the s-th unit is $u_s^1 = U_1(r_1(sP/n, P_{-1})) - U_1(r_1((s-1)P/n, P_{-1}))$, which is again decreasing in s. On the other hand, the marginal utility for agent $i \neq 1$ depends on how many units she receives as well as how many units agent 1 receives (which increases her interference).[4] For two agents, given that agent 2 receives s units at the end of the auction, agent 1 must receive $n-s$ units. Therefore, agent 2's marginal utilities are given by $u_s^2 = U_2(r_2(P_2, (n-s)P/n)) - U_2(r_2(P_2, (n-s+1)P/n))$, which is not necessarily decreasing in s. For example, if $U_2(r_2)$ is linear, then u_s^2 is increasing in s.[5] Here, we focus on the case of two agents, which corresponds to the case where a node has only one dominant interferer. For more than two agents, agent $i \neq 1$'s marginal utilities can not be written in terms of only her allocation, which complicates the analysis.[6]

[4]Note in the bandwidth allocation, the marginal utilities of one agent do not depend on how many units any other agent receives.

[5]Indeed user 2's marginal utilities may be neither increasing nor decreasing for all s. In general this depends on the utility, the choice of channel gains and the power levels. A necessary condition for the marginal utilities to be increasing or decreasing can be given in terms of the utility's coefficient of relative risk aversion, as in [**52**].

[6]In particular for more than two agents whenever an agent $i \neq 1$ is allocated a unit, it decreases the interference for all agents $j \neq 1$ thus providing agents an incentive to "free-ride" on each other.

5.2. Sequential Second-Price Auction

For a given spectrum sharing technique, we consider the case where each of the n resource units is allocated among k agents via a sequential second-price auction. In this auction, the units are allocated sequentially in n rounds. In round $m \leq n$, each agent submits a bid for the m-th unit. The auctioneer allocates this unit to the agent with the largest bid and charges that agent the second largest bid. We refer to this as a bandwidth (power) auction in the FDM (full-spread) case.

This mechanism can be viewed as an extended form game with a balanced k-ary game tree. Each decision node in the game tree designates a state of the world, where a certain quantity of goods (resource units) are allocated to agents $1, \ldots, k$. Let $\mathbf{s} = (s_1, \ldots, s_k)$ denote such an allocation. Since the goods are homogeneous, the decision nodes with the same allocation are indistinguishable and the game tree can be replaced with a directed graph $G = (V, E)$, where $V = \{\mathbf{s} \in [1, \ldots, n]^k | \sum_{i=1}^{k} s_i \leq n\}$ (see Fig. 5.1). A node $\mathbf{s} \in V$ represents the outcome of the $(\sum_{i=1}^{k} s_i)$-th round, in which agent i has been allocated s_i. For $\sum_{i=1}^{k} s_i < n$, each node $\mathbf{s}$ has directed edges to k children $(s_1, \ldots, s_i + 1, \ldots, s_k)$, $i = 1, \ldots, k$; the i-th edge corresponds to agent i winning the current round. The auction begins at the root node $(0, \ldots, 0)$.

Let u_j^i denote the marginal utility of agent i for the j-th unit. Agent i's total utility for receiving s_i units is $\sum_{j=1}^{s_i} u_j^i$. Let H designate the set of observable bidding histories. A *strategy* $\sigma_i : V \times H \rightarrow \Re^+$ is a function mapping states of the allocation and observable histories to bids. The strategy set of an agent is the set of all such functions. The outcome path of a strategy profile $\{\sigma_1, \ldots, \sigma_k\}$ is a directed path $\delta = \{\mathbf{s}^1, \ldots, \mathbf{s}^n\}$ in G such that if $s_i^{t+1} = s_i^t + 1$ and $s_j^{t+1} = s_j^t$ for $j \neq i$ then $\sigma_i(\mathbf{s}^t, \Gamma_t) \geq \sigma_j(\mathbf{s}^t, \Gamma_t)$, for all $j \neq i$, where Γ_t is

the bidding history of the first t units.[7] The total payment of agent i along the path δ is $P_i(\delta) = \sum_{t=1}^{n} p_i(\mathbf{s}^t)$, where for each $\mathbf{s}^t \in \delta$, $p_i(\mathbf{s}^t) = \max\{\sigma_j(\mathbf{s}^t, \Gamma_t) : j \neq i\}$ if $s_i^{t+1} = s_i^t + 1$ and $p_i(\mathbf{s}^t) = 0$, otherwise.

We consider two types of bidding strategies: *myopic* and *sophisticated*. A *myopic* bidding strategy maximizes the immediate payoff during each round. Hence, myopic agents bid their marginal utilities in each round, i.e., $\sigma_i(\mathbf{s}^t, \Gamma_t) = u^k_{s_i^t+1}$. When all agents have decreasing marginal utilities, myopic bidding results in an efficient outcome.[8] This strategy may be an equilibrium depending on the information structure of the extended form game (i.e., the strategy may be rationalized [**85**]). For example, if the agents do not know the number of units on the market or the marginal utilities of the other agents, it may be rational to myopically bid every round under the belief that the current round is the terminal round.[9] We will see, however, that under full information myopic bidding is generally not a dominant strategy.

A *sophisticated* bidding strategy maximizes an agent's payoff over final or expected final outcomes. The ability to make inferences about the final outcome requires that the agent be sufficiently informed about the preferences and strategies of the other agent. Here, we assume full information, i.e., each agent knows the number of units being sold, bidding histories, and the marginal utilities of the other agents.

---

[7] In the case of ties, any tie-breaking rule that allocates the good to one of the agents can be used.
[8] This is not always the case if at least one agent has increasing marginal utilities.
[9] If there are no restrictions on the agent's beliefs then virtually any bidding strategy can be rationalized [**85**].

5.3. Analysis for Two Agents

We consider the sequential second price auction with $k = 2$ agents and an arbitrary number of resource units. First we characterize the outcome of this auction with sophisticated bidding and full information. As we discussed in Section 5.2, this auction is viewed as a 2-ary game tree. Since all agents know when the last unit is being sold, regardless of the bidding history, the last round of the auction is a standard second-price auction for the n-th good. (The valuations for this good will, of course, depend on the outcomes of the previous rounds). Hence it is a weakly dominant strategy for the agents to bid their marginal utilities on the last round.[10] Since those valuations are common knowledge, all agents know beforehand the allocation and payments in the last round. Depending on who wins the unit in the penultimate round, however, the last round auction in which both agents participate is different. There are two possible auctions in the last round: one when agent 1 wins and the other when agent 2 wins in the penultimate round. Thus, we can think of the penultimate round as an auction over the right to participate in one of those two auctions in the last round. Since the payoffs of each one of those auctions is common knowledge, we can think of the penultimate round as a second-price auction with valuation equal to payoff difference between those two auctions. It is therefore a weakly dominant strategy in the penultimate round to bid the payoff difference associated with the outcomes of the two auctions in the last round.

We can proceed in this way inductively until we reach the root. This shows that sophisticated bidding is the only strategy that survives iterative elimination of weakly

[10]A strategy is *weakly dominant* for an agent if no other strategy gives that agent a larger pay-off, for any choice of strategies for the other agents.

dominated strategies.[11] This does not rule out other equilibria and in fact there may exist other Nash equilibria with higher payoffs for both agents (if, for example, they conspire against the seller). However, those equilibria must rely on unreliable threats and commitments. We eliminate those equilibria from consideration by focusing on *subgame perfect equilibria* that survive the iterative elimination of weakly dominated strategies.[12] This discussion is summarized in the following theorem.

Theorem 10. *With two fully informed agents, the sophisticated bidding equilibrium is the only subgame perfect equilibrium that survives iterative elimination of weakly dominated strategies.*

We define the *equilibrium path* to be the outcome path when both agents use a sophisticated bidding strategy, and the *sequential allocation* to be the allocation at the terminal node of the equilibrium path. From the previous discussion if all agents apply a sophisticated bidding strategy, all equilibria have the same equilibrium path, and the same (unique) sequential allocation.

Example: Consider a sequential auction with $n = 2$ units. Figure 1 (c) shows the directed graph G with each node labeled by the allocation (s_1, s_2). Assume that $u_1^1 = u_2^1 = 5$, $u_1^2 = 4$ and $u_2^2 = 1$. Since agent 1 values each unit more than agent 2 values any unit, the efficient allocation is to give both units to agent 1.

Now let us derive the outcome under sophisticated bidding in this example. Assume the game reaches node $v = (1, 0)$, so that the agents bid for the one remaining unit, given that the first unit has gone to agent 1. (See Fig. 1 (a).) In this stage it is weakly dominant

[11] In other words all strategies which are weakly dominated are removed from consideration [**85**].
[12] A subgame perfect equilibrium is a refinement of the concept of Nash equilibrium with the restriction that agents cannot make non-credible threats [**85**].

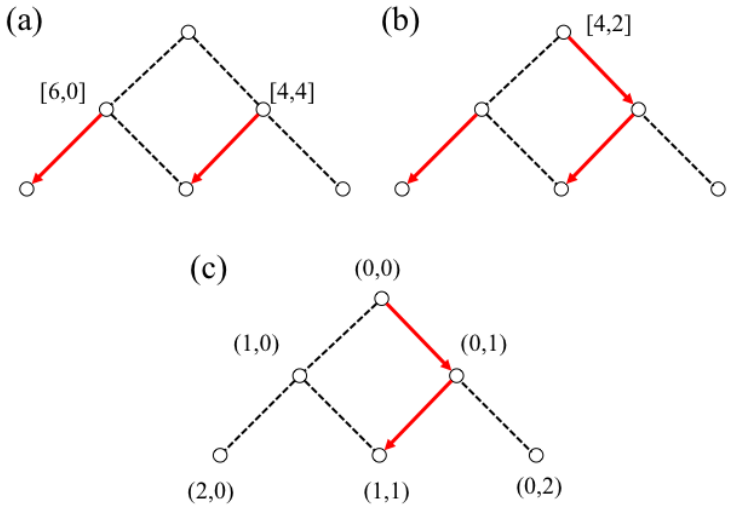

Figure 5.1. Example of the sequential auction with $k = 2$ agents and $n = 2$ resource units. (a) and (b) show the values of each node and (c) shows the equilibrium path.

for the agents to bid their valuations, i.e., agent 1 bids $u_2^1 = 5$ and agent 2 bids $u_1^2 = 4$. The auctioneer then allocates the unit to agent 1 and charges her a price of 4. Hence the value of node $v = (1, 0)$ to agent 1 is $u_1^1 + (u_2^1 - u_1^2) = 6$, where u_1^1 is the value from winning the first unit and $u_2^1 - u_1^2$ is the surplus for winning the second unit. The value of $v = (1, 0)$ to agent 2 is 0. Similarly, the value of $v = (0, 1)$ is 4 to either agent. Given these values, the agents can optimize their bids for the first unit. In particular, agent 1 bids her valuation, which is $6 - 4 = 2$, and agent 2 bids $4 - 0 = 4$. It follows that agent 2 wins the first unit and pays 2. Therefore the equilibrium path is $\delta = \{(0, 0), (0, 1), (1, 1)\}$, i.e., each user receives one unit. Note that δ does not terminate in an efficient allocation. In what follows, we characterize the efficiency loss of this equilibrium.

5.3.1. Efficiency Bound With Decreasing Marginal Utilities

Given n resource units and two agents, let $(l, n-l)$ denote the efficient allocation, and $(l', n-l')$ denote the sequential allocation. The *worst-case efficiency* is defined by

$$\eta(n) = \min_{\{u_i^1\},\{u_i^2\}} \frac{\sum_{i=1}^{l'} u_i^1 + \sum_{i=1}^{n-l'} u_i^2}{\sum_{i=1}^{l} u_i^1 + \sum_{i=1}^{n-l} u_i^2}. \tag{5.3}$$

That is, the worst-case is with respect to the marginal utilities. We refer to $1-\eta(n)$ as the *worst-case efficiency loss*. The next theorem characterizes $\eta(n)$ when each agent has decreasing marginal utilities, as in the bandwidth auction from Section 5.1.

Theorem 11. *In a two-agent sequential second-price auction with decreasing marginal utilities* $\eta(n) \geq 1 - e^{-1}$.

In other words, the worst case efficiency loss is bounded by e^{-1}. Moreover, it can be shown that $\eta(n)$ decreases with n, and the bound $1-e^{-1}$ is asymptotically tight as $n \to \infty$.

5.3.1.1. Worst-Case Utility Profiles. To prove Theorem 11, we first show the worst-case efficiency assuming the marginal utilities of the agents have a particular form. Subsequently, we show that this is also the worst-case efficiency over all possible marginal utilities.

Definition Agent 1's marginal utilities are *dominant* if $u_1^1 \geq \ldots \geq u_n^1 \geq u_1^2 \geq \ldots \geq u_n^2$. We will also refer to this as a *dominant utility profile*. Agent 1's marginal utilities are *flat dominant* if $u_1^1 = \ldots = u_n^1 \geq u_1^2 \geq \ldots \geq u_n^2$.

The efficient allocation for a dominant utility profile is to assign all units to agent 1. In the sequential allocation, however, agent 2 may receive up to $n-1$ units and this

induces the efficiency loss. We denote by $\eta'(n)$ the worst-case efficiency in an auction with n goods when the agents are constrained to having a flat dominant utility profile.

To get some insight, we examine first an example with $n = 2$ goods and $k = 2$ agents with a flat dominant utility profile. Without loss of generality, we assume $u_1^1 = u_2^1 = 1$ for agent 1 and $u_1^2 = b_1, u_2^2 = b_2$ for agent 2. Note that $1 \geq b_1 \geq b_2$. Using backward induction as discussed in the previous example, the value of node $v = (1, 0)$ is $[2 - b_1, 0]$. Similarly, the value of node $v = (0, 1)$ is $[1 - b_2, b_1]$. Given these values, agent 1's bid for the first unit is $(2 - b_1) - (1 - b_2) = 1 - b_1 + b_2$ and agent 2's bid for the first unit is b_1. If $1 - b_1 + b_2 > b_1$, then agent 1 wins the first unit and pays b_1. In this case, the sequential allocation is $(2, 0)$ and there is no efficiency loss. On the other hand, if $1 - b_1 + b_2 < b_1$, the sequential auction reaches the terminal node $(1, 1)$ and the efficiency of the auction becomes $\frac{1+b_1}{1+1}$. This is shown in Figure 5.2. Here, for $\delta = \{(0, 0), (0, 1), (1, 1)\}$ to be equilibrium path we require that

$$\begin{cases} 1 > b_1 > b_2, \\ 1 - b_1 + b_2 < b_1. \end{cases} \tag{5.4}$$

It is easy to see that the lower limit of $\frac{1+b_1}{2}$ subject to (5.4) is approached when $b_1 = 1/2+\epsilon$ and $b_2 = 0$, and so $\eta'(2) = \lim_{\epsilon \to 0} \frac{1+b_1}{2} = 3/4$. Note that when the worst-case efficiency occurs, both $\delta_1 = \{(0, 0), (0, 1), (1, 1)\}$ and $\delta_2 = \{(0, 0), (1, 0), (2, 0)\}$ are equilibrium paths with final values of $[1, 0]$ at the root node $v = (0, 0)$.

We now define a class of subgame perfect equilibrium paths along which agent 2 consumes the first $n - j$ units and agent 1 consumes the remaining j units in that order.

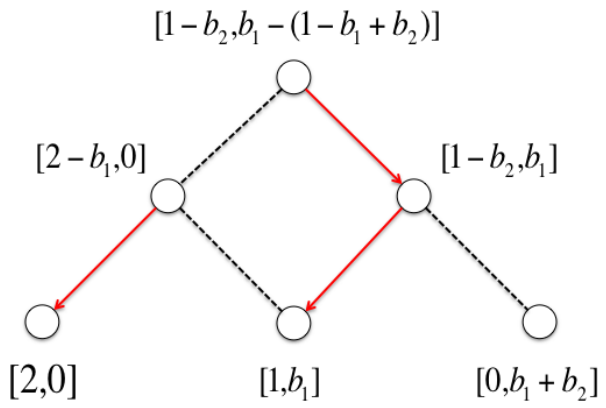

Figure 5.2. The subgame perfect equilibrium path which leads to efficiency loss in the sequential auction with $n = 2$ goods and the following flat dominant utility profile: $u_1^1 = u_2^1 = 1$ for agent 1 and $u_1^2 = b_1$, $u_2^2 = b_2$ for agent 2. The set of constraints required are $1 > b_1 > b_2$ and $1 - b_1 + b_2 < b_1$.

Later, we show that this type of equilibrium path gives the worst-case efficiency for a flat dominant utility profile.

Definition A node on an equilibrium path is a "kink" if immediately prior to that node (on the equilibrium path) one agent wins and immediately following the other agent wins.

Definition A profile of marginal utilities is said to have the *subgame kink property* if (1) each path that corresponds to a subgame perfect equilibrium of the entire game has at most one kink, and (2) each path that corresponds to an equilibrium path for a subgame starting at any node not on a path in (1) has zero kinks.

Definition The subgame perfect equilibrium is called a *subgame kink* when the profile of marginal utilities has the subgame kink property.

The following lemma shows that we can find a flat dominant utility profile such that the subgame perfect equilibrium with n units is a subgame kink.

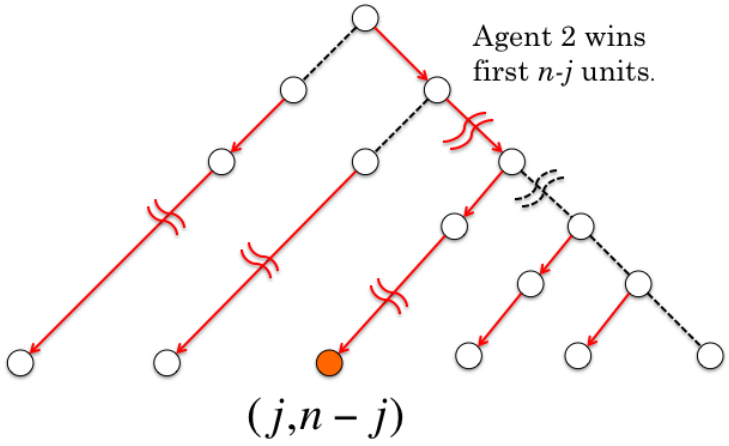

Figure 5.3. An example of a subgame kink equilibrium path resulting in the sequential allocation $(j, n-j)$. There, edges which are part of the equilibrium path of a subgame kink are indicated by a directional solid lines, and off-equilibrium edges are dashed.

Lemma 12. *For any allocation $(j, n-j)$ in a n-unit auction, there is a flat dominant utility profile with the subgame kink property.*

Proof. The following profile of marginal utilities has the subgame kink property with the sequential allocation $(j, n-j)$: $u_1^1 = \cdots = u_n^1 = 1$ for agent 1 and

$$\begin{cases} u_i^2 = 1 - \frac{j}{n-i+1} + \epsilon_i, & i = 1, \cdots, n-j, \\ u_i^2 = 0, & i = n-j+1, \cdots, n, \end{cases} \tag{5.5}$$

for agent 2. Note that $\epsilon_i \to 0^+$ for all i. Backward induction verifies this results in a subgame kink. □

By studying the bids of the agents along the subgame perfect equilibrium path, we come up with the marginal utilities. A detailed explanation is presented in Section 5.7.1. Note that all the sequential allocations $(i, n-i)$ for $i = j, \cdots, n$ are possible with the

marginal utilities in (5.5). In addition, it can be shown that the following relations among the marginal utilities of agent 2 hold:

$$n - n \cdot b_1 = (n-1) - (n-1) \cdot b_2 = \cdots = (j+1) - (j+1) \cdot b_{n-j} = j. \tag{5.6}$$

Lemma 13. *For $n = 2$, the worst-case efficiency among the flat dominant utility profiles is achieved by one with the subgame kink property.*

Proof. We have shown that the worst-case efficiency with $n = 2$ is given by a flat dominant utility profile with $u_1^1 = u_2^1 = 1$, $u_1^2 = 1/2$ and $u_2^2 = 0$ and this profile has the subgame kink property as shown in Figure 5.2. □

For given $b \leq 1$, let $h''(n, b)$ be the worst-case efficiency in a n-unit auction among all flat dominant utility profiles with the subgame kink property *and* for which $b_1 \leq b$ (i.e. agent 2's marginal utility for the first unit is no greater than b). For example, for $n = 2$, if $b < \frac{1}{2}$, then $h''(2, b) = 1$, while for $b \geq \frac{1}{2}$, $h''(2, b) = 3/4$. Note that the first case is achieved when agent 2 has marginal utilities $b_1 = b_2 = 0$, which satisfy Lemma 12 with $j = 2$; the second case is achieved by the marginal utilities $b_1 = \frac{1}{2}$ and $b_2 = 0$ (Lemma 12 with $j = 1$).

Lemma 14. *For all n, $h''(n, b)$ is achieved by one of the marginal utilities in Lemma 12.*

Proof. Proof is by induction on n. As shown above, Lemma 14 is true for $n = 2$. Assume it is true for $n - 1$ and consider the worst-case efficiency of a subgame kink for n units. If the first unit goes to agent 1, we are done since the only subgame kink is for agent 1 to win everything, which corresponds to the marginal utilities in Lemma 12 for $j = n$.

If the first unit goes to agent 2 with a marginal utility of $b_1 < b$, then the worst-case efficiency on the subtree from the node $(0,1)$ must be given by $h''(n-1,b_1)$. By the induction hypothesis this is achieved on the subtree by a set of marginal utilities $b_2, b_3, \ldots, b_n$ given by Lemma 12 for some j. Furthermore, the worst-case efficiency is $(b_1 + (n-1)\cdot h''(n-1,b_1))/n$.

If $b_2, \ldots, b_n$ satisfy Lemma 12 for some j and $n-1$ units, then, in particular, $b_2 = 1 - \frac{j}{n-1}$. At the root node of the n-unit auction, for agent 2 to win the first unit in a subgame kink, it must be that $1 - (n-1)\cdot b_1 + (n-1)\cdot b_2 < b_2$, or

$$n \cdot (1 - b_1) < (n-1) \cdot (1 - b_2). \tag{5.7}$$

By combining this inequality with $b_2 = 1 - \frac{j}{n-1}$, it can be seen that in the worst-case efficiency it should be that $b_1 = 1 - \frac{j}{n}$, which corresponds to Lemma 12. □

Lemma 15. *For all n and $b \leq 1$,*

$$\frac{1 + (n-1)h''(n-1,b)}{n} \geq h''(n,b). \tag{5.8}$$

Proof. Suppose $h''(n-1,b)$ is achieved when agent 1 receives j units. From Lemma 14, it follows that this is achieved by the marginal utilities in Lemma 12 and so $1 - \frac{j}{n-1} < b$.

Consider the marginal utilities from Lemma 12 for n units where agent 1 receives $j+1$ units and note that

$$1 - \frac{j+1}{n} < 1 - \frac{j}{n-1}$$

so that this marginal utility will satisfy $b_1 < b$. Let $\tilde{h}(n,b)$ denote the efficiency achieved with this marginal utility. It can be seen that

$$\begin{aligned} n - n \cdot \tilde{h}(n,b) &= \sum_{i=1}^{n-(j+1)} \frac{j+1}{n-i+1} \\ &\geq \sum_{i=1}^{(n-1)-j} \frac{j}{(n-1)-i+1} \\ &= (n-1) - (n-1) \cdot h''(n-1,b), \end{aligned}$$

or

$$\frac{1+(n-1)\cdot h''}{n} \geq \tilde{h}(n,b) \geq h''(n,b).$$

The bound then follows from noting that $h''(n,b)$ must be no greater than $\tilde{h}(n,b)$. □

Corollary 16. *Amongst all the flat dominant utility profiles with the subgame kink property, the worst-case efficiency is $h''(n,1)$, where $h''(n,1)$ can be obtained explicitly from Lemma 12 and is given by*

$$\eta''(n) \equiv h''(n,1) = \min_{j \in [1,\cdots,n]} \left\{ 1 - \frac{j}{n} \sum_{i=j}^{n-1} \frac{1}{i+1} \right\}. \tag{5.9}$$

Now we are ready to prove the worst-case efficiency of the sequential auction with a flat dominant utility profile. For given $b \leq 1$, let $h'(n,b)$ be the worst-case efficiency in a n-unit auction among all flat dominant marginal utilities for which $b_1 \leq b$. Note that $\eta'(n) = h'(n,1)$.

Theorem 17. *For all n, $h'(n,b)$ is achieved by one of the marginal utilities in Lemma 12, i.e., $h'(n,b) = h''(n,b)$. Especially when $b = 1$, then $\eta'(n) = \eta''(n)$.*

Proof. We prove this by induction on n. From Lemma 13, it is true for $n = 2$. Suppose it is true for $n-1$ and consider a n-unit auction with a given constant b. Let $b_1 \leq b$ be agent 2's marginal utility in the worst-case. If the first unit goes to agent 1, then by induction the equilibrium for the worst-case from $(1,0)$ is a subgame kink with the efficiency $h''(n-1, b_1)$. Suppose that agent 2 wins the second unit, then the worst-case efficiency would be

$$\frac{1 + (n-1) \cdot h''(n-1, b_1)}{1 + n - 1} \geq h''(n, b_1), \tag{5.10}$$

from Lemma 15. If agent 1 wins the second unit, then by induction, the subgame starting at $(1,0)$ has no kinks, and so $h'(n,b) = 1$, which is trivially assumed by the marginal utilities in Lemma 12 for $j = n$.

On the other hand, if the first unit goes to agent 2, by induction we have a subgame kink from the node $(0,1)$ for any marginal utility of b_1 due to Lemma 14. Now we have to show that the subtree starting from the node $(1,0)$ is a line with no kinks for the worst-case efficiency with n units. Given agent 2 wins the first unit in the worst-case, $b_2, \ldots, b_n$ must satisfy Lemma 12 and we have $b_2 = 1 - \frac{j}{n-1}$ for some j. Suppose that the subtree starting from the node $(1,0)$ in the worst-case is not a line. Then it must be that $b_1 < 1 - \frac{j}{n}$. Otherwise, we could lower b_1 to this value and get the subgame kink in Lemma 12 with a lower efficiency. Furthermore, if this subtree is not a line, it must be that for some $m < n$, at node $(n-m, 0)$, $m \cdot (1 - b_1) < (m-1) \cdot (1 - b_2)$. However, this can only be true if $b_1 > 1 - \frac{j}{n}$, which contradicts the above. Therefore, the subtree from the node $(1,0)$ is a line with no kinks for the worst-case efficiency. $\square$

n	Marginals	j^*	$\eta(n)$
2	$1, 1\ ;\ 1/2 + \varepsilon_1, 0$	1	3/4
3	$1, 1, 1\ ;\ 2/3 + \varepsilon_1, 1/2 + \varepsilon_2, 0$	1	13/18
4	$1, 1, 1, 1\ ;\ 1/2 + \varepsilon_1; 1/3 + \varepsilon_2, 0, 0$	2	17/24
$\vdots$	$\vdots$	$\vdots$	$\vdots$
∞			1- $\frac{1}{e}$

Table 5.1. Marginal utilities and corresponding worst-case efficiency achieved by two user the sequential auction for given n.

From Corollary 16 and Theorem 17, the worst-case efficiency of the sequential auction with the flat dominant utility profile $\eta'(n)$ is given by (5.9), which converges to $1 - e^{-1}$ as $n \to \infty$.

In Section 5.7.2, we show that a flat dominant utility profile achieves the worst-case efficiency, so that $\eta(n) = \eta'(n)$. That completes the proof of Theorem 11.

Table 5.1 shows the marginal utilities that give the lowest efficiency $\eta(n)$, which is also shown. As can be seen, $\eta(n)$ is decreasing with n. As $n \to \infty$, these quantities approach the bound from Theorem 11.

5.3.2. Efficiency Bound With Increasing/Decreasing Marginal Utilities

We now assume that agent 1 has increasing marginal utilities, while agent 2's marginal utilities are decreasing. As noted previously, this may arise in the full-spread case due to interference.

Theorem 18. *If the marginal utilities of one agent are decreasing and the other's increasing, then* $\eta(n) \leq \frac{1}{n}$.

Proof. Consider the following marginal utilities: $u_1^1 = a, u_2^1 = \cdots = u_n^1 = \varepsilon$ and $u_1^2 = \cdots = u_{n-1}^2 = 0, u_n^2 = b$ with $b > a + n\varepsilon$ and ε small. If the sequential auction reaches

$(0, n-1)$, then agent 1 bids a for the last unit and agent 2 bids b. Hence, agent 2 wins the unit and pays a. The value of $(0, n-1)$ to agent 2 is therefore $b-a$. By backward induction, the value of $(0,1)$ to agent 2 is $b-(n-1)\,a-\frac{(n-2)(n-1)}{2}\,\varepsilon$, assuming agent 2 wins all $n-1$ units after the first unit. Similarly, the value of $(1,0)$ to agent 1 is $a+(n-1)\,\varepsilon$. The sequential outcome is inefficient if agent 2's value of $(0,1)$ is less than agent 1's value of $(1,0)$, i.e., if $b < n\,a + \frac{(n-1)n}{2}\,\varepsilon$. In that case, the efficiency of the sequential auction outcome is given by

$$\frac{a+(n-1)\,\varepsilon}{b} > \frac{a+(n-1)\,\varepsilon}{n\,a+\frac{(n-1)n}{2}\,\varepsilon}.$$

Letting $a \to \infty$ and/or $\varepsilon \to 0$, the efficiency approaches $\frac{1}{n}$. □

This theorem shows that under Theorem 11 when one agent has increasing marginal utilities the worst-case efficiency can go to zero as the number of goods increases.

5.3.3. Efficiency with Constrained Marginal Utilities

As indicated in the preceding sections, the marginal utilities that achieve the worst-case efficiency in each case are quite special. With additional constraints on the marginal utilities, we expect the worst-case efficiency to increase. Here we illustrate this for $n = 2$ goods.

First, we consider decreasing marginal utilities for both agents, and assume that $u_2^1 = \lambda_1 u_1^1$ and $u_2^2 = \lambda_2 u_1^2$, where $\lambda_1 < 1$ and $\lambda_2 < 1$. In this case, it can be shown that the sequential allocation is not efficient if and only if $u_1^1 > \lambda_1 u_1^1 > u_1^2 > \lambda_2 u_1^2$ or $u_1^2 > \lambda_2 u_1^2 > u_1^1 > \lambda_1 u_1^1$. The worst-case efficiency with these constrained marginal utilities is given by

$$\eta(2; \lambda_1, \lambda_2) = \frac{2+\lambda_1-\lambda_2}{(1+\lambda_1)\cdot(2-\lambda_2)}, \tag{5.11}$$

where $\frac{u_1^2}{u_1^1} < \lambda_1 < 1$ and $0 < \lambda_2 < 1$. Note that $\eta(2; \lambda_1, \lambda_2) \geq 3/4$, which is equal to the bound given in Table 5.1, i.e. restricting the marginal utilities in this way decreases the efficiency loss. As $\lambda_1 \to 1$ and $\lambda_2 \to 0$, this bound holds with equality.

For the case in which one agent has decreasing marginal utilities and the other has increasing marginal utilities, we let $u_2^1 = \lambda_1 u_1^1$, and $u_2^2 = \lambda_2 u_1^2$, where $\lambda_1 < 1$ and $\lambda_2 > 1$. In this case, any ordering of marginal utilities can lead to an inefficient allocation. Hence all orderings must be considered to compute the worst-case efficiency. As an example, assume that $\lambda_2 u_1^2 > u_1^2 > u_1^1 > \lambda_1 u_1^1$. Then the worst-case efficiency is given by

$$\eta(2; \lambda_1, \lambda_2) = \frac{2 - \lambda_1 + \lambda_2}{(2 - \lambda_1) \cdot (1 + \lambda_2)}, \tag{5.12}$$

where $0 < \lambda_1 < 1$ and $1 < \lambda_2 < 2$. Here we have $\eta(2; \lambda_1, \lambda_2) \geq 2/3$, and equality holds as $\lambda_1 \to 0$ and $\lambda_2 \to 2$. Again, restricting the marginal utilities increases the worst-case efficiency.

5.4. Simulation Results

In this section we present simulation results for two-user bandwidth and power auctions. For these results we randomly place two transmitters and receivers within a given region, as illustrated in Fig. 5.4. Specifically, user 1's transmitter is uniformly placed within a circle of radius $d_0 = 50\,m$ centered at user 2's receiver. This captures the scenario in which a user experiences a single dominant interferer. User 1's receiver is then randomly placed within a circle of radius d_0 centered at user 1's transmitter, and similarly, user 2's transmitter is randomly placed within a circle of radius d_0 centered at user 2's receiver. Given these locations, we set each channel gain $h_{ij} = l_{ij}^{-4}$ where l_{ij} is the distance

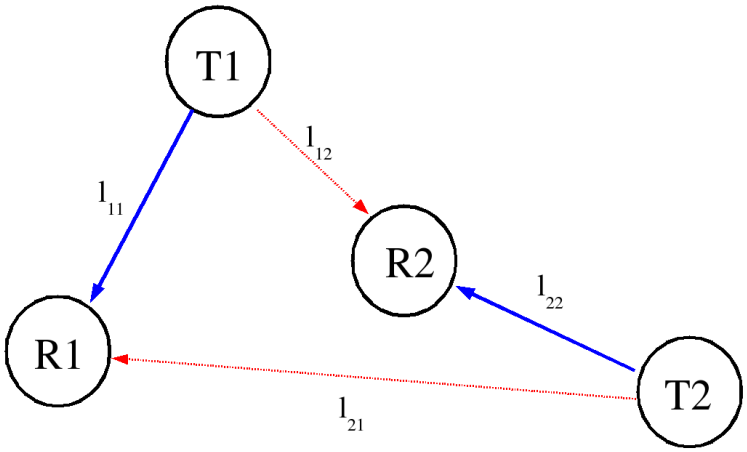

Figure 5.4. Simulation scenario in which the location of the transmitter T1 is uniformly distributed within a circle centered at R2, and R1 and T2 are placed at random locations within circles centered at T1 and R2, respectively. ($l_{11} \leq d_0$, $l_{22} \leq d_0$ and $l_{12} \leq d_0$)

between transmitter i and receiver j. For a given allocation a user's utility is assumed to be the rate given by (5.1) or (5.2), with $W = 25$ MHz, and $N_0 = -174$ dBm/Hz. In the bandwidth auction, W is divided into n units of W/n Hz and both users transmit using power $P_i = P_{max} = 10^{-6}$ watts. In the power auction, we assume that $P_2 = P_{max}$ and $P_1 = n_1 P_{max}/n$, where again $P_{max} = 10^{-6}$ watts. Both users spread over the entire bandwidth W.

5.4.1. Bandwidth Auction

We first show results for the bandwidth auction with $n = 2$ units. We define the *worst possible efficiency* for a given realization as the ratio of minimum sum utility to maximum sum utility over the three possible bandwidth allocations. Figure 5.5 shows the empirical

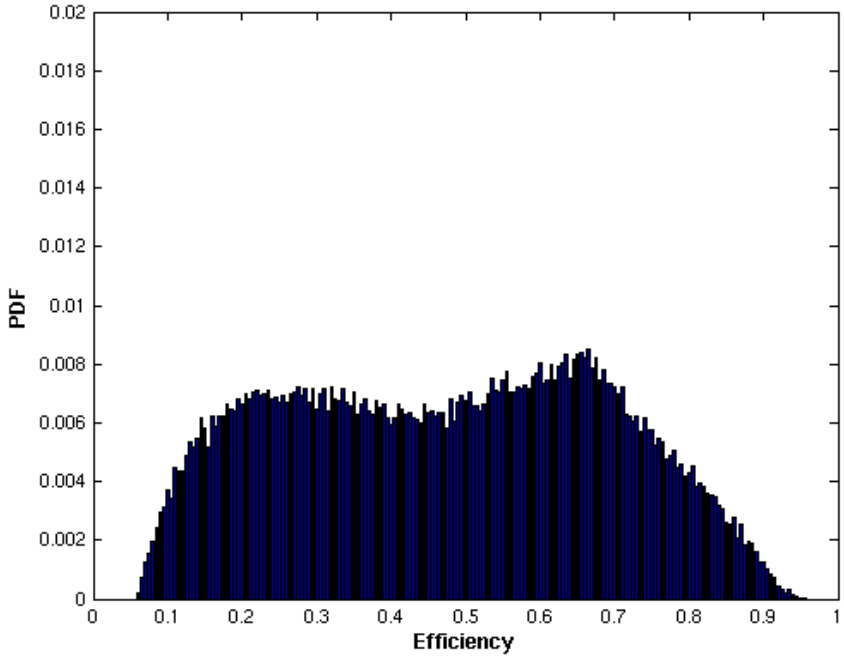

Figure 5.5. Empirical PDF of the worst possible efficiency of the sequential bandwidth auction with two agents and $n = 2$ units.

probability distribution function (PDF) for the worst possible efficiency over 10^4 simulation runs. This shows that without an appropriate resource allocation mechanism, the efficiency can be very low.

Figure 5.6 shows the empirical cumulative distribution function (CDF) of the efficiency of the sequential equilibrium. Curves are shown for different values of n. For $n = 2$ this figure shows a substantial improvement in efficiency relative to the worst possible allocation in Figure 5.5. For $n = 2$, the lowest efficiency is 0.844, and the auction achieves an efficient allocation for more than 80% of the realizations. The lowest efficiency is significantly higher than the worst-case efficiency of 3/4 given in Section 5.3.1. This is due to the nature of the rate utility function, which constrains the possible marginal

utilities as in Section 5.3.3. Here, each agent i's utility function has the form $U_i(s) = s(W/2)\log_2(1 + \frac{2\beta_i}{s})$, where $\beta_i = \frac{|h_{ii}|^2 P_i}{N_0 W}$. For the parameters used in the simulation it follows that $\beta_i \in [1.6, \infty)$. The resulting marginal utilities satisfy the constraints in Sect. 5.3.1, with $\lambda_i \in [.45, 1]$. From (5.11), the worst-case efficiency occurs when $\lambda_1 = 1$ and $\lambda_2 = 0.45$, which gives $\eta(2; 1, 0.45) = 0.82$, only slightly less than the observed lowest efficiency.

As n increases, Figure 5.6 shows that the smallest observed efficiency increases from 0.844 when $n = 2$ to 0.914 when $n = 20$. This is in contrast to the results in Table 5.1, which show that the worst-case efficiency decreases with n. The observed increase is due to the fact that as n increases, the specific marginal utilities, which achieve the worst-case efficiency, are much less likely to occur. However, the fraction of realizations for which the full efficiency is achieved decreases as n increases. In part, this is simply due to the increase in number of possible outcomes (allocations) with n.

5.4.2. Power Auction

Figure 5.7 shows the PDF of the worst possible efficiency for the power auction with $n = 2$ units. Figure 5.8 shows the CDF of the efficiency of the sequential allocation for different values of n. Unlike the bandwidth auction, the smallest efficiencies observed in the simulations are close to $1/n$, as predicted by Theorem 18. (For example, with $n = 2$ the smallest observed efficiency is 0.575.) Because of the interference, the marginal utility of the second unit for agent 2 can be very large relative to the marginal utility of the first unit, which leads to the worst-case efficiency. For $n = 2$ the sequential power auction

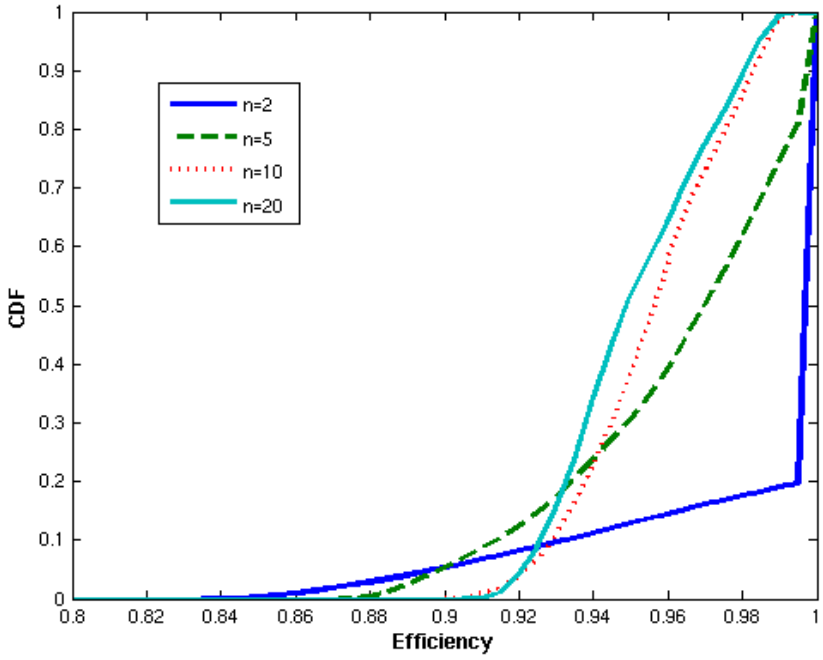

Figure 5.6. Empirical CDFs of the efficiency of the two-user sequential allocation for the bandwidth auction with different n. The transmitted power $P = 10^{-6}$ watts and $d_0 = 50$ m.

still achieves the efficient allocation for more than 85% of the realizations. This fraction decreases as n increases.

Finally, we remark that our results for both the power and bandwidth auctions only indicate efficiency loss relative to the maximum utility for that mechanism. Further results comparing the efficiency across mechanisms show that in addition to having lower efficiency loss, the bandwidth auction typically achieves a higher sum utility than the power auction.

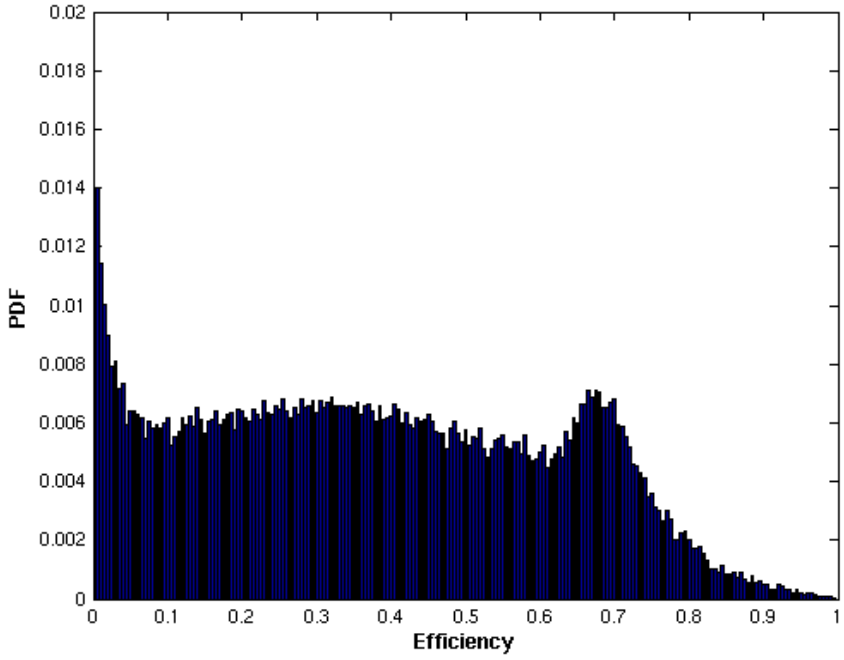

Figure 5.7. Empirical PDF of the worst possible efficiency for the power auction with two users and $n = 2$ units.

5.5. Sequential second price auction for three or more agents

Next we turn to the case where $k > 2$ agents are participating in the bandwidth auction.[13] The main question we address is whether or not the auction has an equilibrium.[14] In a single unit second-price auction, existence of an equilibrium follows from the uniqueness of dominant strategies for all agents. From Theorem 10, a similar argument applies for a two agent sequential auction, namely there is a unique dominant subgame perfect strategy for each agent. However, with $k > 2$ agents, we will show by example that one or more agents may not have a unique dominant strategy. Hence, it is plausible that there

[13]As discussed in Section 5.1, due to the interdependence of the utility functions, the power auction with more than two agents is not considered.

[14]Note that this game has infinite strategy spaces and discontinuous pay-off functions, hence classical equilibria existence theorems may not apply.

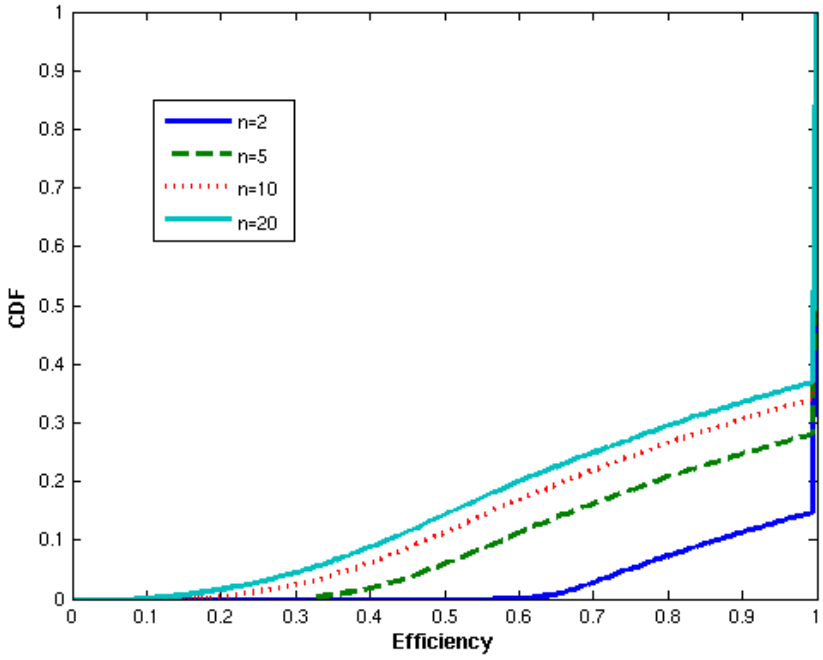

Figure 5.8. Empirical CDF of the efficiency of the sequential equilibrium for the two-user power auction with different values of n.

exist no equilibria (as in first price auctions with full information) or a multiplicity of pure and mixed strategy equilibria. Our main result is to show the existence of at least one pure strategy equilibrium.

Consider sophisticated bidding for $k > 2$ agents in an n-unit auction. As in the two agent case, the last round of the auction is identical to a standard second price auction for the n-th good, and so it is a dominant strategy for all agents to bid their marginal utilities. Given full information, all agents again know the allocations and payments on the last round. Hence, we can think of the penultimate round as a second price auction over the right to participate in one of k possible auctions in the last round whose valuations are known.

In the two agent auction at each node the choice is between two possible sub-auctions. An agent's valuation for one sub-auction over the other is captured by the difference in payoffs between them. Since any sub-auction has a unique equilibrium path, the valuations of the sub-auctions and hence the sophisticated bids are well defined. With $k > 2$ agents, even in the penultimate auction, the choice may be between k alternative second price auctions for which some or all of the agents have different payoffs. Each agent may then have several non-dominated strategies, and as the next example shows, there may be multiple sub-game perfect equilibria. If the equilibrium is not unique, the valuation of the penultimate round may depend on the choice of equilibrium. The same applies, of course, to any node further up the game tree. We therefore define a sophisticated bidding strategy as a strategy that, for each node of the game tree, maximizes the agent's payoff over final outcomes for a given equilibrium strategy on each of the subtrees. In other words, an agent chooses a sophisticated strategy that subsumes some choice of equilibria on the subtrees and maximizes expected payoff for the corresponding valuations.

5.5.1. Example

Figure 5.9 shows an example of a sequential second price auction with three agents and three units which has multiple inefficient equilibria. The marginal utilities of all three units are 10 for agent 1 and 9, 1 and 0 for agents 2 and 3. Since the last round is a second price auction, bidding marginal utility is a equilibrium on each of the final round subtrees. Using these values, in the subtree of the penultimate round corresponding to the allocation of the first unit to agent 1 we get the values $[21, 0, 0]$, $[11, 9, 0]$ and $[11, 0, 9]$

of the second unit being allocated to agents 1, 2 and 3, respectively.[15] This implies that bidding 10 for agent 1 and 9 for agents 2 and 3 are dominant strategies. The value of this subtree is therefore $[12, 0, 0]$. In the penultimate round corresponding to the allocation of the first unit to agent 2 we get the values $[11, 9, 0]$, $[1, 9, 10]$ and $[9, 9, 9]$; hence, the dominant bids are 2, 9, 1 (since agent 1 knows that agent 2 loses regardless of agent 1's bid) and the value is $[9, 9, 7]$. By symmetry, the value of the third penultimate subtree is $[9, 7, 9]$.

Turning to the first round, it follows that agent 1 has a dominant bid of 3 while the two other agents have a choice between 2 and 9. In this case agents 2 and 3 must coordinate to avoid simultaneously bidding high or low thus the pure strategy equilibria bids for this round are 3, 2, 9 and 3, 9, 2. There also exists a mixed strategy where both agents 2 and 3 flip a fair coin and decide between 2 and 9.

5.5.2. Existence

To show that there exists at least one equilibrium with $k > 2$ agents, we define a *second price bidding* mechanism which is a generalization of a second price auction.

Definition A k-second price bidding mechanism is a k-agent mechanism with action profiles in $\Re_+^k$ and a finite outcome set $\{A_1, \ldots, A_k\}$ where the valuation of agent i for A_j is $a_j^i \in \Re$ and $a_j^j \geq a_i^j$ for any $i \neq j$. The outcome as a function of the actions $(b_1, \ldots, b_k)$ is given by $\nu(b_1, \ldots, b_k) = A_i$ when $b_i = \max_j b_j$ and the payment in this case is $p_i(b_1, \ldots, b_k) = \max_{j \neq i} b_j$ and $p_j(b_1, \ldots, b_k) = 0$ for $j \neq i$.

It is easy to see that this reduces to a second price auction if $a_i^j = 0$ for $j \neq i$.

[15] Here each component denotes the corresponding value for that agent.

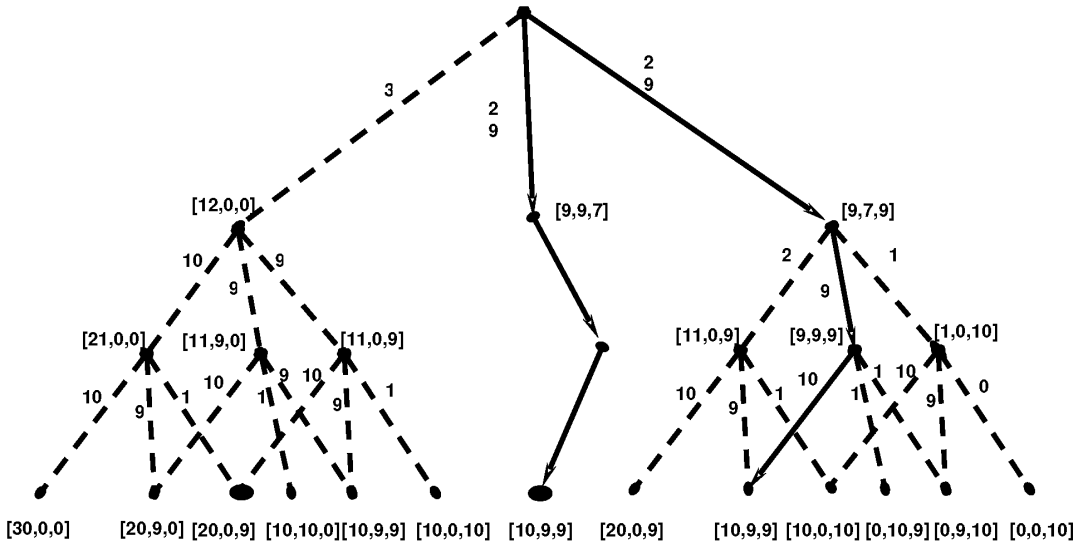

Figure 5.9. Example of a directed graph G representing an auction with $k = 3$ agents and $n = 3$ units. Each node on the graph is labeled with the value of the subtree rooted at that node. The edges are labeled with the valuation of the resource unit to the corresponding agent. The two solid paths correspond to the two pure strategy equilibria.

Lemma 19. *A second price bidding mechanism has at least one pure strategy equilibrium that survives iterated elimination of dominant strategies.*

Proof. For each agent i let $B_i = \{a_i^i - a_j^i : \ j \neq i\}$, the set of valuation differences between outcomes, $\beta_i = \min B_i$. Without loss of generality, $b_1 = a_1^1 - a_2^1 = \max \cup_i B_i$, namely the largest valuation gap is between the valuations of agent 1 for the outcomes A_1 and A_2.

We show that if $b_2 = \max B_2 > \max_{i>2} \beta_i$ then the bidding profile $(b_1, b_2, \beta_3, \ldots, \beta_k)$ is an equilibrium. With this profile the outcome is A_1 with $p_1(b_1, b_2, \beta_3, \ldots, \beta_k) = b_2$ and $p_i(b_1, b_2, \beta_3, \ldots, \beta_k) = 0$ for $i > 1$. Agent 1's payoff is then $a_1^1 - b_2$. The only deviation of agent 1 that would change the outcome is to bid below b_2 which, by the assumption on

b_2, would give the outcome A_2. Agent 1's payoff in this case is a_2^1 and the difference is $a_2^1 - a_1^1 + b_2 = b_2 - b_1 < 0$ from the maximality of b_1. If agent $i > 1$ bids above b_1, then her payoff is $a_i^i - b_1$ compared to a_1^i at A_1, hence by deviating she would gain $a_i^i - b_1 - a_1^i$ which, again by the maximality of b_1, is negative. Thus, no agent can make a positive gain from deviating.

If $b_2 = \max B_2 < \max_{i>2} \beta_i$ then w.l.o.g. $\beta_3 > b_2$. By induction there exists a pure strategy equilibrium for the $k-1$ bidding mechanism derived from excluding agent 2. The base of the induction follows since for two agents trivially it must be that $b_2 > \max_{i>2} \beta_i$.

Since we are removing one of the agents in the new game, the new sets of valuation differences are subsets of the previous B_i's. This implies that their minimal elements β_i' satisfy $\beta_i' \geq \beta_i$, and therefore agent 3 bids above b_2. If agent 3 is not the highest bidder in the new game, or if at least two agents are bidding above b_2, then taking the equilibria bids in the new game and letting agent 2 bid b_2 would give the same allocation and payments as in the k-agent game. Since b_2 is the maximal gain agent 2 could obtain from changing the outcome, she has no incentive to bid above b_2. Any profitable deviation for the other agents would be a profitable deviation in the new game contradicting the choice of bids as an equilibrium. If agent 3 is the highest bidder in the new game and the second highest bid is below b_2 then the same argument shows that adding agent 2 to the equilibrium profile in the new game would not change the bidding incentives of the agents apart from agent 3. Since $a_3^3 - a_3^2 > \beta_3 > b_2$, it follows that agent 3 has no incentive to deviate either. Thus we get a pure strategy equilibrium for the k agent mechanism. These strategies are not dominated hence this equilibrium survives iterated elimination of dominant strategies.

If $\max B_2 = \max_{i>2} \beta_i$ then the outcome depends on the tie breaking rule used in the auction. For any reasonable rule, such as random choice, a pure strategy equilibrium can be constructed in a similar manner. □

Theorem 20. *The multi-agent sequential second price auction has a pure strategy equilibrium.*

Proof. An induction on the depth of the game tree of a sequential second price auction shows that each round of the sequential auction is strategically equivalent to a second price bidding mechanism where the valuations of the subtrees depend on the choice of equilibrium outcome of the bidding mechanism on the subtree. □

5.5.3. Efficiency loss

We conclude this section with a few comments about the worst-case efficiency for $k > 2$ agents. First we note that the worst-case efficiency will not increase as the number of users increase. This follows from the fact that we can always select the marginal utilities of the additional users to be arbitrarily small. In fact for $n = 2$ goods and an arbitrary number of users with decreasing marginal utilities it can be shown that the worst-case efficiency is exactly the same as in the $k = 2$ case (i.e. it is 3/4). Figure 5.10 shows simulation results for the bandwidth auction with $k = 3$ agents and $n = 2$ and $n = 5$ goods. The parameters are the same as those in Section 5.4. For comparison the results to $k = 2$ agents are also shown. It can be seen that the efficiency with $k = 3$ agents is stochastically larger than that with $k = 2$ agents for both $n = 2$ and $n = 5$. A likely explanation for this is that with randomly placed agents the probability of a "bad" choice of marginal utilities arising decreases as the number of agents increase.

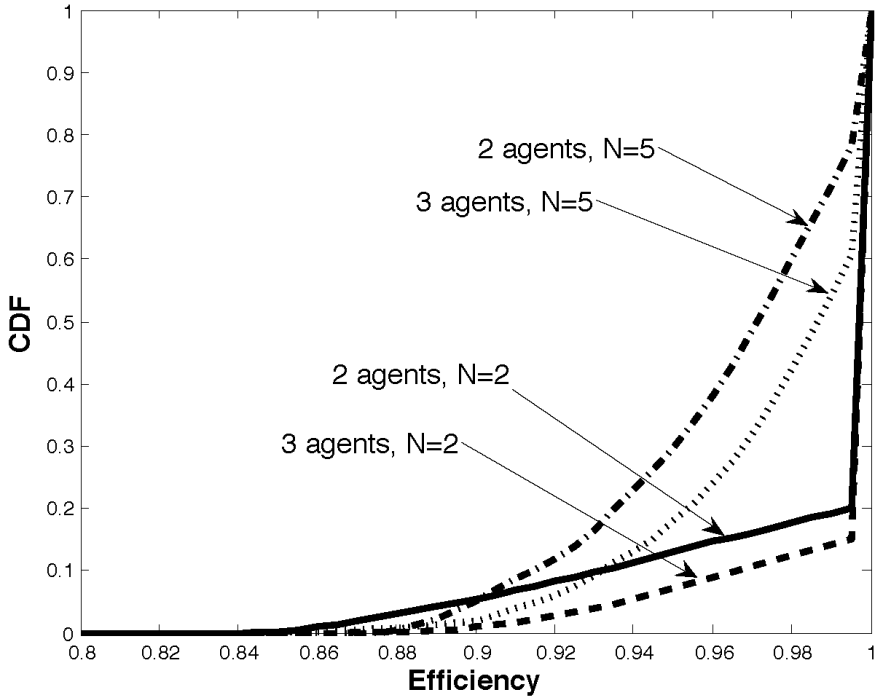

Figure 5.10. Empirical CDFs of the efficiency of the sequential allocation for the bandwidth auction with $k = 2$ and $k = 3$ users and $n = 2$ and $n = 5$ goods.

5.6. Chapter Summary

We have considered a sequential second price auction for allocating n units of bandwidth or power among non-cooperative wireless devices. This mechanism is relatively simple and requires little information exchange among users, which may make it attractive for dynamic bandwidth or power allocation among secondary users who wish to share spectrum with the primary user (spectrum owner or licensee). Our main analytical results characterize the worst-case efficiency of the subgame perfect equilibrium for two users with full knowledge of bidding histories and user utilities. For a bandwidth auction (decreasing marginal utilities), the worst-case efficiency decreases with n and converges

to $1 - e^{-1}$. For the power auction, where one user has decreasing marginal utilities and the other has increasing marginal utilities, the worst-case efficiency bound is no greater than $1/n$.

Although the worst-case efficiency loss due to sophisticated bidding can be significant, simulation results with randomly placed users show that with the rate utility function, the sequential auction typically gives the efficient allocation. Furthermore, when the equilibrium is inefficient, the efficiency loss is typically less than the worst-case efficiency loss. This is due to the rate utility function, which places constraints on the ratios of marginal utilities for the successive units being auctioned.

For more than two users, we show that the sequential second price auction still has a pure strategy equilibrium. In this case, however, the equilibrium may not be unique and so some coordination of the users may be needed to decide on a particular outcome. Assuming a particular equilibrium, simulation results show that for the bandwidth auction the efficiency typically improves when the number of agents increases from 2 to 3.

5.7. Supplement: Proof of Lemma 12 and Theorem 11

5.7.1. Marginal utilities of the agents in Lemma 12

Without loss of generality, we consider the following flat dominant utility profile: $u_1^1 = \cdots = u_n^1 = 1$ for agent 1 and $u_i^2 = b_i$ for agent 2. Note that $1 \geq b_1 \geq b_2 \geq \cdots \geq b_n$. We find a set of constraints such that the marginal utilities above have the subgame kink property with the sequential allocation $(j, n-j)$ through the backward induction as shown in Figure 5.11. At node $(0, n-1)$, agent 1 bids 1 and agent 2 bids b_n for the last unit. Agent 1 wins the last unit and pays b_n. Therefore, the values of node $(0, n-1)$

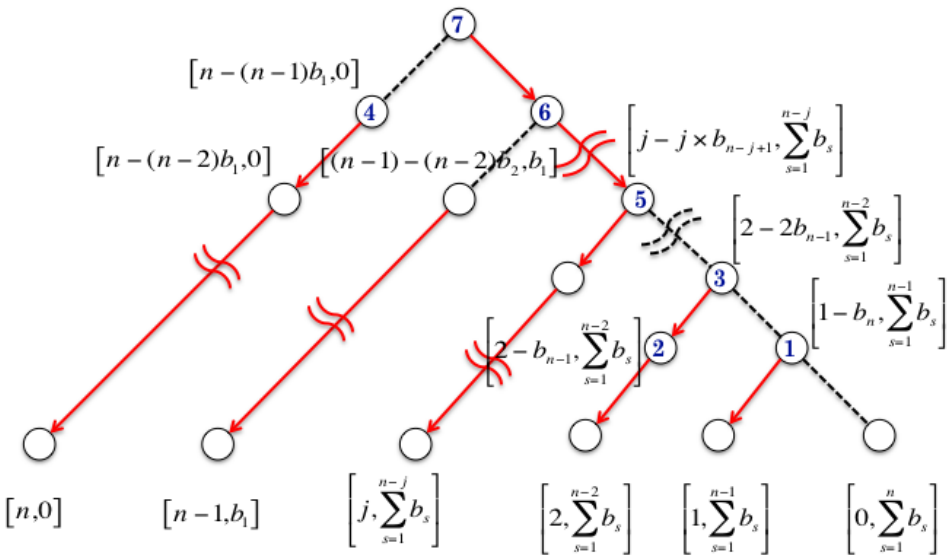

Figure 5.11. Subgame kink property of the marginal utilities considered with sequential allocation $(j, n-j)$

become $1-b_n$ for agent 1 and $\sum_{i=1}^{n-1} b_i$ for agent 2, namely, $[1-b_n, \sum_{i=1}^{n-1} b_i]$. Similarly, the values of node $(1, n-2)$ are $[2-b_{n-1}, \sum_{i=1}^{n-2} b_i]$. Given these values, now we calculate the values of node $(0, n-2)$. Agent 1 bids $(2-b_{n-1})-(1-b_n) = 1-b_{n-1}+b_n$ and agent 2 bids b_{n-1} for the second last unit. Since we assume that the marginal utilities have the subgame kink property, agent 1 wins the second last unit at this node. This implies that $1-b_{n-1}+b_n > b_{n-1}$, or

$$b_{n-1} < \frac{1+b_n}{2}, \tag{5.13}$$

and the values of node $(0, n-2)$ become $[2-2b_{n-2}, \sum_{i=1}^{n-2} b_i]$.

We apply this procedure repeatedly to the straight-line paths where agent 1 wins the units. First, we consider the straight-line with the sequential allocation $(i, n-i)$ where $i \leq j$. We can show that the values of node $(0, n-i)$ become $[i - i \cdot b_{n-i+1}, \sum_{s=1}^{n-i} b_s]$ for $1 = 1, \cdots, j$. Second, for the straight-line path with $i > j$, the values of node $(1, i)$

become $[i-(i-1)\cdot b_{n-i+1}, \sum_{s=1}^{n-i} b_s]$ for $i = j+1, \cdots, n-1$ and $[n-(n-1)\cdot b_1, 0]$ for $i = n$. The following constraints are obtained similar to (5.13).

$$\begin{cases} b_{n-i+1} < \frac{1+(i-1)\cdot b_{n-i+2}}{i}, & i = 2, \cdots, j \\ b_{n-i+1} < \frac{1+(i-2)\cdot b_{n-i+2}}{i-1}, & i = j+1, \cdots, n, \end{cases} \tag{5.14}$$

Now we consider the equilibrium path where agent 2 wins the units. At node $(0, n-j-1)$, agent 1 bids $\{j+1-j\cdot b_{n-j}-(j-j\cdot b_{n-j+1})\} = 1-j\cdot b_{n-j}+j\cdot b_{n-j+1}$ and agent 2 bids b_{n-j} for the $(n-j)$-th unit. From the equilibrium path considered here,

$$p_{n-j} \equiv 1-j\cdot b_{n-j}+j\cdot b_{n-j+1} < b_{n-j}, \tag{5.15}$$

or

$$b_{n-j} > \frac{1+j\cdot b_{n-j+1}}{j+1}. \tag{5.16}$$

Therefore, agent 2 wins the $n-j$-th unit and pays $p_{n-j} = 1-j\cdot b_{n-j}+j\cdot b_{n-j+1}$. Note that (5.15) can be rearranged such that

$$(j+1)-(j+1)\cdot b_{n-j} < j-j\cdot b_{n-j+1}. \tag{5.17}$$

The values of node $(0, n-j-1)$ becomes $[j-j\cdot b_{n-j+1}, \sum_{s=1}^{n-j} b_s - p_{n-j}]$. Similarly, at node $(0, n-j-2)$, the following inequality

$$p_{n-j-1} \equiv 2-(j+1)\cdot b_{n-j-1}+j\cdot b_{n-j+1} < b_{n-j-1}+b_{n-j}-p_{n-j} \tag{5.18}$$

holds and the values of the node $(0, n-j-2)$ become $[j-j\cdot b_{n-j+1}, \sum_{s=1}^{n-j} b_s - p_{n-j-1} - p_{n-j}]$. The payment of agent 2 for $(n-j-1)$-th unit is p_{n-j-1}. (5.18) can be rearranged such

that

$$(j+2)-(j+2)\cdot b_{n-j-1} < j - j\cdot b_{n-j+1} + b_{n-j} - p_{n-j}. \tag{5.19}$$

We repeat this until the backward induction reaches the root node. The values of the root node $(0,0)$ is $[j - j\cdot b_{n-j+1}, \sum_{s=1}^{n-j} b_s - p_s]$, where the payment of agent 2 for the s-th unit is given by

$$p_s \equiv n-j-s+1-(n-s)\cdot b_s + j\cdot b_{n-j+1} < b_s + \sum_{k=s+1}^{n-j}\{b_k - p_k\}, \tag{5.20}$$

where $s = 1, \cdots, n-j-1$. The rearrangement of (5.20) is given by

$$(n-s+1)-(n-s+1)\cdot b_s < j - j\cdot b_{n-j+1} + \sum_{k=s+1}^{n-j}\{b_k - p_k\}. \tag{5.21}$$

The marginal utilities of the agents in Lemma 12 are obtained by setting $b_s = p_s$ or

$$b_s = \frac{1+(n-s)\cdot b_{s+1}}{n-s+1} \tag{5.22}$$

for $s = 1, \cdots, n-j$ and $b_s = 0$ for $s = n-j+1, \cdots, n$.

5.7.2. Proof of Theorem 11

Suppose that $u_1^1 \geq \ldots \geq u_n^1$ and $u_1^2 \geq \ldots u_n^2$, and let $(l, n-l)$ denote the efficient allocation. After auctioning m $(\leq n)$ units, the sequential game reaches a decision node where either agent 1 or agent 2 obtains her efficient allocation (l for agent 1 or $n-l$ for agent 2). For that agent the marginal utilities of the remaining units must be smaller than that for the other agent. (See Figure 5.12.) Up to this decision node, there is no loss in efficiency. Any efficiency loss in the final allocation procures in the subgame tree

rooted at this decision node. Therefore, the efficiency loss of the full game tree cannot be larger than the efficiency loss of this subgame tree. Since the utility profile associated with the subgame tree is dominant, the worst-case efficiency must always correspond to a dominant utility profile.

We now show that changing a dominant utility profile to a flat dominant profile can only decrease efficiency. Given a dominant utility profile, if we replace the marginal utilities of the first agent with $\bar{u}_1^1 = \ldots = \bar{u}_n^1 = u_n^1$, then we must have the sequential allocation $(\bar{s}, \bar{t})$ satisfies $\bar{s} \leq s$. Hence this change in utility profile can only decrease efficiency. ■

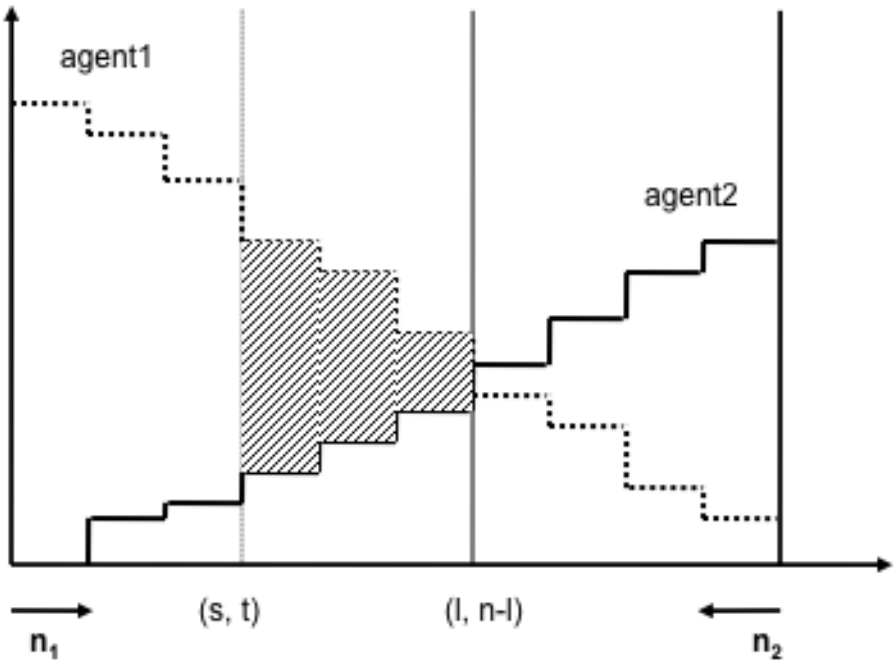

Figure 5.12. Marginal utilities of two agents. n_1 (n_2) is the number of units that agent 1 (2) obtains along the sequential auction. $(l, n-l)$ is the optimal allocation and (s, t) is the sequential allocation. The shadowed region shows the efficiency loss.

CHAPTER 6

An Efficient Dynamic Auction for Convex Utility

In the previous chapter, we considered a sequential second price auction for allocating wireless resources and determined its worst-case efficiency. For the power auction, where one of the agents has a convex utility function, the worst-case efficiency decreases to zero as the number of units increases. In addition, we have assumed complete information among the agents. The impracticality of the complete information assumption as well as the low worst-case efficiency of the power auction leads us to design a new auction mechanism. The main difficulty is the convexity of the agent's utility function in the power auction since most auctions in the literature assume that the utilities of the agents are increasing concave.

Here, we study a new dynamic auction proposed in [**14**], which achieves the efficient outcome for the case where one agent and only one agent has a convex utility function in the scenario considered.[1] This dynamic auction, called a *Fallback auction*, is a modification of Ausubel's ascending auction for multiple units and assumes private information among the agents. We show that the Fallback auction finds a core outcome with minimum revenue to the seller or the auctioneer, which maximizes the "incentive" for the agents to report truthfully.[2] As discussed later, the core outcome is necessary for stability of

[1]As briefly discussed in Chapter 5, the analysis becomes complicated if there is more than one agent with a convex utility function due to the "free-rider" problem [**29**].
[2]As we show later, this does not mean that the Fallback auction is incentive compatible.

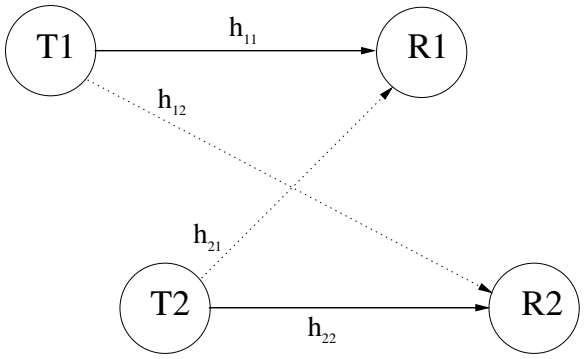

Figure 6.1. Interference channel with two transmitter-receiver pairs

the auction. Moreover, the Fallback auction achieves efficient resource allocation with truthful biddings, which implies that it has a full information equilibrium.

6.1. Spectrum Sharing Model

We consider a model with K agents, where each agent is represented by a distinct transmitter-receiver pair. An example of two such agents is shown in Figure 6.1. Let agent 1 be the primary agent so that agents $2, \ldots, K$ are the secondary agents. As in [**51**], we assume that the utility derived by each agent i is a function of that agent's received *Signal-to-Interference and Noise Ratio (SINR)* given by

$$\gamma_i(\mathbf{q}) = \frac{q_i h_{ii}}{\sigma^2 + \sum_{j \neq i} q_j h_{ji}}, \tag{6.1}$$

where $\mathbf{q} = \{q_i\}$ is the vector of transmission powers across all agents, σ^2 is the noise power and h_{ji} is the channel gain from agent j's transmitter to agent i's receiver. The externality that agent j causes agent i is due to the interference term $q_j h_{ji}$ in this expression. Letting $U_i(\gamma_i)$ denote agent i's utility, an efficient allocation of power $\mathbf{q}$ maximizes $\sum_i U_i(\gamma_i)$.

We assume that the primary user transmits at a fixed power q_1 and is guaranteed that the interference from the secondary users does not exceed a given level q^{max}. The spectrum manager's task is then to allocate this total received power at the primary user's receiver through the auction such that the total power of the secondary users is constrained to satisfy $\sum_{i=2}^{K} q_i h_{i1} \leq q^{max}$. We also allow the primary user to participate in this auction. Each unit of power the primary user is allocated corresponds to a reduction in the total interference it sees, i.e. if it receives q_1' units of power, its total interference becomes $q^{max} - q_1'$. Let $x_1 = \frac{q_1'}{q^{max}}$ and $x_i = \frac{q_i h_{i1}}{q^{max}}$, represent the normalized resources allocated to each agent, so that the resource constraint can be written as $\sum_{i=1}^{K} x_i \leq 1$.

The utility function $U_i(\gamma_i)$ is assumed to be a monotonic increasing concave function of γ_i for all i. However, it is more useful to consider this as a function of x_i. For each agent $i \geq 2$, we assume that the interference from the primary user is much larger than the interference from any secondary user, so that

$$\gamma_i(x_i) \approx \frac{x_i \frac{q_{max} h_{ii}}{h_{i1}}}{\sigma^2 + q_1 h_{1i}}, \tag{6.2}$$

in which case clearly $U_i(x_i)$ is also a monotonically increasing concave function of x_i.[3] On the other hand, for agent 1, we have

$$\gamma_1(x_1) = \frac{q_1 h_{11}}{\sigma^2 + q^{max}(1 - x_1)}, \tag{6.3}$$

[3]If there is more than one secondary user and the interference from the other secondary users is not negligible, once again users may free ride.

in which case $U_1(x_1)$ is an increasing function of x_1. Moreover, $U_1(x_1)$ is a convex function of x_1 if the following relation holds:

$$\frac{d^2U_1(x_1)}{dx_1^2} = \frac{h_{11}q_1(q^{max})^2}{(\sigma^2 + q^{max}(1-x_1))^3}\left\{\frac{d^2U_1}{d\gamma_1^2}\,\gamma_1 + 2\,\frac{dU_1}{d\gamma_1}\right\} > 0, \tag{6.4}$$

or equivalently, if the coefficient of relative risk aversion, $-\frac{\gamma_1 U_1''(\gamma_1)}{U_1'(\gamma_1)}$, is less than 2 for all γ_1.

6.2. Ausubel's Ascending Auction

We describe an auction setting, which captures key features of power allocation described in the previous section. A seller wishes to allocate one unit of a divisible good among K agents. Agent i obtains utility $U_i(x)$ from consuming $x \leq 1$ units of the good. Utilities are assumed to be private and quasi-linear with derivative $\frac{\partial U_i(x)}{\partial x} = u_i(x)$. When all $U_i(x)$ are concave, Ausubel's ascending auction can be used to allocate one unit of good [**12**]. In this auction, truthful bidding is a dominant strategy that leads to an *ex post perfect equilibrium* and the VCG outcome is obtained. On the other hand, if one of the agents has a convex utility function, then Ausubel's auction cannot be applied and a 'Fallback' auction is proposed in the following section. Here, we describe Ausubel's ascending auction in detail. For convenience we initially assume all $U_i(x)$ to be strictly concave.

If p is the per unit price of the good, strict concavity of $U_i(x)$ implies that

$$x_i(p) = \arg\max_{0\leq x\leq 1} U_i(x) - p\cdot x \tag{6.5}$$

is unique for any price p. Call $x_i(p)$ agent i's demand at price p. Notice that $x_i(p)$ is continuous and strictly decreasing. In addition, $x_i(0) = 1$ and $x_i(p) \to 0$ as $p \to \infty$ are assumed.

Initially the price is set to 0 and increases continuously. At each price p, bidder i is asked to report $x_i(p)$. We assume that each agent reports truthfully. We show later that Ausubel's auction encourages truthful reporting. Whenever the sum of demands from all agents is larger than supply (one unit of good), namely, $\sum_{i=1}^{n} x_i(p) > 1$, the auctioneer or the seller increases the price. The auction terminates when the market clearing price p^* is reached, which satisfies $\sum_{i=1}^{n} x_i(p^*) = 1$. Notice that the existence of such a price follows from the the fact that $x_i(p)$ is continuous and decreasing.

As the price increases from p to $p + \Delta p$, each agent i clinches, i.e., is allocated the additional quantity $\Delta C_i(p) = C_i(p + \Delta p) - C_i(p)$ with the payment $p \cdot \Delta C_i(p)$ to the seller. Here, $C_i(p) = \max\{0, 1 - \sum_{j \neq i} x_j(p)\}$ is the total clinched quantity of agent i at price p. If p^{-i} is the market clearing price when agent i is excluded, it is easy to see that $C_i(p) = 0$ for $p \leq p^{-i}$. Hence, the total payment of agent i for the clinched quantity $C_i(p)$ is the following:

$$P_i^{\mathrm{AA}}(p) = \int_0^p \rho \frac{dC_i(\rho)}{d\rho} d\rho = -\int_{p^{-i}}^p \rho \frac{d(\sum_{j \neq i} x_j(\rho))}{d\rho} d\rho. \tag{6.6}$$

Notice that $p^{-i} \leq p^*$ and, therefore, $x_j(p^{-i}) \geq x_j(p^*)$ for all $j \neq i$.

When Ausubel's ascending auction ends with the market clearing price p^*, the final allocation of one unit of good among agents is socially optimal, namely, maximizes the sum of all agents' utilities. Now we show that the total payment $P_i^{\mathrm{AA}}(p^*)$ of agent i after the auction ends is the same as the VCG payment. The VCG payment for agent i is given

by

$$P_i^{\mathrm{VCG}} = \sum_{j \neq i} \left\{ U_j(x_j(p^{-i})) - U_j(x_j(p^*)) \right\}. \tag{6.7}$$

Using information revealed from the agents during the auction and the first-order condition $u_j(x_j(p)) = p$ for all j, the VCG payment becomes

$$\begin{aligned} P_i^{\mathrm{VCG}} &= \sum_{j \neq i} \int_{x_j(p^*)}^{x_j(p^{-i})} u_j(x)dx = -\sum_{j \neq i} \int_{p^{-i}}^{p^*} u_j(x_j(\rho)) \frac{dx_j}{d\rho} d\rho \\ &= -\sum_{j \neq i} \int_{p^{-i}}^{p^*} \rho \frac{dx_j}{d\rho} d\rho = -\int_{p^{-i}}^{p^*} \rho \frac{d(\sum_{j \neq i} x_j)}{d\rho} d\rho, \end{aligned} \tag{6.8}$$

which is the same as the payment (6.6) at price p^*. Therefore, the ascending auction with concave utilities generates the VCG outcome. Moreover, reporting $x_i(p)$ truthfully at given price p is incentive compatible for all agents [**43**].

So far we have not considered the demand of an agent appropriately in (6.5). When the auctioneer asks agent i to report her demand at the current price, we assume that each agent reports $x_i(p)$ that maximizes $U_i(x) - p \cdot x$. However, this ignores the fact that agent i has already clinched $C_i(p) \geq 0$ with the payment $P_i^{\mathrm{AA}}(p)$ by the time the price in the auction has reached p. Therefore, she only pays for the additional amount of demand $x_i' - C_i(p)$ at the unit price p, where x_i' is agent i's demand that maximizes the following payoff $\pi_i(x, p)$:

$$\pi_i(x, p) = U_i(x) - p \cdot \max\{x - C_i(p), 0\} - \int_0^p \rho \frac{dC_i(\rho)}{d\rho} d\rho. \tag{6.9}$$

As we can see, $x_i'(p) = x_i(p)$. This is because the payment of an agent does not depend on her bidding strategy (demand). This is the main reason why truthful reporting of

demand is incentive compatible in the ascending auction. Note that concavity of the utility function means that $x_i(p) \geq C_i(p)$ throughout the auction. Algorithm 1 describes the ascending auction.

Algorithm 1 Alg1 $(p, x_1, x_2, \ldots, x_K)$: Ausubel's Ascending Auction

Initialization:
$p \leftarrow 0$; $x_i, x_i^- \leftarrow 1$ for $i = 1, \ldots, K$
Dynamic:
while $\sum_{i=1}^{K} x_i > 1$ **do**
  $p \leftarrow p + \Delta p$
  Ask each agent her demand x_i for given price p.
  $x_i \leftarrow \max\{x_i, 1 - \sum_{j \neq i} x_j^-\}$,
  $C_i \leftarrow \max\{0, 1 - \sum_{j \neq i} x_j\}$, $C_i^- \leftarrow \max\{0, 1 - \sum_{j \neq i} x_j^-\}$,
  $P_i \leftarrow P_i + p \cdot (C_i - C_i^-)$,
  $x_i^- \leftarrow x_i$ for $i = 1, \ldots, K$
end while
Return $(x_1, \ldots, x_K)$ and $(P_1, \ldots, P_K)$

6.3. Fallback Auction

We now present the Fallback auction. The Fallback auction modifies Ausubel's ascending auction to adapt to the presence of a single agent with a non-concave utility function, henceforth, called agent 1. All other agents have strictly concave utilities. In this case there may be no price p such that $\sum_{i=1}^{K} x_i(p) = 1$. The difficulty arises because $x_1(p)$, while non-increasing, may have discontinuities. Namely, there may be a price p^t such that $\lim_{p \nearrow p^t} \sum_{i=1}^{K} x_i(p) > 1$ and $\sum_{i=1}^{K} x_i(p) < 1$ for all $p > p^t$. This means there is an excess supply when the auction reaches the price $p > p^t$. In addition, $x_1(p) = 0$ for all $p > p^t$ because of the non-concavity of her utility function. Hence, agent 1's demand at a price $p > p^t$ is less than what she has clinched. In Ausubel's ascending auction an agent is not allowed to relinquish her clinch. Therefore, if agent 1's utility is convex, her surplus

is forced to be zero or negative, creating an incentive to deviate from truthful reporting of her demand.

The Fallback auction surmounts this difficulty by allowing only agent 1 to relinquish some of the units she has clinched. If a fallback price (defined below) is reached and agent 1 has clinched some amount of the good, we allow agent 1 to choose a smaller quantity clinched earlier and the auction terminates. The relinquished units from agent 1 must then be reallocated to other agents. On the other hand, if $\sum_{i=2}^{K} x_i(p) > 1$ at the fallback price, then agent 1 could not have clinched anything. She then falls back to a price $p < p^t$ with $x_1 = 0$. All of the good may not be allocated when agent 1 falls back, in which case the auction continues without agent 1 until it reaches the market clearing price.

Definition p^t is called a fallback price if $\lim_{p \nearrow p^t} \sum_{i=1}^{K} x_i(p) > 1$ and $x_1(p) = 0$ for all $p > p^t$.

To understand what occurs at the fallback price, suppose that agent 1 decides to fall back at some price p^t. At this price agent 1 is free to choose any quantity clinched earlier, i.e., $C_1(p')$ where $p' < p^t$. Agent 1's payoff from choosing $C_1(p')$ would be $U_1(C_1(p')) - \int_{p^{-1}}^{p'} \rho \frac{dC_1(\rho)}{d\rho} d\rho$. Clearly, she would choose the price p' that maximizes her payoff. Depending on whether $C_1(p^t) > 0$ or $C_1(p^t) = 0$, the auction follows one of two different paths after agent 1 falls.

6.3.1. Case I: $p^t \geq p^{-1}$

If the fallback price p^t is higher than the market clearing price p^{-1} without agent 1, then $C_1(p^t) > 0$. Therefore, agent 1 chooses a price $p < p^t$, which maximizes her payoff and the auction ends. This motivates the following definition.

Definition The price

$$p^* = \arg \max_{p^t \geq p \geq p^{-1}} \left[\pi_1(p) = U_1(C_1(p)) - \int_{p^{-1}}^{p} \rho \frac{dC_1(\rho)}{d\rho} d\rho \right] \tag{6.10}$$

is called the security price.

The security price is the price, which maximizes agent 1's payoff π_1 when she falls back. Therefore, the following equality holds at the fallback price:

$$\overline{\pi}_1(p^t) = \pi_1(p^*), \tag{6.11}$$

where $\overline{\pi}_1$ is the payoff that agent 1 would receive if she were allocated her entire demand $x_1(p^t)$.[4] Note that in the definition of the security price, the payoff maximization could be taken over the interval $[p^{-1}, p^t]$. If the Fallback auction terminates at a fallback price, namely $p^* = p^t$, then the auctioneer allocates the quantity $x_i(p^*)$ to each agent $i \geq 2$ and the amount $1 - \sum_{i \geq 2} x_i(p^*)$ to agent 1.

Once the auction ends, the payment that agent 1 makes for the allocation $C_1(p^*)$ is

$$P_1^{\mathrm{FB}} = \int_{p^{-1}}^{p^*} \rho \frac{dC_1(\rho)}{d\rho} d\rho, \tag{6.12}$$

and the payment that agent $i \geq 2$ makes is

$$\begin{aligned} P_i^{\mathrm{FB}} &= p^t \cdot \lim_{p \nearrow p^t} x_i(p) - \int_{p^*}^{p^t} \rho \frac{dx_i}{d\rho} d\rho \\ &= p^t \cdot \lim_{p \nearrow p^t} x_i(p) + U_i(x_i(p^*)) - U_i(x_i(p^t)). \end{aligned} \tag{6.13}$$

[4] If $p > p^t$, $\overline{\pi}_1(p) < \pi_1(p^*)$. Otherwise, agent 1 would not fall back because she expects better payoff at price $p > p^t$. See an example in Section 6.4 for further explanation.

The payment consists of two terms. The first term is her demand multiplied by the fallback price p^t and the second term is the increase in agent i's utility for the quantity re-allocated to her when agent 1 falls back. Since the gain from reallocation is the same as the payment, agent $i > 0$ is indifferent to whether she gets additional quantity relinquished from agent 1.

6.3.2. Case II: $p^t < p^{-1}$

Since the sum demand of all agents except agent 1 is $\sum_{i=2}^{K} x_i(p) > 1$ at the fallback price, agent 1 could not have clinched any quantity, namely, $C_1(p) = 0$. Therefore, agent 1 falls back to any price $p < p^t$ with no allocation. Since $\sum_{i=2}^{K} x_i(p) > 1$ after agent 1's fallback, the auction continues without agent 1 from the fallback price p^t until it reaches the market clearing price p^{-1}. The market clearing price exists because all agents in the auction have concave utility functions.

The allocation of agent 1 is $x_1 = 0$ once the auction ends, and the payment of agent 1 is $P_1^{\mathrm{FB}} = 0$. On the other hand, agent $i \neq 1$'s allocation is $x_i(p^{-1})$. For allocation $x_i(p^{-1})$ of agent $i \geq 2$, $C_i(p^t) = \max\{0, 1 - \sum_{j \neq 1,i} x_j(p^t)\}$ is obtained with the unit price p^t right after agent 1 falls back. The corresponding payment is then

$$P_i^{\mathrm{FB}} = p^t \cdot C_i(p^t) + \lim_{p \searrow p^t} \int_p^{p^{-1}} \rho \frac{dC_i(\rho)}{d\rho}\, d\rho. \tag{6.14}$$

A pseudo-code description of the complete Fallback auction is given in Algorithm 2.

Algorithm 2 Fallback Auction

Initialization:
fallback flag down ; $p \leftarrow 0$; $x_i, x_i^- \leftarrow 1$ for $i = 1, \ldots, K$
Dynamic:
while $\sum_{i=1}^{K} x_i > 1$ **and** fallback flag down **do**
$p \leftarrow p + \Delta p$
ask each agent her demand x_i for price p.
$x_i \leftarrow \max\{x_i, 1 - \sum_{j \neq i} x_j^-\}$
$C_i \leftarrow \max\{0, 1 - \sum_{j \neq i} x_j\}$, $C_i^- \leftarrow \max\{0, 1 - \sum_{j \neq i} x_j^-\}$,
$P_i \leftarrow P_i + p \cdot (C_i - C_i^-)$,
ask agent 1 if p is secure.
if 'yes' **then**
$x_i^* \leftarrow x_i$ for $i = 2, \ldots, K$
$P_1^* \leftarrow P_1$
end if
if $x_i, x_i^- \geq x_i^*$ **then**
$P_{i1} \leftarrow P_{i1} + p \cdot \max\{0, x_i^- - x_i\}$ for $i = 2, \ldots, K$
end if
if agent 1 request fallback, **then**
Fallback flag up
if $C_1 > 0$ **then**
$P_1 \leftarrow P_1^*$
$P_i \leftarrow p \cdot x_i + P_{i1}$ for $i = 2, \ldots, K$
$x_i \leftarrow x_i^*$ for $i = 2. \ldots, K$
$x_1 \leftarrow 1 - \sum_{i=2}^{K} x_i^*$
end while;
else
$x_1 = 0$; $P_1 = 0$;
$(x_2, \ldots, x_K, P_2, \ldots, P_K) = \text{Alg1}(p, x_2, \ldots, x_K)$ call Ausubel's algorithm
end while;
end if
end if
$x_i^- \leftarrow x_i$ for $i = 1, \ldots, K$
end while
Return $(x_1, \ldots, x_K)$ and $(P_1, \ldots, P_K)$

6.4. Examples

In this section, we illustrate the Fallback auction with examples. We consider a divisible good with unit quantity, as assumed in Section 6.3, and extend this auction to the case where there are multiple units of an indivisible good to be auctioned off.

6.4.1. Divisible Good

Example Consider the allocation of one unit of a divisible good among three agents with the following utility functions:

$$U_1(x_1) = \frac{1}{3}x_1^3 + \frac{11}{10}x_1, \tag{6.15}$$

$$U_2(x_2) = 2x_2 - x_2^2, \tag{6.16}$$

$$U_3(x_3) = 2x_3 - x_3^2. \tag{6.17}$$

VCG Outcome: The efficient allocation is the solution to the following maximization problem:

$$\max \quad \frac{1}{3}x_1^3 + \frac{11}{10}x_1 + 2x_2 - x_2^2 + 2x_3 - x_3^2 \tag{6.18}$$

$$\text{s.t.} \quad x_1 + x_2 + x_3 = 1 \ ; \ x_1, x_2, x_3 \geq 0 \tag{6.19}$$

Since agents 2 and 3 have identical concave utilities, the solution should be $x_2 = x_3 = \frac{1-x}{2}$ and $x_1 = x$. The maximization problem is then equivalent to

$$\max_{0 \leq x \leq 1} \frac{1}{3}x^3 + \frac{11}{10}x + 2\left\{2(\frac{1-x}{2}) - (\frac{1-x}{2})^2\right\}, \tag{6.20}$$

which gives the optimal allocation $x_1 = 0.1127$ and $x_2 = x_3 = 0.44365$. Moreover, the VCG payments of all agents can be calculated easily and are given by $P_1^{\text{VCG}} = 0.1191$ and $P_2^{\text{VCG}} = P_3^{\text{VCG}} = 0.6184$.

Fallback Outcome: Agent 1 has a convex utility function and her demand is $x_1(p) = 1$ until she falls back to her security clinch. Agents 2 and 3 demand the quantities for which their marginals exceed the price, i.e., $x_2(p) = x_3(p) = 1 - \frac{p}{2}$. If $0 \leq p \leq 1$, the sum of the demands for any two agents exceeds the supply and therefore no agent clinches anything. For $1 \leq p \leq 2$, the total demand of agents 2 and 3, $x_2(p) + x_3(p) = 2 - p$ drops below 1, and agent 1 clinches $C_1(p) = p - 1$. This continues until either agent 1 falls back or the price reaches $p = 2$ at which point the demands of agents 2 and 3 drop to zero and the market clears. The clinch rate in this interval is constant, namely, $\frac{\partial C_1(\rho)}{\partial \rho} = 1$.

If agent 1's demand ($x_1(p) = 1$ due to convexity of utility function) is satisfied without fallback, the expected payoff at price $p < p^t$ would therefore be

$$\begin{aligned} \overline{\pi}_1(p) &= U_1(x_1(p)) - p \cdot \{x_1(p) - C_1(p)\} - \int_1^p \rho \frac{\partial C_1(\rho)}{\partial \rho} d\rho \\ &= \frac{43}{30} - p \cdot (2 - p) - \int_1^p \rho \, d\rho = \frac{1}{2} p^2 - 2\, p + \frac{29}{15}. \end{aligned} \tag{6.21}$$

On the other hand, the payoff of agent 1 with her actual clinch is given by

$$\begin{aligned} \pi_1(p) &= U_1(C_1(p)) - \int_1^p \rho \frac{\partial C_1(\rho)}{\partial \rho} d\rho \\ &= \frac{(p-1)^3}{3} + \frac{11}{10}(p-1) - \frac{p^2}{2} + \frac{1}{2}. \end{aligned} \tag{6.22}$$

The security price is then obtained by

$$\begin{aligned} p^* &= \arg\max\{\pi_1(p) : \text{s.t. } 1 \leq p \leq 2\} \\ &= \frac{3-\sqrt{0.6}}{2} = 1.1127. \end{aligned} \tag{6.23}$$

The Fallback auction, therefore, has the following dynamics. As the price rises above $p = 1$, agent 1 begins to clinch. Her payoff increases until $p = p^*$, at which $\pi_1(p^*) = 0.0054$. As the auction continues, however, the security price of agent 1 remains $p^* = 1.1127$ since the surplus decreases with $p > p^*$. The price continues to increase until it reaches the fallback price p^t. At this price, $\overline{\pi}_1(p^t) = \pi_1(p^*)$, or

$$\frac{1}{2} \cdot (p^t)^2 - 2 \cdot p^t + \frac{29}{15} = \pi_1(p^*) = 0.0054, \tag{6.24}$$

which gives the fallback price $p^t = 1.6202$. Once agent 1 falls back to the allocation at the security price, the auction terminates and the final allocations among the agents are

$$x_1(p^*) = p^* - 1 = 0.1127, \tag{6.25}$$

$$x_2(p^*) = 1 - \frac{p^*}{2} = 0.44365, \tag{6.26}$$

$$x_3(p^*) = 1 - \frac{p^*}{2} = 0.44365. \tag{6.27}$$

Table 6.1. Marginal valuations of three agents A, B and C.

	1	2	3
A	0	0	7
B	4	2	0
C	4	1	0

At the fallback price, the demands of agent 2 and 3 are $x_2(p^t) = x_3(p^t) = 1 - \frac{p^t}{2} = 0.1899$ and the payments of the agents when the auction ends are then:

$$P_1^{\text{FB}} = \int_1^{p^*} \rho \frac{\partial C_1(\rho)}{\partial \rho} d\rho = 0.1191, \tag{6.28}$$

$$P_2^{\text{FB}} = 2\,x_2(p^*) - (x_2(p^*))^2 - 2\,x_2(p^t) + (x_2(p^t))^2 + p^t \cdot x_2(p^t) = 0.6543, \tag{6.29}$$

$$P_3^{\text{FB}} = 0.6543. \tag{6.30}$$

Note that the final allocation of the Fallback auction is same as that of the VCG auction. Moreover, the payment of agent 1 is the same for both auctions. However, $P_i^{\text{FB}} \neq P_i^{\text{VCG}}$ for $i = 2, \ldots, K$. Therefore, the Fallback auction is not incentive compatible. Later, in Section 6.5, we show that the Fallback auction is a core-selecting auction [**31**].

6.4.2. Indivisible Goods

Example (Case I in Section 6.3) Suppose we wish to allocate Allocate three units of an indivisible good among three agents with marginal valuations given in Table 6.1.

VCG outcome: The efficient allocation is $x_A = 0, x_B = 2, x_C = 1$ with the following VCG payments: $P_{\text{A}}^{\text{VCG}} = 0$, $P_{\text{B}}^{\text{VCG}} = 3$, $P_{\text{C}}^{\text{VCG}} = 1$.

Table 6.2. Fallback Dynamics

	x_A	x_B	x_C	C_1
$0 \leq p < 1$	3	2	2	0
$1 \leq p < 2$	3	2	1	0
$p = 2$	3	1	1	1
$2 < p < 2.5$	3	1	1	1
$p = 2.5$	F	1	1	$*$

Table 6.3. Marginal valuations of three agents A, B and C.

	1	2	3
A	0	0	9
B	5	3.4	1.1
C	4.3	3.1	0.5

Fallback outcome: For $0 \leq p < 1$, A bids for 3 units, B and C bid for 2 units. For $1 \leq p < 2$, agent A bids for 3 units, B for two, and C for one.[5] So far, no agent has clinched unit. At $p = 2$, B reduces demand to one and A clinches to $3 - (1 + 1) = 1$ with $p = 2$. Since A pays 2 for one unit, she can pay up to 5 for the other two units. Therefore, the demand of agent A remains 3 until p reaches 2.5. When the price becomes $p = 2.5$, agent A decides to fall back to the security quantity $x_A^* = 0$ and relinquishes one unit to agent B with the price she paid. Since agents B and C ask for one unit, respectively, at the fallback price $p = 2.5$, the final allocation becomes $x_B = 1 + 1 = 2$ and $x_C = 1$. The payments of agents with the Fallback auction are $P_A^{\text{FB}} = 0$, $P_B^{\text{FB}} = 2.5 \times 1 + 2 = 4.5$ and $P_C^{\text{FB}} = 2.5 \times 1 = 2.5$.

Example (Case II in Section 6.3) Suppose we wish to allocate three units of an indivisible good among three agents with marginal valuations given by Table 6.3.

[5]We assume that an agent does not ask for the unit when the marginal value of the unit is the same as the current price.

Table 6.4. Fallback Dynamics

	x_A	x_B	x_C	C_1	C_2	C_3
$0 \leq p < 3$	3	2	2	0	0	0
$p = 3$	F	2	2	0	1	1
$3 < p < 3.1$		2	2	0	1	1
$p = 3.1$		2	1	0	2	1

VCG outcome: The efficient allocation among all three agents is $x_A = 0$, $x_B = 2$, and $x_C = 1$ with the following VCG payments: $P_A^{\text{VCG}} = 0$, $P_B^{\text{VCG}} = 4.7$, $P_C^{\text{VCG}} = 1.1$.

Fallback outcome: For $0 \leq p < 3$, A bids for 3 units, B bids for 2 units, and C bids for 2 units. At $p = 3$, A falls back to a price $p' < 3$ with no clinch. The auction continues without agent A from the current price $p = 3$. Since B's demand is 2 units, C clinches one unit at price $p = 3$. Similarly, B clinches one unit at this price. When the price reaches $p = 3.1$, the demand of C becomes 1 unit, B clinches an additional unit and the auction ends. The final allocation of the Fallback auction is $x_A = 0$, $x_B = 2$, and $x_C = 1$, and the payments of the agents are $P_A^{\text{FB}} = 0$, $P_B^{\text{FB}} = 3 + 3.1 = 6.1$, $P_C^{\text{FB}} = 3$.

6.5. Fallback Auction as a Core-Selecting Auction

As shown in Section 6.4, the final allocation of the Fallback auction is the same as that of the VCG auction, which maximizes the sum utilities of the agents. This is only possible when agents reveal their demand truthfully. However, the payments of all agents except agent 1 are not the VCG payments, and therefore sincere bidding (truthful reporting) is not a dominant strategy [**75**]. Instead, we prove that the Fallback auction with truthful bidding leads to a core allocation with minimum total payment of all agents to the seller. This is stated on the following Theorem.

Theorem 21. *When all agents but one have concave utility functions, the Fallback auction has a full information equilibrium in the core.*

The proof relies on concepts from [**31**], which we repeat here. The seller is denoted as player 0, and the bidders as agents $i = 1, \ldots, K$. The set of all players including the seller is denoted by $\mathcal{N}$. Agent 1 has an increasing convex utility $U_1(x_1) \geq 0$ and agent $i \neq 1$ has an increasing concave utility $U_i(x_i) \geq 0$. One unit of a divisible good is allocated to the agents through the Fallback auction. In addition, we assume $U_i(0) = 0$. For any coalition $\mathcal{S}$, an assignment $\{x_i\}$ is feasible for coalition $\mathcal{S}$, written $\{x_i\} \in F(\mathcal{S})$, if (1) $\sum_{i \in \mathcal{S}} x_i \leq 1$ and (2) for all i, if $i \notin \mathcal{S}$ or $0 \notin \mathcal{S}$, then $x_i = 0$. Namely, a bidder can have a non-zero assignment when coalition S forms only if that bidder and the seller are both in the coalition. The coalition value or characteristic function is defined by

$$w(\mathcal{S}) = \max_{x \in F(\mathcal{S})} \sum_{j \in \mathcal{S}} U_j(x_j). \tag{6.31}$$

If the payment of the auction P_j is made to the seller by each agent j, then the associated payoffs are given by $\sum_{j=1}^{K} P_j$ for the seller and $\pi_j = U_j(x_j) - P_j$ for each bidder j. The payoff profile is individually rational if $\pi_j \geq 0$ for all j. An *imputation* is a feasible, non-negative payoff profile. An imputation is in the core if it is efficient and unblocked:

$$Core(\mathcal{N}, w) = \left\{ \pi \geq 0 \,|\, \sum_{j \in \mathcal{N}} \pi_j = w(\mathcal{N}) \text{ and } \left(\forall \mathcal{S} \subseteq \mathcal{N}\right) \sum_{j \in \mathcal{S}} \pi_j \geq w(\mathcal{S}) \right\}. \tag{6.32}$$

Now we consider the Fallback auction. If the Fallback auction terminates with the fallback flag down, the final allocation among the agents is the same as that of Ausubel's ascending auction assuming that agent 1 does not exist. It is easy to prove that the

Fallback auction in this case is the core-selecting auciton. We, therefore, assume the algorithm terminates with the fallback flag up, and prove that we obtain an equilibrium outcome in the core. The following proof is for the case when $p^t \geq p^{-1}$. We present the proof for the case when $p^t < p^{-1}$ in Section 6.7.2. This can be done in several steps. First, we show that the resulting allocation of the Fallback auction is efficient under truthful bidding. Second, for two agents, the VCG outcome is obtained, i.e., the payments of all agents are the same as the VCG payments. From a standard argument (see for example [**13**] or [**33**]), it follows that bidding truthfully is an ex-post perfect equilibrium. Finally, we show that for $K > 2$, the truthful bidding outcome of the Fallback auction lies in the core and minimizes the seller's payoff. From [**18**], the bidding strategies of the agents according to a *truncation profile* is a full information equilibrium.[6]

Lemma 22. *Assuming truthful bidding among agents, the allocation of the Fallback auction is efficient.*

Proof. We show that $x_2(p^*), \ldots, x_K(p^*)$ and $x_1(p^*) = 1 - \sum_{i \geq 2} x_i(p^*)$ are solutions to the following maximization problem $\mathbf{\Pi}$:

$$\begin{aligned} \max \quad & U_1(x_1) + \sum_{i=2}^{K} U_i(x_i) \\ \text{s.t.} \quad & \sum_{i=1}^{K} x_i = 1 \\ & x_i \geq 0 \ \forall i \in N \setminus \{0\}. \end{aligned} \tag{6.33}$$

[6]A report $\hat{u}_j$ is a *truncation* report if and only if there exists some $\alpha \geq 0$ such that for all $x_j \in X_j$, $\hat{u_j}(x_j) = u_j(x_j) - \alpha$. A set of $\hat{u}_j$ is a *truncation profile*.

For given $Q \in [0,1]$, consider the following problem:

$$\begin{aligned} F(Q) \quad = \quad & \max \sum_{i=2}^{K} U_i(x_i) \\ & \text{s.t.} \quad \sum_{i=2}^{K} x_i = Q \\ & x_i \geq 0 \ \forall i \in N \setminus \{0,1\}. \end{aligned} \tag{6.34}$$

There is a Lagrange multiplier p that corresponds to the market clearing price such that Q units are distributed among the agents $N \setminus \{0,1\}$. Therefore, $F(Q) = \sum_{i=2}^{K} U_i(x_i(p))$. For example, when $Q = 1$, the corresponding Lagrange multiplier is p^{-1}. Now problem **Π** can be reformulated as

$$\max_{p \geq p^{-1}} U_1(1 - \sum_{i \geq 2} x_i(p)) + \sum_{i \geq 2} U_i(x_i(p)). \tag{6.35}$$

The objective function can be expressed as

$$\begin{aligned} U_1(1 - \sum_{i \geq 2} x_i(p)) + \sum_{i \geq 2} \int_{p^{-1}}^{p} u_i(x_i(\rho)) \frac{dx_i(\rho)}{d\rho} d\rho \\ = U_1(C_1(p)) - \int_{p^{-1}}^{p} \rho \frac{dC_1(\rho)}{d\rho} d\rho, \end{aligned} \tag{6.36}$$

and this is maximized by the security price p^* (See Definition 6.3.1). □

Lemma 23. *Suppose $K = 2$ and agent 1 has an increasing convex utility function. Then truthful bidding is an* ex post perfect equilibrium *of the Fallback auction that charges the VCG payment to each agent.*

Proof. When the fallback flag is up, the payment of agent 1 is

$$\begin{aligned} P_1^{\mathrm{FB}} &= \int_0^{p^*} \rho \, \frac{dC_1(\rho)}{d\rho} \, d\rho = \int_{p^{-1}}^{p^*} \rho \, \frac{dC_1(\rho)}{d\rho} \, d\rho \\ &= U_2(x_2(p^{-1})) - U_2(x_2(p^*)), \end{aligned} \tag{6.37}$$

which is by definition the VCG payment. Moreover, the payment of agent 2 is given by (6.13).

$$P_2^{\mathrm{FB}} = p^t \cdot \lim_{p \nearrow p^t} x_2(p) + U_2(x_2(p^*)) - U_2(x_2(p^t)). \tag{6.38}$$

From the definition of the fallback price, $\overline{\pi}_1(x_1(p^t), p^t) = \pi_1(x_1(p^*), p^*)$. Namely,

$$\begin{aligned} U_1(1) - p^t \cdot (1 - C_1(p^t)) - \int_0^{p^t} \rho \frac{dC_1(\rho)}{d\rho} d\,\rho \\ = U_1(C_1(p^*)) - \int_{p^{-1}}^{p^*} \rho \frac{dC_1(\rho)}{d\rho} d\,\rho, \end{aligned} \tag{6.39}$$

or

$$\begin{aligned} U_1(1) - p^t \cdot x_2(p^t) &= U_1(x_1(p^*)) + \int_{p^*}^{p^t} \rho \, \frac{dC_1(\rho)}{d\rho} d\,\rho \\ &= U_1(x_1(p^*)) + U_2(x_2(p^*)) - U_2(x_2(p^t)). \end{aligned} \tag{6.40}$$

Here, we use the following facts in the auction: $x_1(p^t) = 1$ and $C_1(p^t) = 1 - x_2(p^t)$. Therefore, the payment of agent 2 becomes

$$P_2^{\mathrm{FB}} = U_1(1) - U_1(x_1(p^*)) = U_1(x_1(p^{-2})) - U_1(x_1(p^*)), \tag{6.41}$$

which is exactly the VCG payment for agent 2. For $K = 2$, the Fallback auction with truthful bidding achieves the efficient allocation with VCG payments. From [**43**], any incentive compatible, individually rational and efficient mechanism must charge VCG

payments. Therefore, for $K = 2$, truthful bidding is an *ex post perfect equilibrium* of the Fallback auction that generates the VCG outcome. □

In [**31**], Day and Milgrom argue that core-selecting auctions that minimize the seller's payoff maximize incentives for truthful reporting and they produce the Vickrey outcome when it lies in the core. Theorem 3 in [**31**], especially, shows that a truncation report is a full information equilibrium. For a given $\alpha \geq 0$, a truncation report for agent i corresponds to an α-truncation of her true utility, i.e. $U_i(x_i) - \alpha$. The following Lemma states that the Fallback auction minimizes the seller's payoff, and the payoffs of all agents, including the seller, lies in the core.

Lemma 24. *For $K > 2$, if all agents bid truthfully, the Fallback auction finds an imputation in the core with minimum payoff to the seller.*

Proof. See Section 6.7.1. □

Corollary 25. *The bidding strategies of agents according to the profile of π_i truncations of $U_i(x_i)$ for $i = 1, 2, \ldots, K$ are a full information equilibrium in the Fallback auction.*

Proof. The allocation of the Fallback auction with truthful bidding is a bidder optimal allocation according to [**31**]. Therefore, the bidding strategy of agent i according to the profile of π_i truncations of $U_i(x_i)$, or $\widehat{U}(x_i) = U_i(x_i) - \pi_i$, is a full information equilibrium in the Fallback auction (See Theorem 3 in [**31**].) It only remains to prove that the Fallback auction with $\widehat{U}_i(x_i)$ gives the same allocation as with $U_i(x_i)$. As the unit price increases from 0, agent i asks for the quantity $x_i = \arg\max_{0 \leq x_i \leq 1} \widehat{U}_i(x_i) - p \cdot x_i =$

$\arg\max_{0\leq x_i\leq 1} U_i(x_i) - \pi_i - p\cdot x_i$. Therefore, each concave agent asks for the same quantity as if it were responding with the true utility except for the fact that at a certain price $\widetilde{p}$, demand suddenly becomes zero. Hence we need to show that $\widetilde{p} \geq p^t \geq p^*$ for all concave agents, which can be easily done since $\pi_i = U_i(x_i(p^t)) - p^t \cdot x_i(p^t)$ for $\forall i \in N \setminus \{0, 1\}$. □

The bidding strategies of agents according to the profile of π_i truncations of $U_i(x_i)$ for all i is, therefore, a full information equilibrium in the Fallback auction and this leads to the efficient outcome.

6.6. Chapter Summary

We studied an auction model motivated by spectrum sharing in which there is one bidder with a non-concave valuation and $K-1$ bidders with concave valuations. For this setting we presented the Fallback auction, a dynamic ascending auction which has a full information equilibrium in the core. For $K = 2$ agents, this produces the VCG outcome; for $K > 2$ agents, the auction outcome is the core allocation with minimum revenue to the seller. This auction dynamically elicits information from the agents to determine an efficient outcome. It would be of interest to determine if this is a minimal amount of information that must be elicited for obtaining such an outcome.

6.7. Supplement: Proof of Lemma 24 and Additional Discussion

6.7.1. Proof of Lemma 24

6.7.1.1. The payoff profile is in the core. We prove that the payoff profile of the Fallback auction is in the core if each agent bids truthfully. In this case, the payment of

each agent is shown by (6.12) or (6.13). For agent 1,

$$\begin{aligned} P_1^{\mathrm{FB}} &= \int_0^{p^*} \rho \frac{dC_1(\rho)}{d\rho} d\rho = \int_{p^{-1}}^{p^*} \rho \frac{dC_1(\rho)}{d\rho} d\rho \\ &= \sum_{l=2}^{K} U_l(x_l(p^{-1})) - \sum_{l=2}^{K} U_l(x_l(p^*)), \end{aligned} \tag{6.42}$$

and for agent $i \geq 2$,

$$P_i^{\mathrm{FB}} = p^t \cdot x_i(p^t) + U_i(x_i(p^*)) - U_i(x_i(p^t)). \tag{6.43}$$

Note that the payment of agent 1 is the VCG payment. The payoffs of all players in the Fallback auction are, therefore, given by

$$\begin{aligned} \pi_1 &= U_1(x_1(p^*)) - P_1^{\mathrm{FB}} \\ &= \sum_{l=1}^{K} U_l(x_l(p^*)) - \sum_{l=2}^{K} U_l(x_l(p^{-1})) \end{aligned} \tag{6.44}$$

for agent 1,

$$\pi_i = U_i(x_i(p^*)) - P_i^{\mathrm{FB}} = U_i(x_i(p^t)) - p^t \cdot x_i(p^t) \tag{6.45}$$

for agent $i \geq 2$, and

$$\begin{aligned} \pi_0 &= \sum_{l=1}^{K} P_l^{\mathrm{FB}} \\ &= \sum_{l=2}^{K} U_l(x_l(p^{-1})) + \sum_{l=2}^{K} \left\{ p^t \cdot x_l(p^t) - U_l(x_l(p^t)) \right\} \end{aligned} \tag{6.46}$$

for the seller. In addition, from the Fallback price condition (6.11), we have the following equality:

$$\sum_{l=1}^{K} U_l(x_l(p^*)) = U_1(1) + \sum_{l=2}^{K} \left\{ U_l(x_l(p^t)) - p^t \cdot x_l(p^t) \right\}. \tag{6.47}$$

Note that $\sum_{l=2}^{K} P_l^{\mathrm{FB}} = U_1(1) - U_1(x_1(p^*))$.

From Lemma 22, the Fallback auction is efficient with truthful bidding, namely, $\sum_{l\in\mathcal{N}} \pi_l = w(\mathcal{N})$. Now we have to prove that $\sum_{l\in\mathcal{S}} \pi_l \geq w(\mathcal{S})$ for any coalition $\mathcal{S} \subset \mathcal{N}$. To do this, a set $\mathcal{S}'$ which has one agent $i \neq 1$ and the seller is considered. Then, we would like to prove

$$\pi_0 + \pi_i = \sum_{l=2}^{K} U_l(x_l(p^{-1})) + \sum_{j\neq 1,i} \left\{ p^t \cdot x_j(p^t) - U_j(x_j(p^t)) \right\} \geq w(\mathcal{S}') \tag{6.48}$$

or

$$\sum_{l=2}^{K} U_l(x_l(p^{-1})) \geq U_i(1) + \sum_{j\neq 1,i} \left\{ U_j(x_j(p^t)) - p^t \cdot x_j(p^t) \right\}. \tag{6.49}$$

Here, $w(\mathcal{S}') = U_i(1)$. Since p^{-1} is the market clearing price among all concave agents, it maximizes sum utilities of all concave agents, or $\sum_{l=2}^{K} U_l(x_l(p))$. Agent 1 starts to clinch when $p > p^{-1}$ in the Fallback auction and this implies $p^t \geq p^{-1}$. Hence, (6.49) is evident. For example, Figure 6.2 shows the case where $K = 3$ and $i = 2$. In a similar way, for a set $\mathcal{S}''$ with any number of concave agents, we can prove that $\sum_{l\in\mathcal{S}''} \pi_l \geq w(\mathcal{S}'')$.

Now we consider a set $\widehat{\mathcal{S}}$, which includes agent 1. If this set has only agent 1 with the seller, then $\pi_0 + \pi_1 = U_1(1) = w(\widehat{\mathcal{S}})$. Therefore, we consider a set $\widehat{\mathcal{S}}$ with at least one concave agent along with agent 1 and the seller. Then we have to prove

$$\pi_0 + \pi_1 + \sum_{l\in\widehat{\mathcal{S}}\setminus\{0,1\}} \pi_l = U_1(1) + \sum_{l\in\widehat{\mathcal{S}}\setminus\{0,1\}} \left\{ U_l(x_l(p^t)) - p^t \cdot x_l(p^t) \right\} \geq w(\widehat{\mathcal{S}}). \tag{6.50}$$

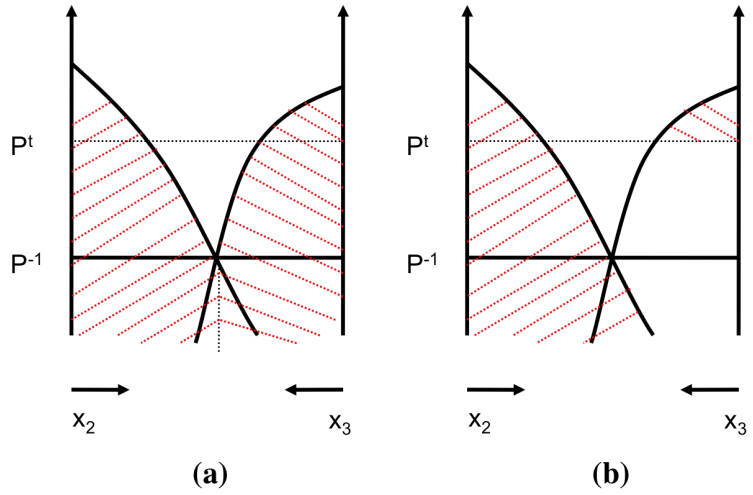

Figure 6.2. Illustration of (6.49) when $K = 3$ and $i = 2$. (a) Area of $\sum_{l=2}^{3} U_l(x_l(p^{-1}))$. (b) Area of $U_2(1) + U_3(x_3^t) - p^t \cdot x_3(p^t)$.

At the fallback price p^t, the expected gain of agent 1 is the same as the total loss of agent 1 from the security price p^* up to the fallback price p^t, and this is shown in Figure 6.3. The sum demand of all concave agents at price p in this Figure is obtained by $D(\mathcal{N}\backslash\{0,1\}) = \sum_{l=2}^{K} x_l$, where $x_l = \arg\max U_l(x_l) - p \cdot x_l$. For the Fallback auction, the sum demand of all concave agents in the coalition $\widehat{\mathcal{S}}$ is $D(\widehat{\mathcal{S}}\backslash\{0,1\}) \leq D(\mathcal{N}\backslash\{0,1\})$. Figure 6.4 shows the sum demand $D(\widehat{\mathcal{S}}\backslash\{0,1\})$ and optimal sum utilities when $K = 4$ and $\widehat{\mathcal{S}} = \{0,1,2\}$. In the figure, p^t is the fallback price of the auction with all agents K, and hence, is the same as in Figure 6.3. This shows that the area of $U_1(1)+U_2(x_2(p^t))-p^t\cdot x_2(p^t)$ is larger than the area of $w(\widehat{\mathcal{S}})$. In a similar way, we can prove (6.50) for any coalition with agent 1. Therefore, the payoff profile of the Fallback auction is in the core when agents report their demands truthfully.

6.7.1.2. Minimum payoff for the seller. Next we prove that the payoff to the seller is minimized over all payoff profiles in the core. This is easily shown. Since, $P_1^{\mathrm{FB}} =$

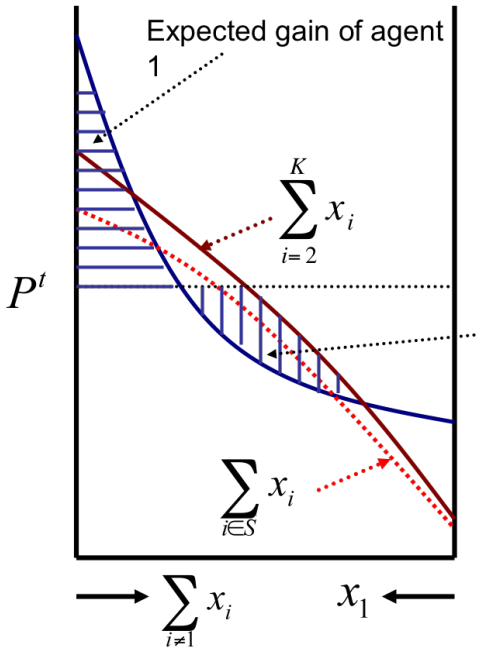

Figure 6.3. Fallback price condition. The forward expected gain of agent 1 is the same as the total loss of agent 1 from the security price p^* up to the fallback price p^t.

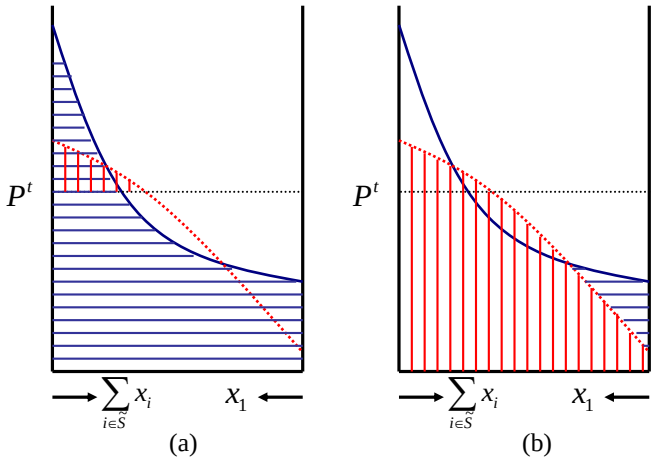

Figure 6.4. Illustration of (6.50) when $K = 4$ and $\widehat{\mathcal{S}} = \{0, 1, 2\}$. (a) Area of $U_1(1) + U_2(x_2(p^t)) - p^t \cdot x_2(p^t)$. (b) Area of $w(\widehat{\mathcal{S}})$.

$\sum_{l=2}^{n} U_l(x_l(p^{-1})) - \sum_{l=2}^{K} U_l(x_l(p^*))$ is the VCG payment of agent 1, and this is the minimum payment that agent 1 can have. In addition, $\sum_{l=2}^{K} P_l^{\mathrm{FB}} = U_1(1) - U_1(x_1(p^*))$. Namely, the sum payment of all concave agents is also the disutility that they impose on agent 1, and this is also the minimum sum payment they all can make. Therefore, the seller's payoff $\pi_0 = \sum_{l=1}^{K} P_l^{\mathrm{FB}}$ is the minimum in the core of the Fallback auction.

6.7.2. Fallback Auction when $p^t < p^{-1}$

Lemma 26. *Assuming truthful bidding among agents, the allocation of the Fallback auction is efficient.*

Proof. The final allocation of the Fallback auction is $x_1 = 0$ and $x_i = x_i(p^{-1})$ for all $i \neq 1$. (In addition, $\sum_{l=2}^{K} x_l(p^{-1}) = 1$.) By increasing agent 1's allocation to $x_1 = \delta$ and decreasing $x_i = x_i(p^{-1}) - \delta$ for any $i \neq 1$, we reduce the sum utility because $U_1(\delta) < p^t \cdot \delta$ and $U_i(x_i(p^{-1})) - U_i(x_i(p^{-1}) - \delta) > p^t \cdot \delta$. Therefore, the allocation of the Fallback auction is efficient. □

Lemma 27. *Suppose $K = 2$ and agent 1 has an increasing convex utility function. Then truthful bidding is an ex post equilibrium of the Fallback auction that charges the VCG payment to each agent.*

Proof. Since agent 2 gets $x_2 = 1$, we only need to prove that the payment of agent 2 is $P_2^{\mathrm{FB}} = U_1(1)$. We have $p^t \cdot 1 = U_1(1)$ from the fallback condition, and this is what agent 2 pays with demand $x_2 = 1$. Therefore, for $K = 2$ truthful bidding is an ex-post perfect equilibrium of the Fallback auction that generates the VCG outcome. □

Lemma 28. *For $K > 2$, if all agents bid truthfully, the Fallback auction finds an imputation in the core with minimum payoff to the seller.*

Proof. First, we prove that the payoff profile is in the core if each agent bids truthfully. In the case where $p^t < p^{-1}$, the payment of agent 1 is $P_1^{\mathrm{FB}} = 0$ and the payoff is $\pi_1 = U_1(0) - P_1^{\mathrm{FB}} = 0$. The payment of agent $i \neq 1$ is given by (6.14) and the payoff is $\pi_i = U_i(x_i(p^{-1})) - P_i^{\mathrm{FB}}$. In addition, the seller's payoff is given by $\pi_0 = \sum_{i=1}^{K} P_i^{\mathrm{FB}}$. From the fallback condition, $U_1(1) = p^t \cdot 1$.

We consider a coalition $S = \{0, 1, \cdots, K\}$. Then,

$$\begin{aligned}
\pi_0 + \pi_1 &= \sum_{i=2}^{K} P_i^{\mathrm{FB}} \\
&\geq \sum_{i=2}^{K} p^t \cdot (1 - \sum_{l \neq 1,i} x_l(p^t)) + p^t \cdot \left\{ \sum_{l \neq 1,i} (x_l(p^t) - x_l(p^{-1})) \right\} \\
&= p^t \cdot \left\{ 1 + K - 2 - (K-2) \cdot \sum_{l=2}^{K} x_l(p^{-1}) \right\} \\
&= p^t = U_1(1),
\end{aligned} \tag{6.51}$$

where $\sum_{l=2}^{K} x_l(p^{-1}) = 1$. Here, we assume that $C_i(p^t) = \max\{0, 1 - \sum_{l\neq 1,i} x_l(p^t)\} = 1 - \sum_{l\neq 1,i} x_l(p^t)$ to make the analysis simple. Also,

$$\begin{aligned}
\pi_0 + \pi_2 &= \sum_{i\neq 1,2}^{K} P_i^{\mathrm{FB}} + U_2(x_2(p^{-1})) \\
&= p^t \cdot \left\{1 - x_2(p^t)\right\} + U_2(x_2(p^t)) \\
&\quad + (K-3) \cdot \sum_{l=2}^{K} \left\{U_l(x_l(p^t)) - U_l(x_l(p^{-1}))\right\} \\
&\geq p^t \cdot \left\{1 - x_2(p^t)\right\} + U_2(x_2(p^t)) \\
&\geq U_2(1).
\end{aligned} \tag{6.52}$$

Similarly, we can prove that $\pi_0 + \pi_l \geq U_l(1)$ for $l = 3, \ldots, K$. Next we consider the following.

$$\begin{aligned}
\pi_0 + \pi_2 + \pi_3 &= \sum_{i\neq 1,2,3}^{K} P_i^{\mathrm{FB}} + U_2(x_2(p^{-1})) + U_3(x_3(p^{-1})) \\
&= p^t \cdot \left[1 - \{x_2(p^t) + x_3(p^t)\}\right] + U_2(x_2(p^t)) + U_3(x_3(p^t)) \\
&\quad + (K-4) \cdot \sum_{l=2}^{K} \left\{U_l(x_l(p^t)) - U_l(x_l(p^{-1}))\right\} \\
&\geq p^t \cdot \left[1 - \{x_2(p^t) + x_3(p^t)\}\right] + U_2(x_2(p^t)) + U_3(x_3(p^t)) \\
&\geq \max_{x_2+x_3\leq 1} U_2(x_2) + U_3(x_3).
\end{aligned} \tag{6.53}$$

The last inequality is illustrated in Figure 6.5. Moreover, we can prove that the payoff profile of a set S with any number of concave agents is in the core. Finally, we consider the payoff profile of a set with agent 1 and any number of concave agents. For example,

with agent 1 and agent 2,

$$\begin{aligned}
\pi_0 + \pi_1 + \pi_2 &= \sum_{i \neq 1,2}^{K} P_i^{\mathrm{FB}} + U_2(x_2(p^{-1})) \\
&= p^t \cdot \left\{1 - x_2(p^t)\right\} + U_2(x_2(p^t)) \\
&\quad + (K-3) \cdot \sum_{l=2}^{K} \left\{U_l(x_l(p^t)) - U_l(x_l(p^{-1}))\right\} \\
&\geq p^t \cdot \left\{1 - x_2(p^t)\right\} + U_2(x_2(p^t)) \\
&\geq \max_{x_1 + x_2 \leq 1} U_1(x_1) + U_2(x_2).
\end{aligned} \tag{6.54}$$

The last inequality is illustrated in Figure 6.6.

Second, we show that the sum of the payments to the seller is the minimum over all possible payoff profiles in the core. The minimum unit price at which the seller is willing to sell the good is p^t since agent 1 will buy the entire unit with this price (fallback condition). Therefore, the payoff of the seller should satisfy $\pi_0 \geq p^t \cdot 1$. With this, we can rewrite the core condition without agent 1:

$$\pi_0' + \sum_{j \in \mathcal{S} \setminus \{0,1\}} \pi_j \geq w(\mathcal{S}) - p^t, \tag{6.55}$$

for any $\mathcal{S} \subseteq \mathcal{N}$. The seller's payoff is redefined as $\pi_0' = \pi_0 - p^t$. The ascending auction with only concave agents generates the minimum revenue to the seller. Therefore, the seller's payoff is minimized among all payoff profiles in the core.

□

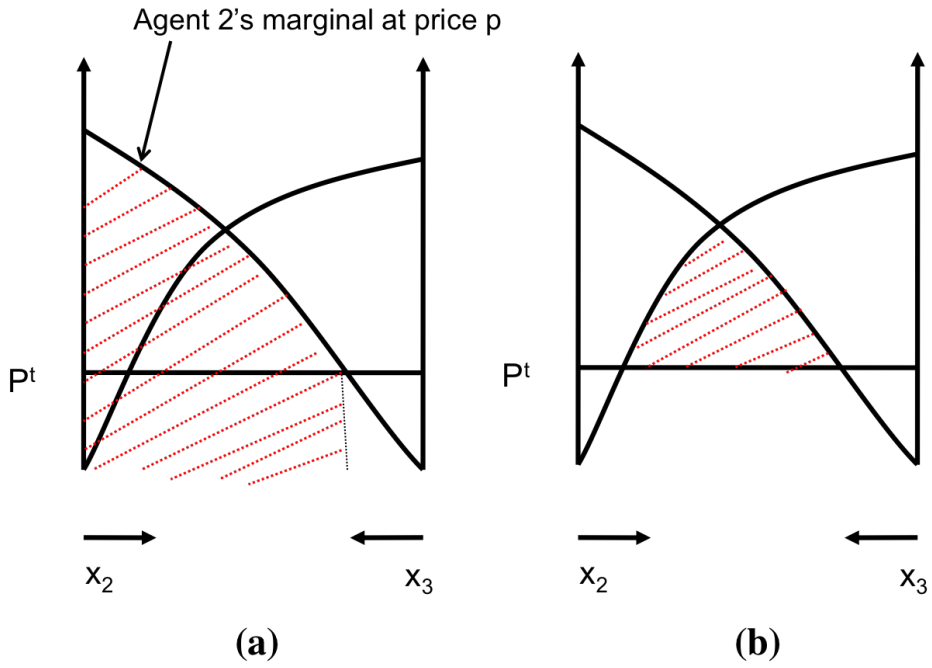

Figure 6.5. Illustration of last inequality in (6.53). (a) Area of $U_2(x_2(p^t))$. (b) Area of $U_2(x_2(p^t)) + U_3(x_3(p^t)) - p^t \cdot \{(x_2(p^t) + x_3(p^t) - 1\} - \max_{x_2+x_3\leq 1}\{U_2(x_2) + U_3(x_3)\}$.

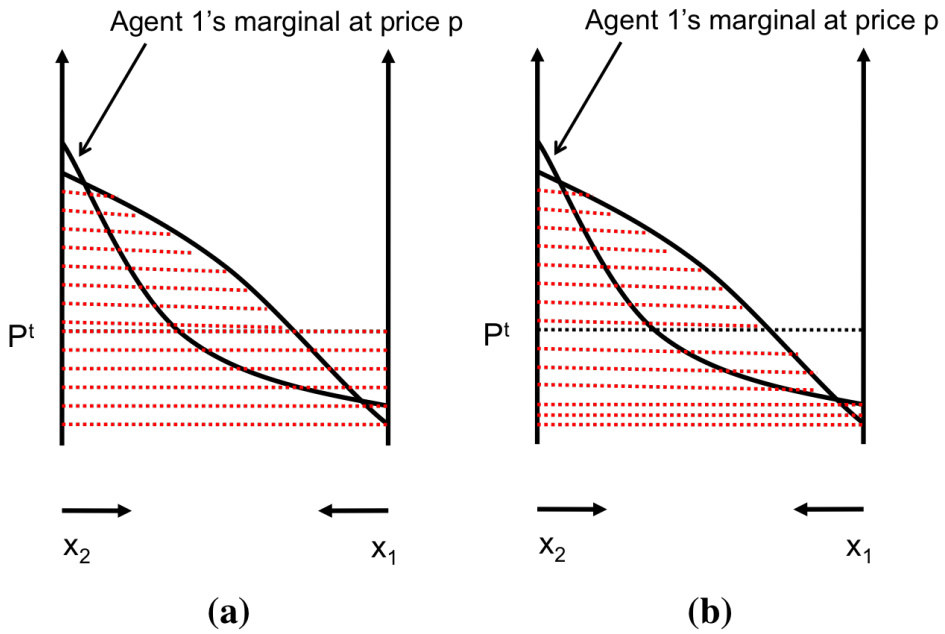

Figure 6.6. Illustration of last inequality in (6.54). (a) Area of $U_2(x_2(p^t)) + p^t \cdot \{1 - x_2(p^t)\}$. (b) Area of $\max_{x_1+x_2\leq 1} U_1(x_1) + U_2(x_2)$.

CHAPTER 7

Conclusions

In this thesis, we have studied resource allocation in wireless communication networks using a utility function framework. A utility function can reflect the degree of satisfaction of individual users in the network, and makes it possible to allocate the constrained resources such that appropriate trade-offs among system efficiency, fairness and QoS, are obtained. Depending on the degree of cooperation among users in the network, two methods for the resource allocation problem are investigated: centralized vs. distributed. In Chapters 2 and 3, we studied centralized time and power allocation in a cellular network with a relay extension and showed that the relay offers significant gains in capacity. Chapters 4, 5, and 6 focused on distributed resource allocation mechanisms for dynamic spectrum sharing, and their associated efficiencies. In the commons model considered in Chapter 4, interference management using rate sharing among users was formulated as a potential game and the efficiency of the game at a Nash equilibrium was studied. In Chapter 5, a sequential second-price auction was applied to bandwidth and power allocation, and the worst-case efficiency was obtained using backward induction in the extended form game of the sequential auction. In Chapter 6, the modified ascending auction, i.e., the Fallback auction, which can be applied to the case where one of the agents has an increasing convex utility function, was analyzed.

In Chapter 2, we analyzed the uplink capacity gain in a cellular network with dedicated fixed relays such as in the *IEEE* 802.16j standard. The relays are assumed to use the

same frequency as the base station and the optimized resource is time within the frame allocated to the relay. Our first-order analysis, as well as detailed system simulations, show that with two relays deployed in the system, uplink capacity increases more than 40% for data and more than 100% for voice. These gains are, however, realized at the cost of relay deployment in the system, such as associated hardware and its installation.

Relay extension using Wi-Fi access points was considered in Chapter 3 as an attempt to exploit existing Wi-Fi nodes. In that scenario, the relays use a different frequency band from the base station (out-of-band relay). Assuming one unit of bandwidth is assigned to each user, we have studied the power allocation at the base station, which maximizes total throughput for data traffic or the total number of active users for voice traffic. We assumed a linear model of a single cell site with two access points (relays) located symmetrically around a base station. In addition to relay traffic, we assumed that the access point has its own customers to serve, which means that if the access point relays data for cellular users, it must reduce the resources available for its own users. We studied two different flow conservation constraints, which correspond to whether or not the relay traffic from the base station is jointly encoded.

Our results show that under both flow constraints, the total transmission rate of data traffic increases by around 40% for the case considered. Moreover, each relay scheme alters the cellular user rate distribution by slightly reducing the rates of users near the base station and increasing the rates of users near the relay. Similarly, for voice traffic, when the sets of active users are optimized, the total number of cellular users increases significantly under both flow rate conservation schemes, but at the cost of reducing the access point users. This corresponds to extending the coverage of the cellular network.

Even though the relay increases the throughput and the coverage of the base station as shown in Chapters 2 and 3, a key assumption is that the relay is cooperative. Namely, it should be willing to share resources with the base station. If the base station and the relay do not belong to the same service provider, relay cooperation can be achieved with an agreement on usage of relay resources, for example, through a bargaining process. Recently, the Nash bargaining solution concept has received some attention in wireless applications [**123, 76**]. We can apply this solution concept for bargaining with an appropriate relay model. If both the base station and the relay have complete information about each other's utility function, then it can be shown that the Nash bargaining solution maximizes the social welfare. An interesting research topic may be to analyze bargaining protocols between the base station and the relay with incomplete information.

Switching from centralized resource allocation among cooperative agents to decentralized methods, we focused on the development of allocation mechanisms and their efficiency. For dynamic spectrum allocation among non-cooperative agents, the commons model and secondary spectrum market have been considered. In Chapter 4, access point deployment was considered in a commons model framework. Interference is managed through a rate sharing scheme among users, which is formulated as a potential game. With various boundary conditions, we showed that there exist pure and mixed Nash equilibria, and by choosing the shared rate appropriately, an efficient Nash equilibrium can be achieved. However, as the density of users increases, local rate sharing is insufficient for adequately managing interference among users. Hence, spectrum markets become attractive for dynamic spectrum sharing.

Auction mechanisms have been considered for a secondary spectrum market. In Chapter 5, we studied a sequential second-price auction for allocating n units of bandwidth or power among non-cooperative wireless devices. This mechanism is relatively simple and requires little information exchange among users, which may make it attractive for dynamic bandwidth or power allocation among secondary users who wish to share spectrum with the primary user (spectrum owner or licensee). Our main analytical results characterize the worst-case efficiency of the subgame perfect equilibrium for two users with full knowledge of bidding histories and user utilities. For a bandwidth auction (decreasing marginal utilities), the worst-case efficiency decreases with n and converges to $1 - e^{-1}$. For the power auction, where one user has decreasing marginal utilities and the other has increasing marginal utilities, the worst-case efficiency is upper bounded by $1/n$.

Although the worst-case efficiency loss due to sophisticated bidding can be significant, simulation results with randomly placed users show that with the rate utility function, the sequential auction typically achieves the efficient allocation. Furthermore, even when the equilibrium is inefficient, the efficiency loss is typically less than the worst-case efficiency loss. This is due to the rate utility function, which places constraints on the ratios of marginal utilities for the successive units being auctioned.

For more than two users, we showed that the sequential second-price auction still has a pure strategy equilibrium. In that case, however, the equilibrium may not be unique and some coordination of the users may be needed to decide on a particular outcome. Assuming a particular equilibrium, simulation results show that for the bandwidth auction the efficiency typically improves when the number of agents increases from 2 to 3. We suspect that this conclusion can be generalized, namely, the worst-case efficiency for any

number of agents might be bounded by that for $k = 2$ agents. In fact, an exhaustive search for the worst-case efficiency with $k = 3$ agents and $n = 3$ units of good has shown that the worst-case efficiency is the same as that for $k = 2$ agents. Completely characterizing the efficiency with an arbitrary number of goods and agents is an open problem.

We applied the sequential second-price auction to the scenario where the total number of agents in the auction is fixed. It might be interesting to extend it to the scenario where agents enter and leave the system at arbitrary times. That more accurately reflects spectrum sharing in a wireless communications network. Moreover, in the absence of full information about other users' utilities, each user may attempt to strategize bidding by assuming a distribution over those utilities. Computing equilibria and efficiency loss in that case is another open problem, although in general less information seems more likely to encourage bidding according to marginal utilities, which leads to an efficient allocation in the bandwidth auction. Extensions to joint power and bandwidth auctions are also interesting possibilities for future work.

In Chapter 6 we studied the Fallback auction motivated by spectrum sharing in which the resource is a potential user's power, so that there is one bidder with a convex utility function, and $n - 1$ bidders with a concave utility function. We showed that the Fallback auction is a core-selecting auction, which minimizes the seller's revenue. Those characteristics minimize the incentive for bidders to misreport bids and collude. At the same time, the seller cannot benefit from excluding bidders. In the case with $k = 2$ agents, the VCG outcome is in the core and the Fallback auction achieves the VCG outcome, which makes the auction incentive compatible even when there is an agent with a convex utility function. On the other hand, for $k > 2$ agents, the VCG might not be in the core, so

that the Fallback auction is not incentive compatible. From [**31**], however, the auction provides "optimal" incentives for truthful reporting and this leads to a full information equilibrium.

The Fallback auction dynamically elicits information from agents to determine an efficient outcome. It would be of interest to determine if this is the minimal information that must be elicited for obtaining such an outcome. In the spectrum sharing model we presented there was only one agent with a convex utility function. It would also be of interest (for spectrum sharing and other applications) to extend these ideas to scenarios in which multiple users have convex utility functions.

Another interesting related challenge is the free rider problem. The free rider problem occurs when there is an externality such as interference. For example, when agent A buys agent B's power to reduce her own interference, it would also benefit agent C (the free rider) who happens to be close to agent B. This may induce agents to buy less power even when the interference is severe. It may be useful to investigate the free rider problem in the context of spectrum sharing and explore possible options to reduce its effect.

References

[1] IEEE P802.11n/D3.00, Wireless LAN Medium Access Control (MAC) and Physical Layer (PHY) specifications: Amendment 4: Enhancements for Higher Throughput.

[2] IEEE Std 802.16j Draft Amendment to IEEE Standard for Local and Metropolitan Area Networks - Part 16: Air Interface for Fixed and Mobile Broadband Wireless Access Systems - Multihop Relay Specification.

[3] Title 47 of the Code of Federal Requlation (CFR). It regulates everything from spurious emissions to unlicensed low-power broadcasting.

[4] IEEE 802.22 draft standard, "IEEE P802.22/D0.3 Draft Standard for Wireless Regional Area Networks," http://www.ieee802.org/22/, doc. no. 22-07-0086-01-0000, May 2007.

[5] *http://wirelessman.org/tgm/*. IEEE 802.16 Task Group m (TGm).

[6] *http://www.ieee802.org/16/relay/*. IEEE 802.16's Relay Task Group.

[7] *http://www.wimaxforum.org/*.

[8] *http://www.zytrax.com/tech/wireless/free.htm*. Unlicensed Frequencies in US.

[9] *Long term evolution of the 3gpp radio technology*. http://www.3gpp.org/Highlights/LTE/LTE.htm.

[10] *www.wesm.ph*. Philippine Wholesale Electricity Spot Market.

[11] E. Altman, Y. Hayel, and H. Kameda, *Evolutionary dynamics and potential games in non-cooperative routing*, Modeling and Optimization in Mobile, Ad Hoc and Wireless Networks and Workshops, 2007. WiOpt 2007. 5th International Symposium on, (2007), pp. 1–5.

[12] L. M. Ausubel, *An efficient ascending bid auction for multiple objects*, American Economic Review, 94 (2004), pp. 1452–1475.

[13] L. M. Ausubel and P. R. Milgrom, *Ascending auctions with package bidding*, Frontiers of Theoretical Economics, 1 (2002), p. Article 1.

[14] J. Bae, E. Beigman, R. Berry, M. L. Honig, and R. Vohra, *An efficient ascending auction for non-concave valuation*, in Annual Allerton Conference on Communication, Network games and algorithms, Monticello, IL, USA, 2007. invited paper.

[15] J. Bae, R. Berry, and M. Honig, *Power allocation, rate, and coverage for relay-assisted downlink data transmission*, in Communications, 2006. ICC '06. IEEE International Conference on, vol. 10, 2006, pp. 4451–4456.

[16] J. Bae, R. Berry, and M. L. Honig, *Power allocation and coverage for a relay-assisted downlink with voice users*, in Global Telecommunications Conference, 2006. GLOBECOM '06. IEEE, 2006, pp. 1–6.

[17] K. Balachandran, J. Kang, K. Karakayali, and J. Singh, *Capacity benefits of relays with in-band backhauling in cellular networks*, Communications, 2008. ICC '08. IEEE International Conference on, (2008), pp. 3736–3742.

[18] B. D. Bernheim and M. D. Whinston, *Menu auctions, resource allocation, and economic influence*, The Quarterly Journal of Economics, 101 (1986), pp. 1–32.

[19] S. Bikhchandani, *Reputation in repeated second-price auctions*, Journal of Economic Theory, 46 (1988), pp. 97–119.

[20] H. Bolukbasi, H. Yanikomeroglu, D. Falconer, and S. Periyalwar, *On the capacity of cellular fixed relay networks*, Electrical and Computer Engineering, 2004. Canadian Conference on, 4 (2004), pp. 2217–2220.

[21] C. Boutilier, M. Goldszmidts, and B. Sabata, *Sequential auctions for the allocation of resources with complementarities*, in Proceedings of 16th International Joint Conference on Artificial Intelligence (IJCAI-99), 1999, pp. 527–534.

[22] M. Bykowsky, *A secondary market for the trading of spectrum: promoting market liquidity*, Telecommunications Policy, 27 (2003), pp. 533–541.

[23] B. Carbunar, B. Lindsley, M. Pearce, and V. Vasudevan, *Verifiable credit based transfers in wireless ad hoc networks*, Parallel and Distributed Processing Symposium, 2007. IPDPS 2007. IEEE International, (2007), pp. 1–10.

[24] J. Chapin and W. Lehr, *The path to market success for dynamic spectrum access technology*, Communications Magazine, IEEE, 45 (2007), pp. 96–103.

[25] L. Chen and J. Leneutre, *On the power and rate control in ieee 802.11 wlans - a game theoretical approach*, Computer Communications and Networks, 2007. ICCCN 2007. Proceedings of 16th International Conference on, (2007), pp. 450–456.

[26] J. Cho and Z. Haas, *On the throughput enhancement of the downstream channel in cellular radio networks through multihop relaying*, Selected Areas in Communications, IEEE Journal on, 22 (2004), pp. 1206–1219.

[27] M. Cooper, *The economics of collaborative production in the spectrum commons*, New Frontiers in Dynamic Spectrum Access Networks, 2005. DySPAN 2005. 2005 First IEEE International Symposium on, (2005), pp. 379–400.

[28] C. Cordeiro, M. Ghosh, D. Cavalcanti, and K. Challapali, *Spectrum sensing for dynamic spectrum access of tv bands*, in Second International Conference on Cognitive Radio Oriented Wireless Networks and Communications, 2007.

[29] R. Cornes and T. Sandler, *The Theory of Externalities*, Cambridge University Press, 1986.

[30] Z. Dawy, S. Davidovic, and I. OikonomidisZ, *Coverage and capacity enhancement of cdma cellular systems via multihop transmission*, in Global Telecommunications Conference, 2003. GLOBECOM '03. IEEE, vol. 2, December 2003, pp. 1147–1151.

[31] R. Day and P. Milgrom, *Core-selecting package auctions*, International Journal of Game Theory, 36 (2008), pp. 393–407.

[32] A. S. de Vany, R. D. Eckert, C. J. Meyers, D. J. O'Hara, and R. C. Scott, *A property system for market allocation of the electromagnetic spectrum: A legal-economic-engineering study*, Stanford Law Review, 21 (1969), pp. 1499–1561.

[33] S. de Vries, J. Schummer, and R. V. Vohra, *On ascending vickrey auctions for heterogeneous objects*, Journal of Economic Theory, 132 (2007), pp. 95–118.

[34] K. Doppler, C. Wijting, and K. Valkealahti, *On the benefits of relays in a metropolitan area network*, Vehicular Technology Conference, 2008. VTC Spring 2008. IEEE, (2008), pp. 2301–2305.

[35] L. Doyle and T. Forde, *Towards a fluid spectrum market for exclusive usage rights*, New Frontiers in Dynamic Spectrum Access Networks, 2007. DySPAN 2007. 2nd IEEE International Symposium on, (2007), pp. 620–632.

[36] R. Etkin, A. Parekh, and D. Tse, *Spectrum sharing for unlicensed bands*, Selected Areas in Communications, IEEE Journal on, 25 (2007), pp. 517–528.

[37] FCC, *The development of secondary markets - report and order and further notice of proposed rule making*. Federal Communications Commission Report 03-113, 2003.

[38] ——, *Second report and order: Promoting efficient use of spectrum through elimination of barriers to the development of secondary markets*. Federal Communications Commission Report 04-167, Sept. 2004.

[39] ——, *Promoting efficient use of spectrum through elimination of barriers to the development of secondary markets - third report and order*. Federal Communications Commission Report 07-52, 2007.

[40] T. Forde and L. Doyle, *Exclusivity, externalities & easements: Dynamic spectrum access and coasean bargaining*, New Frontiers in Dynamic Spectrum Access Networks, 2007. DySPAN 2007. 2nd IEEE International Symposium on, (2007), pp. 303–315.

[41] A. Fujiwara, S. Takeda, H. Yoshino, and T. Otsu, *Area coverage and capacity enhancement by multihop connection of cdma cellular network*, in Vehicular Technology Conference, 2002. Proceedings. VTC 2002-Fall. 2002 IEEE 56th, vol. 4, 2002, pp. 2371–2374 vol.4.

[42] D. Ghosh, *An efficient multi-unit auction with increasing marginal values*. working paper, Octorber 2006.

[43] J. Green and J.-J. Laffont, *Characterization of satisfactory mechanisms for the revelation of preferences for public goods*, Econometrica, 45 (1977), pp. 427–438.

[44] T. Groves, *Incentives in teams*, Econometrica, 41 (1973), pp. 617–631.

[45] G. Hardin, *The tragedy of the commons*, Science, 162 (1968), pp. 1243 – 1248.

[46] T. Harrold and A. Nix, *Performance analysis of intelligent relaying in utra tdd*, in Vehicular Technology Conference, 2002. Proceedings. VTC 2002-Fall. 2002 IEEE 56th, vol. 3, 2002, pp. 1374–1378 vol.3.

[47] D. B. Hausch, *Multi-object auctions: Sequential vs. simultaneous sales*, Management Science, 32 (1986), pp. 1599–1610.

[48] T. Heikkinen, *A potential game approach to distributed power control and scheduling*, Computer Networks, 50 (2006), pp. 2295–2311.

[49] S. Hon-Snir, D. Monderer, and A. Sela, *A learning approach to auctions*, Journal of Economic Theory, 82 (1998), pp. 65–88.

[50] J. Horner and J. Jamison, *Private information in repeated auctions*, The Review of Economic Studies, (2008).

[51] J. Huang, R. Berry, and M. L. Honig, *Auction-based spectrum sharing*, ACM/Springer Mobile Networks and Applications Journal (MONET), 11 (2006), pp. 405–418.

[52] J. Huang, R. A. Berry, and M. L. Honig, *Distributed interference compensation for wireless networks*, IEEE Journal on Selected Areas in Communications, 24 (2006), pp. 1074–1084.

[53] S. Hunt and G. Shuttleworth, *Competition and Choice in Electricity*, John Wiley & Sons, May 1996.

[54] O. Ileri, D. Samardzija, T. Sizer, and N. Mandayam, *Demand responsive pricing and competitive spectrum allocation via a spectrum server*, in First IEEE International Symposium on New Frontiers in Dynamic Spectrum Access Networks (DySPAN), 2005, pp. 194–202.

[55] R. Johari and J. N. Tsitsiklis, *Efficiency loss in a network resource allocation game*, Mathematics of Operations Research, 29 (2004), pp. 407–435.

[56] H. R. Karimi, L. T. W. Ho, H. Claussen, and L. G. Samuel, *Evolution towards dynamic spectrum sharing in mobile communications*, Personal, Indoor and Mobile Radio Communications, 2006 IEEE 17th International Symposium on, (2006), pp. 1–5.

[57] F. P. Kelly, *Charging and rate control for elastic traffic*, European Transactions on Telecommunications, 8 (1997), pp. 33–37.

[58] F. P. Kelly, A. K. Maulloo, and D. K. H. Tan, *Rate control for communication networks: shadow prices, proportional fairness and stability*, Journal of the Operational Research Society, 49 (1998), pp. 237–252.

[59] G. Kramer, M. Gastpar, and P. Gupta, *Cooperative strategies and capacity theorems for relay networks*, Information Theory, IEEE Transactions on, 51 (2005), pp. 3037–3063.

[60] E. R. Kwerel and J. R. Williams, *Moving toward a market for spectrum*, Regulation: The Review of Business and Government, (1993).

[61] M. Kwiek, *Reputation and cooperation in the repeated second-price auctions*. Discussion Paper Series In Economics And Econometrics from University of Southampton, Economics Division, School of Social Sciences.

[62] J. Laneman, D. Tse, and G. Wornell, *Cooperative diversity in wireless networks: Efficient protocols and outage behavior*, Information Theory, IEEE Transactions on, 50 (2004), pp. 3062–3080.

[63] J.-W. Lee, R. Mazumdar, and N. Shroff, *Non-convex optimization and rate control for multi-class services in the internet*, Networking, IEEE/ACM Transactions on, 13 (2005), pp. 827–840.

[64] W. Lehr and J. Crowcroft, *Managing shared access to a spectrum commons*, New Frontiers in Dynamic Spectrum Access Networks, 2005. DySPAN 2005. 2005 First IEEE International Symposium on, (2005), pp. 420–444.

[65] K. Leung and B.-J. Kim, *Frequency assignment for ieee 802.11 wireless networks*, Vehicular Technology Conference, 2003. VTC 2003-Fall. 2003 IEEE 58th, 3 (2003), pp. 1422–1426.

[66] P. Liu, R. Berry, and M. Honig, *A fluid analysis of utility-based wireless scheduling policies*, in Decision and Control, 2004. CDC. 43rd IEEE Conference on, vol. 3, 2004, pp. 3283–3288 Vol.3.

[67] P. Liu, M. Honig, and S. Jordan, *Forward-link cdma resource allocation based on pricing*, in Wireless Communications and Networking Conference, 2000. WCNC. 2000 IEEE, vol. 3, 2000, pp. 1410–1414 vol.3.

[68] Y. Liu, R. Hoshyar, X. Yang, and R. Tafazolli, *Integrated radio resource allocation for multihop cellular networks with fixed relay stations*, Selected Areas in Communications, IEEE Journal on, 24 (2006), pp. 2137–2146.

[69] H. Luo, X. Meng, R. Ramjee, P. Sinha, and L. Li, *The design and evaluation of unified cellular and ad-hoc networks*, Mobile Computing, IEEE Transactions on, 6 (2007), pp. 1060–1074.

[70] J. MacDonald and D. Roberson, *Spectrum occupancy estimation in wireless channels with asymmetric transmitter powers*, in Second International Conference on Cognitive Radio Oriented Wireless Networks and Communications, 2007.

[71] P. Mahonen, J. Riihijarvi, and M. Petrova, *Automatic channel allocation for small wireless local area networks using graph colouring algorithm approach*,

Personal, Indoor and Mobile Radio Communications, 2004. PIMRC 2004. 15th IEEE International Symposium on, 1 (2004), pp. 536–539.

[72] M. H. Manshaei, J. Freudiger, M. Felegyhazi, P. M. adn, and J.-P. Hubaux, *On wireless social community networks*, in INFOCOM, 2008.

[73] P. Marbach and Y. Qiu, *Cooperation in wireless ad hoc networks: A market-based approach*, IEEE/ACM Transactions on Networking, 13 (2005), pp. 1325–1338.

[74] R. Marbach, P.; Berry, *Downlink resource allocation and pricing for wireless networks*, INFOCOM 2002. Twenty-First Annual Joint Conference of the IEEE Computer and Communications Societies. Proceedings. IEEE, 3 (2002), pp. 1470–1479 vol.3.

[75] A. Mas-Colell, M. D. Whinston, and J. R. Green, *Microeconomic Theory*, Oxford University Press, 1995.

[76] S. Mathur, L. Sankaranarayanan, and N. B. Mandayam, *Coalitional games in gaussian interference channels*, Information Theory, 2006 IEEE International Symposium on, (2006), pp. 2210–2214.

[77] P. R. Milgrom and R. J. Weber, *A theory of auctions and competitive bidding*, Econometrica, 50 (1982), pp. 1089–1122.

[78] D. Mishra and D. C. Parkes, *Ascending price vickrey auctions for general valuations*. CORE Discussion Paper No. 2005/52, August 2005.

[79] D. Monderer and L. S. Shapley, *Potential games*, Games and Economic Behavior, 14 (1996), pp. 124–143.

[80] S. Mukherjee and H. Viswanathan, *Resource allocation strategies for linear symmetric wireless networks with relays*, in Communications, 2002. ICC 2002. IEEE International Conference on, vol. 1, 2002, pp. 366–370.

[81] ——, *Analysis of throughput gains from relays in cellular networks*, in Global Telecommunications Conference, 2005. GLOBECOM '05. IEEE, vol. 6, 2005, pp. 3471–3476.

[82] J. F. Nash, *The bargaining problem*, Econometrica, 18 (1950), pp. 155–162.

[83] D. Niyato and E. Hossain, *Integration of ieee 802.11 wlans with ieee 802.16-based multihop infrastructure mesh/relay networks: A game-theoretic approach to radio resource management*, Network, IEEE, 21 (2007), pp. 6–14.

[84] A. Ortego-Reichert, *Models for Competitive Bidding under Uncertainty*, Stanford University, 1968.

[85] M. Osborne and A. Rubinstein, *A course in Game Theory*, MIT Press, 1994.

[86] R. Pabst, B. Walke, D. Schultz, P. Herhold, H. Yanikomeroglu, S. Mukherjee, H. Viswanathan, M. Lott, W. Zirwas, M. Dohler, H. Aghvami, D. Falconer, and G. Fettweis, *Relay-based deployment concepts for wireless and mobile broadband radio*, Communications Magazine, IEEE, 42 (2004), pp. 80–89.

[87] J. M. Peha, *Developing equipment and services for shared spectrum: is it a good gamble?*, in Proceedings of the fifth international conference on electronic commerce, 1997, pp. 955–958.

[88] J. M. Peha and S. Panichpapiboon, *Real-time secondary markets for spectrum*, Telecommunications Policy, 28 (2004), pp. 603–618.

[89] R. Peterson, K. Cutts, and J. Haug, *System performance prediction for personal communication systems*, in Vehicular Technology Conference, IEEE 45th, vol. 2, 1995, pp. 749–753.

[90] M. R. Preston and V. Daniel, *The declining price anomaly*, Journal of Economic Theory, 60 (1993), pp. 191–212.

[91] W. Project, *Wireless world initiative new radio*. http://www.ist-winner.org/.

[92] C. Raman, R. D. Yates, and N. B. Mandayam, *Scheduling variable rate links via a spectrum server*, in New Frontiers in Dynamic Spectrum Access Networks (DySPAN), 2005, pp. 110–118.

[93] F. Reif, *Fundamentals of Statistical and Thermal Physics*, McGraw-Hill, 1985.

[94] J. Riihijarvi, M. Petrova, and P. Mahonen, *Frequency allocation for wlans using graph colouring techniques*, Wireless On-demand Network Systems and Services, 2005. WONS 2005. Second Annual Conference on, (2005), pp. 216–222.

[95] T. Roughgarden and E. Tardos, *How bad is selfish routing?*, Journal of the ACM, 49 (2002), pp. 236–259.

[96] C. Saraydar, N. Mandayam, and D. Goodman, *Efficient power control via pricing in wireless data networks*, Communications, IEEE Transactions on, 50 (Feb 2002), pp. 291–303.

[97] D. Satapathy and J. Peha, *Etiquette modification for unlicensed spectrum: approach and impact*, Vehicular Technology Conference, 1998. VTC 98. 48th IEEE, 1 (1998), pp. 272–276.

[98] R. Schoenen, R. Halfmann, and B. Walke, *Mac performance of a 3gpp-lte multihop cellular network*, Communications, 2008. ICC '08. IEEE International Conference on, (2008), pp. 4819–4824.

[99] G. Senarath and et al., *Multi-hop relay system evaluation methodology (channel model and performance metric)*. IEEE 802.16j Task Group, November 2006. C802.16j-06/013r1.

[100] S. Shakkottai, E. Altman, and A. Kumar, *Multihoming of users to access points in wlans: A population game perspective*, Selected Areas in Communications, IEEE Journal on, 25 (2007), pp. 1207–1215.

[101] N. Shankar, C. Cordeiro, and K. Challapali, *Spectrum agile radios: utilization and sensing architectures*, in New Frontiers in Dynamic Spectrum Access Networks, 2005. DySPAN 2005. 2005 First IEEE International Symposium on, 2005, pp. 160–169.

[102] S. Shenker, *Fundamental design issues for the future internet*, Selected Areas in Communications, IEEE Journal on, 13 (1995), pp. 1176–1188.

[103] S. Simoens, O. Munoz, and J. Vidal, *Achievable rates of compress-and-forward cooperative relaying on gaussian vector channels*, Communications, 2007. ICC '07. IEEE International Conference on, (2007), pp. 4225–4231.

[104] G. Song and Y. Li, *Cross-layer optimization for ofdm wireless networks-part i: theoretical framework*, Wireless Communications, IEEE Transactions on, 4 (2005), pp. 614–624.

[105] I. Spectrum Bridge, *Spectrum licensing and secondary markets primer*. White paper, available at www.spectrumbridge.com, March 2008.

[106] V. Srivastava, J. Neel, A. Mackenzie, R. Menon, L. Dasilva, J. Hicks, J. Reed, and R. Gilles, *Using game theory to analyze wireless ad hoc networks*, Communications Surveys & Tutorials, IEEE, 7 (2005), pp. 46–56.

[107] K. Steiglitz, *Snipers, Shills, and Sharks: eBay and Human Behavior*, Princeton University Press, March 2007.

[108] J. Sun, E. Modiano, and L. Zheng, *Wireless channel allocation using an auction algorithm*, Selected Areas in Communications, IEEE Journal on, 24 (2006), pp. 1085–1096.

[109] W. Vickrey, *Counterspeculation, auctions, and competitive sealed tenders*, Journal of Finance, 16 (1961), pp. 8–37.

[110] H. Viswanathan and S. Mukherjee, *Performance of cellular networks with relays and centralized scheduling*, Wireless Communications, IEEE Transactions on, 4 (2005), pp. 2318–2328.

[111] F. Wang, M. Krunz, and S. Cui, *Price-based spectrum management in cognitive radio networks*, Selected Topics in Signal Processing, IEEE Journal of, 2 (2008), pp. 74–87.

[112] J. M. Ward, *Secondary markets in spectrum: Making spectrum policy as flexible as the spectrum market it must foster*, CommLaw Conspectus: Journal of Communication Law and Policy, 10 (2001), pp. 103–132.

[113] R. J. Weber, *Multiple-object auctions*. Discussion Papers 496, Northwestern University, Center for Mathematical Studies in Economics and Management Science, 1983.

[114] H.-y. Wei and R. Gitlin, *Wwan/wlan two-hop-relay architecture for capacity enhancement*, in Wireless Communications and Networking Conference, 2004. WCNC. 2004 IEEE, vol. 1, 2004, pp. 225–230 Vol.1.

[115] M. Wellens, J. Wu, and P. Mahonen, *Evaluation of spectrum occupancy in indoor and outdoor scenario in the cognitive wireless networks*, in Second International Conference on Cognitive Radio Oriented Wireless Networks and Communications, 2007.

[116] K. Werbach, *Open spectrum: The new wireless paradigm*. New America Foundation, Spectrum Policy Program, Spectrum Series Working Paper #6 October 2002.

[117] W. C. Wong, J. Sydir, H. H. Lee, K. Johnson, R. Peterson, E. Visotsky, M. Asa, and F.-C. Ren, *Frame structure to support multi-hop relay operation*, January 2007. C80216j-07/109r1.

[118] H. Wu, C. Qiao, S. De, and O. Tonguz, *Integrated cellular and ad hoc relaying systems: icar*, Selected Areas in Communications, IEEE Journal on, 19 (2001), pp. 2105–2115.

[119] L. Xiao, T. E. Fuja, and D. J. Costello, *An analysis of mobile relaying for coverage extension*, Information Theory, 2008. ISIT 2008. IEEE International Symposium on, (2008), pp. 2262–2266.

[120] M. Xiao, N. Shroff, and E. Chong, *A utility-based power-control scheme in wireless cellular systems*, Networking, IEEE/ACM Transactions on, 11 (2003), pp. 210–221.

[121] Y. Xiao, X. Shan, and Y. Ren, *Game theory models for ieee 802.11 dcf in wireless ad hoc networks*, Communications Magazine, IEEE, 43 (2005), pp. S22–S26.

[122] F. Xu, L. Zhang, Z. Zhou, and Q. Liang, *Adaptive power control for cooperative uwb network using potential game theory*, Wireless Communications and Networking Conference, 2007.WCNC 2007. IEEE, (2007), pp. 1620–1624.

[123] H. Yaiche, R. Mazumdar, and C. Rosenberg, *A game theoretic framework for bandwidth allocation and pricing in broadband networks*, Networking, IEEE/ACM Transactions on, 8 (2000), pp. 667–678.

[124] S. Yang and B. Hajek, *Vcg-kelly mechanisms for allocation of divisible goods: Adapting vcg mechanisms to one-dimensional signals*, Selected Areas in Communications, IEEE Journal on, 25 (2007), pp. 1237–1243.

[125] E. Yanmaz and O. Tonguz, *Dynamic load balancing and sharing performance of integrated wireless networks*, Selected Areas in Communications, IEEE Journal on, 22 (2004), pp. 862–872.

[126] J. T. yi Wang, *The ebay market as sequential second price auctions: Theory and experiments*. unpulbished manuscript, November 2006.

[127] C. Zhou, P. Zhang, M. Honig, and S. Jordan, *Two-cell power allocation for downlink cdma*, Wireless Communications, IEEE Transactions on, 3 (2004), pp. 2256–2266.